Università degli Studi della Tuscia di Viterbo

Dipartimento di Scienze Agrarie e Forestali (DAFNE)

Corso di Dottorato di Ricerca in

Ecologia e Gestione Sostenibile delle Risorse Ambientali XXXVI° ciclo

A NEW APPROACH FOR THE REDUCTION OF SOIL EROSION IN FOREST ENVIRONMENTS

Settore scientifico-disciplinare
s.s.d. AGR/05

Tesi di dottorato di:
Dott. Pietro Salvaneschi

Firma

Coordinatore del corso
Prof. Claudio Carere

Firma

Tutore
Prof. Bartolomeo Schirone

Firma

Co-tutors
Prof. Ciro Apollonio
Prof. Kevin Cianfaglione

Firma

A.A. 2023/24 (A.Y. 2023/24)

Summary

List of acronyms (a-z)

ADF	Amount-Duration-Frequency
AGI	American Geosciences Institute
AMR	Annual Maximum Rainfall
BSM	Banded Standards Method
DEM	Digital Elevation Model
EEA	European Environment Agency
EUROSTAT	European Community Statistics
FAO	Food and Agriculture Organisation
GIS	Geographical Information System
GSM	Grouped Standards Method
INFC	Italian National Forest Inventory
IPCC	Intergovernmental Panel on Climate Change
ISPRA	Istituto Superiore per la Protezione e la Ricerca Ambientale
ITPS	Intergovernmental Technical Panel on Soils
LIDAR	Light Detection and Ranging
MASE	Italian Ministry of Environment and Energetic Security
MFI	Modified Fournier Index
NDVI	Normalized difference Vegetation Index
NOOA	National Oceanic and Atmospheric Administration
NSRP	Neyman Scott Rectangular Pulses
PVC	Polyvinyl Chloride
RUSLE	Revised Universal Soil Loss Equation
SA	Standards Arrangement
SOM	Soil Organic Matter
SRG	Stochastic Rainfall Generator
SSM	Scattered Standards Method
TOC	Total Organic Carbon
USDA	United States Department of Agriculture
USGS	United States Geological Survey
USLE	Universal Soil Loss Equation

Abstract

This PhD project had, as its main objective, the comprehension of the dynamics involved in the formation of soil erosion after logging. To reach this goal we created a new sylvicultural model, called Banded Standards Method (BSM), to be used in hilly coppice forest, aimed to the reduction of soil erosion after cuts. To test the validity of this model we first tested the model theoretically, then we tested the model on field, by comparing the BSM method with the Italian traditional coppice standard arrangement, the Scattered Standards Method (SSM). To collect the sediment created by the soil erosion we created a prototype of a new soil erosion plot, that we called Natural Erosion Trap (NET), created with the aim to be utilized in forests and more in general in natural environments. Both theoretically and on field experiment suggested that our method decreased soil erosion after logging, in particular with regards to the gravels and rocks. We also studied deeply the USLE and RUSLE model to understand which formulas were better to use in central Italy. We discovered that the R factor of the USLE and RUSLE models affect the final result. We so evaluate the R factor equations that fit better in the internal part of central Italy. We found out three equation and we used them to evaluate the soil erosion by using the RUSLE model in the study area where the field experiment was carried out. Also, the RUSLE model created for the study area showed a reduction of the soil erosion in the BSM plot, even the result were very different with the experimental campaign.

1. Introduction

Aim of the PhD project.

Italy is one of the European countries with the highest value of hydrogeological instability due to natural and anthropogenic causes, 94% of Italian municipalities suffer some kind of hydrological instability (Trigila et Al., 2021).

It is well known that a key factor to reduce soil erosion so, consecutively, hydrological instability, is the conservation of forest areas (Chapter 2, Schirone et Al., 2021). An improvement in the management of Italian forests could help to reduce hydrological instability in the country. According to the Italian National Forest Inventory, (INFC 2015), in Italy, coppice stand forests represent 42.3% of the total forest Italian surface, while the high forests represent 41.9%. The coppice stands management of forest is the one that produces more erosion because of the more frequent logging of the forest in comparison with other managements.

Given this context, it becomes imperative to explore innovative management approaches aimed at minimizing soil erosion and hydrological risks within coppice forests. Because of that, this PhD project has, as its main objective, the realization of a new silvicultural method that can help the reduction of soil erosion caused by water after logging.

Our proposed model involves modifying the geometry of the standards left behind after a cut in hilly coppice forests. Instead of the traditional Scattered Standards Method (SSM), we have adopted the Banded Standards Method (BSM). By arranging these standards in bands, we create a natural barrier—a sort of "dam"—that can intercept water flow and traps gravel of varying sizes, thus mitigating erosion. To reach our goal, we divided the project into several steps.

The first step was based on a bibliography search to better understand what soil erosion by water is, and how it is calculated both using models and field experiments.

As the second step, we run into a search for soil erosion studies in forests and studies that put in relationship the coppicing geometry and the soil erosion.

Once the theoretical model had been formulated, we tested its feasibility inside a forest. For that, we counted the trees inside that forest, and we mapped them to understand if it was possible to create bands of standards. Finally, we tested the BSM model by comparison with the typical SSM method using the Universal Soil Loss Equation, USLE (Wischmeier and Smith, 1978). The results of this study allowed the publication of a scientific article (Chapter 2).

The research brings us to the conclusion that the results of USLE models can vary a lot depending on the factors chosen to create the equation. These factors can bring different errors, overestimating or underestimating the erosion. One of the more relevant is the R factor, the Rainfall Erosivity Factor. Because the literature presents a large variety of R factor formulas (e.g. Wischmeier and Smith, 1978; Arnoldus, 1980; Ferreira et al., 2014), we decided to try to find the best R factor for central Italy, the zone of our studies, and the next studies. So, we tested 12 different R factor equations using data from Rieti Province, and we created different Rieti province maps. Finally, we chose the equations that fit better in the province. The results of this study let us the publication of an article (chapter 3).

In the final step (chapter 4 and 5), we realized two experimental plots, inside a coppice forest located in Popoli, Abruzzo Region, with the help of the Maiella National Park and Raggruppamento Carabinieri per la Biodiversità Pescara.

We first cut the two plots, one using the SSM method and the second with our method (BSM). Then, on the perimeter of the two plots, we created two erosion plots, we collected the soil erosion generated from the cuts, and we compared them. We also collected the leaves moved from the logged areas to the base of the erosion plots and we compared them within the two methods (chapter 4). Finally, we created different soil erosion models, for each plot before and after the cut. We developed these models using the Revised Universal Soil Loss Equation, RUSLE (Renard et Al., 1997), an equation developed for GIS use. We tried to use data as much high-detailed as possible (chapter 5).

Soil Erosion.

Soil erosion is a natural phenomenon, that occurs under all climatic conditions and on all continents, typically when water or wind removes the topsoil from the land surface (Pimentel and Kounang, 1998; FAO and ITPS, 2015 and FAO, 2019). Soil erosion can be increased and accelerated by unsustainable human activities such as intensive agriculture, deforestation, overgrazing, and improper land use changes (FAO and ITPS, 2015; FAO, 2019).

It is very important to reduce soil erosion and to prevent it because it has been proved that erosion rates in arable and grazing land are much higher than in natural environments, while the formation of new soil is slower, as much as it can be considered as a non-renewable resource (Pimentel and Kounang 1998; FAO and ITPS, 2015).

As said before soil erosion takes place in the topsoil, which is also the most fertile part of it, where is located most of the Soil Organic Matter (SOM) present in the soil, so losing it means a loss in SOM and a loss in fertility (FAO and ITPS, 2015).

Soil erosion causes a decrease in agricultural productivity and a degradation in ecosystem functions, it amplifies hydrogeological risks such as landslides or floods, causes significant losses in biodiversity, and finally, it can damage urban infrastructure elevating the risk for human health (FAO, 2019). It is considered the major threat to soil functions in five of the seven FAO regions (Africa, Asia, Latin America, Near East and North Africa, and North America) (FAO and ITPS 2015, FAO 2019).

Soil erosion is caused by three major factors, water, wind, and tillage. They can act individually, in dual combination, or all together (Pimentel and Kounang 1998; FAO, 2019).

Water erosion is the one that affects the greatest land area. It occurs in two different ways: when the raindrop splashes on the soil surface, and, after that, when the water flows across the surface (runoff). The runoff erosion occurs first in thin sheets (sheet erosion), but often it is concentrated in different channels, when they are small, we call it rill erosion, if they are deeper, we call it gully erosion, in both types of channels the erosive power of the flow is amplified. When there are no barriers to block the runoff and the sediment eroded, they are carried to a stream system and are removed from the landscape (Pimentel and Kounang 1998; FAO, 2019). There are other two forms of water erosion, those are erosion by snow and by ice. The first one, erosion by snow, is the erosion caused by the melting of the snow, typically during spring, where the melted snow flows down and causes erosion (Středová et al., 2017). The second type is related to glaciers, and it is called glacial erosion or ice erosion. It occurs when glaciers move, where the ice present at the bottom and on the sides of a glacier freezes onto rocks. As glaciers move continuously, it causes the breakdown of rocks from the ground and sometimes even from the sides of a valley. There are two types of glacial erosion, the first one is plucking, which is related to the water and ice that percolate into crack of rocks. The water inside these cracks melts, freezes, and so on, generating big forces that cause the formation of bigger cracks and finally the breaking of the rocks into small pieces. The second type is abrasion, it occurs when broken rock particles rub against each other. The huge volume of the glacier, along with broken rock particles and sediments, generally rub and carve the surface of the rock present below the glacier, leaving behind scratch marks on the rock's surface (AGI; Iverson, 2002; Fu and Harbor, 2011;).

Wind Erosion Wind erosion, also known as eolian erosion, is a natural geomorphic process that shapes the Earth's surface by moving soil particles through the action of wind. It occurs in various landscapes, from deserts to agricultural fields, and has significant implications for soil health, land productivity, and environmental sustainability. It is a natural process, but human activities can exacerbate its effects.

Several factors contribute to wind erosion. The first one is wind velocity, the force of the wind plays a crucial role. Strong winds can detach and transport soil particles more effectively. Then there is soil properties, soil texture, structure, and moisture content influence its susceptibility to erosion. Sandy soils are more prone to wind erosion than clayey soils. Vegetation cover, vegetation acts as a protective shield against wind erosion. Deforestation or removal of native vegetation increases vulnerability. Land Use Practices, agricultural activities, construction, and mining disturb the soil surface, making it more susceptible to erosion. Finally, there is the climate, arid and semi-arid regions experience more frequent wind erosion due to the lack of vegetation and high wind speeds.

The wind erosion process involves several stages, detachment, transport, and deposition. The detachment occurs when wind lifts soil particles from the surface. The impact of windblown sand and dust on rocks and other surfaces leads to abrasion and detachment. After this process starts the transport of particles, soil particles move through the air. There are three primary modes of transport. The first one is suspension, when fine particles (silt and clay) remain suspended in the air for extended periods, forming atmospheric dust. The second is saltation, when larger particles (sand-sized) bounce along the ground in short hops and as third way of transportation, the surface Creep, when Coarser particles roll or slide along the surface. The last process of wind erosion is deposition, and it occurs when the wind speed decreases or encounters an obstacle (such as vegetation or topography), it deposits the transported particles. Deposition contributes to soil formation in some areas.

Wind erosion can lead to soil degradation because it removes the fertile topsoil, reducing soil quality and nutrient content, which affects agricultural productivity. It can also lead to a loss of ecosystem services because of the disruption of ecosystem functions, including nutrient cycling, water retention, and carbon sequestration. Also, air quality can be affected by wind erosion, suspended dust particles contribute to poor air quality and respiratory issues. Finally, it contributes to landform modification, it shapes dune, loess deposits and other landforms (Lal, 2001; Shao, 2009; FAO, 2019).

Finally, tillage erosion is the erosion caused by human tillage practice and it causes a net downslope movement of soil (FAO, 2019). It is a significant form of soil erosion that occurs in cultivated fields due to the movement of soil caused by tillage practices. It involves the downslope movement of soil due to gravity. It primarily occurs on sloping and hilly lands where intensive cropping and tillage practices are used. Unlike water erosion, which mainly affects midslope and lowerslope segments, tillage erosion specifically impacts hilltops. The process of tillage erosion depends on two factors: tillage erosivity and tillage erodibility. The first one refers to the propensity of a tillage operation to erode soil. it’s influenced by factors like the design and operation of the tillage implement. Landscape erodibility describes the landscape’s susceptibility to erosion by tillage, considering topography and soil properties. typical patterns of tillage erosion include the hilltop erosion that is the soil loss from convex hilltops and, depression accumulation, that is the soil accumulation in concave depressions. Tillage erosion can lead to soil degradation, reduced crop yield, and economic losses for farmers. it’s essential to manage tillage practices carefully to minimize its impact on agricultural lands (Van Oost and Govers, 2006; Blanco and Lal, 2008) .

In this PhD project, we focused our attention on soil erosion by water, so, from this moment till the end we will use the term soil erosion to intend soil erosion by water.

Soil erosion in forest areas.

Soil erosion inside an undisturbed forest is typically low (Elliott et al., 1996; Pimentel and Kounang 1998; Borrelli et al., 201), if the forest is located on a flat surface, it is almost null, if it is located on a hilly or steep surface, the quantity of soil erosion depends on the species and the geometry of the canopy of the trees (Rodrigues et al., 2020). In any case, if there is no intervention of human activities, soil erosion in those areas is negligible in comparison with agricultural land. Soil erosion starts after a disturbance, which can be natural as a forest fire or an avalanche, or human, such as deforestation, logging, or the construction of forest roads (Elliott et al., 1996; Sudarmadji, 2001; Stott et al., 2001; Golijanin et al., 2022).

Talking about deforestation and forest logging, it has been proved, in Italy, that soil erosion passes from 0.33 Mg ha^{-1} yr^{-1} to 13.9 Mg ha^{-1} yr^{-1}(mean of 4 years of soil erosion after a cut) (Borrelli et al., 2017). This happens because, without tree cover, the rain falls directly on the topsoil, the retention function of roots is less powerful, and there is more compaction (Elliott et al.,1996), so water rills on the surface creating a lot of erosion and augmenting the hydrological risk.

Soil erosion estimation.

Soil erosion of a specific area can be calculated in two ways. The first one is the empirical way, and it is done using equations or models created for that purpose. The second one is the experimental way, which is done by creating different plots that can collect the sediment yields of a specific limited area. The first approach is generally used to assess a big area, where it would be impossible to create an immense quantity of plots. The results can have errors and can be considered more as potential results than real (e.g. Van Der Knijff et al. 1999; Panagos et al., 2014; Sidi Almouctar et al., 2021). The second method is used to do experimental studies in very small areas, often in the agricultural field (e.g. Bagarello et al., 2008; Porto et al., 2009; Kastridis et al., 2022), the results are real, but not every time statistically valid, because the experiments should last for years and anyway, they represent only the area where they are made.

There are different equations or models to estimate the soil erosion of an area. The most used of all is the Universal Soil Loss Equation, USLE (Wischmeier and Smith, 1978), and his revision, the Revised Universal Soil Loss Equation, RUSLE (Renard et Al., 1997). The

USLE was created after many years of field experiments, using experimental plots. the experimental plot created by the two researchers is still the plot model of most of today's field research. The RUSLE has been developed for use in a GIS (Geographic Information System) environment. The two equations are very utilized because even if they cannot be precise as a field experiment, their simple use overcomes the errors committed and the results can be useful anyway as a Guideline for interventions.

The concept of the two equations is the same, soil erosion is calculated by the product of different factors, the same factors for both equations, the only difference between them is that in the USLE the factors are numbers while in the RUSLE every factor is a map.

Soil erosion in USLE and RUSLE is calculated as follows:

$A= L \times S \times R \times K \times C \times P$

Where:

A = Annual soil erosion (t/ha/year),

L = Length factor (-),

S = Slope factor (-),

R = Rainfall erosivity factor (MJ*mm/ha/h/year),

K = Soil erodibility factor (t*h/MJ/mm),

C = Soil coverage factor (-),

P = Erosion control measures factor (-).

L and S factors measure the influence of the topography on soil erosion. The longer and steeper the hillside, the higher the erosion. The L factor is related to the runoff length of the study area, while the S factor represents the hillside slope of it.

The R factor for a given considered period is obtained by summing, for each rainstorm, the product of total storm energy (E), expressed in MJ/ha, and the maximum 30-minute intensity (I_{30}), expressed in mm/min, (Van Der Knijff et al. 1999). Because of the difficulty of getting such high-resolution data, over the years several empirical formulas have been proposed as alternatives, aiming to express the R factor using monthly or annual cumulative rainfall values.

The K factor is the soil erodibility factor. It considers the soil properties during a rainfall event, so how much the soil can be eroded during it.

The C factor is related to the capacity of vegetation cover to mitigate soil erosion, the more vegetation is present, the less erosion will be.

Finally, the P factor is related to the cultural practices aiming to reduce soil erosion, it is used only in agriculture, not in natural environments, such as forests.

As said before the are several other equations or models to estimate soil erosion, in the next table (table 1.1), from Borrelli 2011 (Borrelli, 2011), a list of the principal equations or models used for soil erosion estimation.

Table 1.1: This table shows the principal models used to estimate soil erosion. Extract from Borrelli 2011.

Model	Type	Spatial scale	Temporal scale	Outputs	
USLE	Empirical	Hillslope	Annual	Erosion	Wischmeier and Smith, (1978)
RUSLE	Empirical	Hillslope	Annual	Erosion	Renard et al., (1997)
RUSLE-3D	Empirical/conceptual	Watershed	Annual	Erosion	Mitasova et al., (2009)
USPED	Empirical/conceptual	Watershed	Event/ Annual	Erosion/deposition	Mitas and Mitasova, (1998)
AGNPS	Conceptual	Small watershed	Event/continuous	Run-off, peak rate, erosion, sediment yield	Young et al., (1989)
LASCAM	Conceptual	Watershed	Continuous	Run-off, sediments	Viney and Sivapalan, (1999)
SWAT	Conceptual	Watershed	Continuous	Run-off, peak rate, erosion, sediment yield	Arnold and Williams, (1995)
AGWA	Conceptual/physical	Watershed/basin	Continuous	Run-off, peak rate, erosion, sediment yield	
EMSS	Conceptual	Watershed	Continuous	Run-off, sediment loads	Vertessey et al., (2001)
HSPF	Conceptual	Watershed	Continuous	Run-off, flow rate, sediment load	Johanson et al., (1980)
SEDNET	Conceptual/empirical	Watershed/basin	Annual/continuous	Suspended sediment, relative contribution from overland flow, gully and bank erosion processes	Prosser et al., (2001)
THORNES	Conceptual/empirical	Hillslope/watershed	Annual	Run-off, erosion	Thornes (1990)
SEDEM/WaTEM	Conceptual	Watershed	Annual	Erosion	Van Rompaey et al., (2001)
SEAGIS	Empirical/conceptual	Watershed	Annual	Erosion, sediment yield	
SPL	Empirical/conceptual	Watershed/river	Annual	Fluvial erosion, river incision	Stock and Montgomery, (1999)

Regarding experimental studies, three typical methods are used to calculate soil erosion.

The first one, the most common method, is the creation of an experimental plot like the ones created by Wischmeier and Smith (Wischmeier and Smith, 1978). It consists of a fence that isolates the plot from the outside environment, it is posed on the top of the plot, and the two sides and it is made of cement or iron. On the base of the plot, there is a collector, that collects the water runoff and the sediment yields (Figure 1.1). The collector is typically a tank. Because of the difficulties of creating such a plot, it is not widely used in natural environments, much more in agricultural experiments.

The second method is the pegs method (e.g. Takei et al., 1981; Smith and Dragovich, 2008; Borrelli, 2011), which consists of the positioning of a series of pegs along a specific place, typically perpendicular to the contour lines. The erosion is calculated by taking soil blocked by the pins (Figure 1.2). This method is very simple to do, but it is not precise because the pegs are sparse, so the erosion between them is lost, but it gives anyway a real estimation. It is used typically in natural environments.

The final method is the silt fence method (Kastridis et al., 2022), which consists of the positioning of a silt fence along a contour line (Figure 1.3). This method is more precise than the pins method, but the fence is positioned only in the base, so the system is not isolated from the rest of the environment, and the fence is made of a Nonwoven fabric, that is permeable, so it lost the smallest particles of soil eroded. This method is also used in natural environments.

For this research, we developed a new erosion plot type. Our erosion plot has the objective of being as precise as the Wischmeier plot but easier to build. It doesn't need mechanization or the remotion of soil for the creation, and it is easy to remove, so the environment can return to its original state with not so much time. This plot can be used in all environments, natural or artificial, but we create it specifically for natural forests (Figure 1.4). More specific details can be found in Chapter 4.

Figure 1.1: This image represents the Wischmeier plots built for the development of the USLE. Source: Agricultural Research Service, USDA.

(A)

(B)

Figure 1.2: pegs method. (A): details of the pegs. (B): soil erosion plot made using pegs. Source: Borrelli, 2011.

Figure 1.3: Silt fence method. Source: Kastridis et al. 2022.

(A)

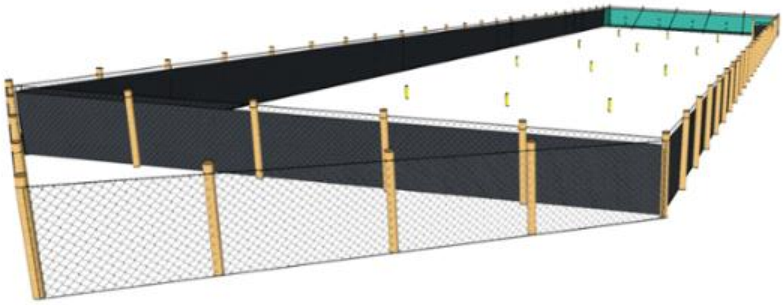

(B)

(C)

Figure 1.4: Soil erosion plot proposed by our research team. (A and B): 3d render of the soil erosion plot. (C): image of the soil erosion plot mounted in the Popoli Study area, Chapter 4.

References

1. AGI: https://www.americangeosciences.org/education/k5geosource/content/rocks/what-is-glacial-erosion
2. Arnoldus, H. M. J. (1980). An approximation of the rainfall factor in the Universal Soil Loss Equation. 127–132.
3. Lal, R. (2001). Soil degradation by erosion. Land Degradation & Development, 12(6), 519–539. https://doi.org/https://doi.org/10.1002/ldr.472
4. Iverson, N. R. (2002). 5 - Processes of glacial erosion (J. B. T.-M. and P. G. E. Menzies (ed.); pp. 131–145). Butterworth-Heinemann. https://doi.org/10.1016/B978-075064226-2/50008-8
5. Van Oost, K., & Govers, G. (2006). Tillage Erosion. Soil Erosion in Europe, 40(3), 599–608. https://doi.org/10.1002/0470859202.ch43

6. Bagarello, V., Di Piazza, G.V., Ferro, V. and Giordano, G. (2008), Predicting unit plot soil loss in Sicily, south Italy. Hydrol. Process., 22: 586-595. https://doi.org/10.1002/hyp.6621
7. Blanco-Canqui, H., & Lal, R. (2008). Tillage Erosion - Principles of Soil Conservation and Management (H. Blanco-Canqui & R. Lal (eds.); pp. 109–135). Springer Netherlands. https://doi.org/10.1007/978-1-4020-8709-7_5
8. Shao, Y. (2009). Physics and Modelling of Wind Erosion. Physics and Modelling of Wind Erosion, April. https://doi.org/10.1007/978-1-4020-8895-7
9. Borrelli, P. (2011). Risk assessment of human-induced accelerated soil erosion processes in the intermountain watersheds of Central Italy: A Case Study of the Upper Turano Watershed (Latium-Abruzzi) (Doctoral dissertation).
10. Fu, P., & Harbor, J. (2011). Glacial erosion. Encyclopedia of Snow, Ice and Glaciers, Edited by: Singh, VP, Singh, P., and Haritashya, UK, Springer Netherlands, Dordrecht, 332–341.
11. Borrelli, P., Panagos, P., Märker, M., Modugno, S., & Schütt, B. (2017). Assessment of the impacts of clear-cutting on soil loss by water erosion in Italian forests: First comprehensive monitoring and modelling approach. *Catena*, *149*, 770–781. https://doi.org/10.1016/j.catena.2016.02.017
12. Elliot, W. J., Page-Dumroese, D., & Robichaud, P. R. (1996). The Effects of Forest Management on Erosion and Soil Productivity*. In R. Lal (A c. Di), Soil Quality and Soil Erosion (1ª ed., pp. 195–208). CRC Press. https://doi.org/10.1201/9780203739266-12
13. FAO and ITPS. 2015. Status of the World's Soil Resources (SWSR) – Main Report. Food and Agriculture Organization of the United Nations and Intergovernmental Technical Panel on Soils, Rome, Italy
14. FAO. 2019. Soil erosion: the greatest challenge to sustainable soil management. Rome. 100 pp. Licence: CC BY-NC-SA 3.0 IGO.
15. Ferreira, V., & Panagopoulos, T. (2014). Seasonality of Soil Erosion Under Mediterranean Conditions at the Alqueva Dam Watershed. Environmental Management, 54(1), 67–83. https://doi.org/10.1007/s00267-014-0281-3
16. Golijanin, J., Nikolić, G., Valjarević, A., Ivanović, R., Tunguz, V., Bojić, S., Grmuša, M., Lukić Tanović, M., Perić, M., Hrelja, E., & Stankov, S. (2022). Estimation of potential soil erosion reduction using GIS-based RUSLE under different land cover management models: A case study of Pale Municipality, B&H. Frontiers in Environmental Science, 10, 945789. https://doi.org/10.3389/fenvs.2022.945789
17. INFC 2015, Gasparini, P., Di Cosmo, L., Floris, A., & De Laurentis, D. (A c. Di). (2022). Italian National Forest Inventory—Methods and Results of the Third Survey: Inventario Nazionale delle Foreste e dei Serbatoi Forestali di Carbonio—Metodi e Risultati della Terza Indagine. Springer International Publishing. https://doi.org/10.1007/978-3-030-98678-0
18. Kastridis, A., Margiorou, S., & Sapountzis, M. (2022). Check-Dams and Silt Fences: Cost-Effective Methods to Monitor Soil Erosion under Various Disturbances in Forest Ecosystems. Land, 11(12), 2129. https://doi.org/10.3390/land11122129
19. Panagos, P., Meusburger, K., Liedekerke, M. Van, Alewell, C., Hiederer, R., Montanarella, L., Panagos, P., Meusburger, K., & Liedekerke, M. V. A. N. (2014). Soil Science and Plant Nutrition Assessing soil erosion in Europe based on data collected through a European network Assessing soil erosion in Europe based on

data collected through a European network. *Soil Science and Plant Nutrition*, *60*(1), 15–29. https://doi.org/10.1080/00380768.2013.835701

20. Pimentel, D., & Kounang, N. (1998). Ecology of soil erosion in ecosystems. *Ecosystems*, *1*(5), 416–426. https://doi.org/10.1007/s100219900035
21. Porto, P., Walling, D. E., & Callegari, G. (2009). Investigating the effects of afforestation on soil erosion and sediment mobilization in two small catchments in Southern Italy. Catena, 79(3), 181–188. https://doi.org/10.1016/j.catena.2009.01.007
22. Renard, K., Foster, G., Weesies, G., McCool, D. and Yoder, D. (1997) Predicting Soil Erosion by Water: A Guide to Conservation Planning with the Revised Universal Soil Loss Equation (RUSLE). US Department of Agriculture, Agriculture Handbook No.703USDA, USDA, Washington DC.
23. Rodrigues, A. R., Botequim, B., Tavares, C., Pécurto, P., & Borges, J. G. (2020). Addressing soil protection concerns in forest ecosystem management under climate change. *Forest Ecosystems*, *7*(1). https://doi.org/10.1186/s40663-020-00247-y
24. Schirone, B., Salvaneschi, P., Cianfaglione, K., Pecci, M., Andrisano, T., Vessella, F., & Petroselli, A. (2021). A proposal for modifying coppicing geometry in order to reduce soil erosion in the forest areas. *Notulae Botanicae Horti Agrobotanici Cluj-Napoca*, *49*(2), 1–17. https://doi.org/10.15835/nbha49212325
25. Sidi Almouctar, M.A.; Wu, Y.; Zhao, F.; Dossou, J.F. Soil Erosion Assessment Using the RUSLE Model and Geospatial Techniques (Remote Sensing and GIS) in South-Central Niger (Maradi Region). Water 2021, 13, 3511. https://doi.org/10.3390/w13243511
26. Smith, H. G., & Dragovich, D. (2008). Post-fire hillslope erosion response in a sub-alpine environment, south-eastern Australia. Catena, 73(3), 274–285. https://doi.org/10.1016/j.catena.2007.11.003
27.
28. Stott, T., Leeks, G., Marks, S., & Sawyer, A. (2001). Environmentally sensitive plot-scale timber harvesting: Impacts on suspended sediment, bedload and bank erosion dynamics. Journal of Environmental Management, 63(1), 3–25. https://doi.org/10.1006/jema.2001.0459
29. Středová, H., Středa, T., & Rožnovský, J. (2017). *Snow as a cause of soil erosion-methodological approach of determination*. *September*. https://www.researchgate.net/publication/319964644
30. Sudarmadji, T. (2001). *Impact of logging and forest fires on soil erosion in tropical humid forest in Kalimantan*. *November 1999*, 35–44. http://www.cifor.cgiar.org/Knowledge/Publications/Detail?pid=934
31. Takei, A., Kobashi, S., & Fukushima, Y. (1981). Erosion and sediment transport measurement in a weathered granite mountain area (Tanakami region, Japan). Erosion and Sediment Transport Measurement. Proc. Florence Symposium, June 1981, (International Association of Hydrological Sciences, IAHS-AISH Publication 133), 133, 493–502.
32. Trigila A., Iadanza C., Lastoria B., Bussettini M., Barbano A. (2021) Dissesto idrogeologico in Italia: pericolosità e indicatori di rischio - Edizione 2021. ISPRA, Rapporti 356/2021
33. Van der Knijff JM, Jones RJ, Montanarella L (1999) Soil erosion risk assessment in Italy. European Soil Bureau, Joint Research Center of the European Commission. Scientific-Technical Reports, EUR 19044 EN, 34 pp.
34. Wischmeier, W.H. and Smith, D.D. (1978) Predicting Rainfall Erosion Losses. A Guide to Conservation Planning. The USDA Agricultural Handbook No. 537, Maryland.

2. A proposal for modifying coppicing geometry in order to reduce soil erosion (research article).

Bartolomeo SCHIRONE[1]*, Pietro SALVANESCHI[1], Kevin CIANFAGLIONE[2], Massimo PECCI[3], Teodoro ANDRISANO[4], Federico VESSELLA[1], Andrea PETROSELLI[5]

1 Tuscia University, Department of Agriculture and Forest Sciences (DAFNE), San Camillo del Lellis s.n.c., 01100 Viterbo, Italy; schirone@unitus.it (*corresponding author); salvaneschi@unitus.it; vessella@unitus.it
2 Université de Lorraine, Faculté des Sciences et Techniques, UMR UL/AgroParisTech/INRAE 1434 Silva, BP 70239, CEDEX 54506 Vandoeuvre-lès-Nancy, France; kevin.cianfaglione@univ-lorraine.fr
3 Department of Regional Affairs and Autonomies (DARA) – Presidency of the Council of Ministers, Via della Stamperia 8, 00186 Rome, Italy; m.pecci@palazzochigi.it
4 Majella National Park, Via Badia 28, 67039 Sulmona, Italy; teodoro.andrisano@parcomajella.it
5 Tuscia University, Department of Economics, Engineering, Society and Business Organisation (DEIM), 01100 Viterbo, Italy; petro@unitus.it

---

Abstract

A key factor to reduce soil erosion and soil instability is the conservation of forest areas. In the last years, in all Europe, forest logging has increased. The Italian situation is paradigmatic because more than 70% of the broadleaved forests are managed as coppices and new exploitations concerning biomass for energy production have tripled since 2001. The common coppicing method leaves standards uniformly distributed on the ground, but this geometry has proven to not play an effective role in soil erosion control. In this paper, we propose a different method for coppicing geometry, aimed to decrease the soil erosion risk. In particular, the theoretical framework of the model is presented here, employing the USLE framework and discussing a real case study, while the results of the experimental tests, which are in progress, will be discussed in future papers. The theoretical results seem to demonstrate the method's validity, which is expected to reduce soil erosion amount in the range 29%-42%.

Keywords: Coppice; mountain slopes; soil erosion; standards; barriers

---

Introduction

Italy is one of the European countries with the highest value of hydrogeological instability due to natural and anthropogenic causes: more than 300 people died in the last 10 years in Italy due to this problem (Trigila et al. 2018). The hydrogeological risk could become more frequent in the next years because of the climate changes that should modify the precipitation regime, causing an increase of intense rainfall events with a very short duration. From projections of the Regional Climate Models for Europe, in the future, higher rainfall intensities and longer dry periods are generally expected (EEA 2017). Considering the projections related to a future period in Italy (until 2090), a decrease of the annual cumulative rainfall value, a modest increase of the annual maximum daily rainfall, and a significant increase of the time interval between two consecutive rainfall events should occur (Desiato et al. 2015).

A key factor to reduce soil erosion and hydrogeological instability is the conservation of forest areas, that is the object of this paper. Indeed, it is well known that forests exercise a protective action on soil (Borrelli et al. 2017a; Nikolic et al. 2018). The efficiency of soil protection by forest is due to the forest coverage. In general, every interruption of the forest coverage causes a reduction on the capacity to intercept the rainfall by the tree canopies with a consequent increase of soil erosion. However, this could be mitigated by the adoption of particular silvicultural treatment (Altieri et al. 2018; Iovino 2009). According to Ceccherini *et al.* (2020) in the last ten years, in all Europe, logging is increased, with an increase of 49% for the harvest surface and of 60% for the biomass exploitation. The mean area of the harvested patch size is becoming bigger; for instance, in Italy the increase reached +125%, that was the highest value in Europe after Portugal (Ceccherini *et al.*, 2020). The Italian situation must be highlighted because more than 70% of the broadleaved forests are managed as coppice and new utilizations concerning biomass for energy production are tripled since 2001 (Eurostat, *https://ec.europa.eu/eurostat/web/energy/data/energy-balances*). Additionally, the last national policy on forests risks to aggravate the situation, promoting the tampering and the exploitation of forests, rather than encouraging natural dynamics (Bottacci, 2018; Searchinger et al. 2018).

The effects of this forest policy are already evident: in the last years, the area of a single coppicing could reach even 20 ha on very steep slopes, hence it is crucial to mitigate the damages of these larger and more frequent coppicing. Coppice management activities modify indeed the soil structure and the biodiversity affecting the successional processes, reducing progressively the soil quality by a frequent rejuvenation of pedological profiles, and, in general, rapidly increasing the superficial soil erosion due to the frequent cuttings (the rotation period typically is lower than 25 years) (Clauser 1989; Borrelli et al. 2017b; Vacca et al. 2017). Thinking about that, we should start considering new approaches in coppicing, with the aim to reduce soil erosion without decreasing biomass production.

The prevalent coppicing method in Italy is the “coppice with standards” and the word “matricinatura” is used to indicate both the number and the type of standards (“matricine” in Italian language) per surface unit. In this work, we will use the term Standards Arrangement (SA) for indicating such system. According to the classic silviculture, the number of standards per hectare is variable, but the range should be between 80 and 120 per hectare (with a minimum of 30 for some species), so that the soil that remains covered after a cut typically does not exceed 10% of the total area.

Usually, the standards are scattered on the ground (Scattered Standards Method, SSM), although several studies propose alternative solutions to limit the inconveniences of such distribution. For example, the distribution of standards in groups (Grouped Standards Method, GSM) would guarantee a lower impact on the landscape and more ecological benefits, especially for nemoral species (Grohmann et al. 2002).

After a coppice cutting, standards are left mainly because they should be useful to: a) progressively substitute old stumps with plantlets; b) promote the conservation of genetic diversity; c) keep safe soil coverage and reduce soil erosion (Piussi 2000). Notwithstanding, it has been demonstrated that standards do not significantly play a role in any of those functions, while it has been shown that they depress the generation of new shoots on stumps (Amorini et al. 1998; Bianchi and Giovannini 2006). Actually, the SSM is the heritage of an old coppicing practice that included the saving of some adult trees useful to guarantee not only firewood but also lumber (Zanzi Sulli and Di Pasquale 1993).

Despite a frequent occurrence of coppices, Italian studies on relationships between coppicing and soil erosion are scarce. There is a lack of studies about forest coverage before and after a cutting, although soil use is a key factor for methods that aim to estimate the soil erosion. On the contrary, many investigations focus on SA density: the main goal is always the search for the optimal number of standards to be left, according to the target species and local environmental conditions, in order to guarantee the wood production (Corona et al. 1986; La Marca et al. 1987; La Marca et al. 1996).

Among the authors who studied soil erosion in coppices, Garfì et al. (2006) and Iovino (2007) recommend some actions to limit soil erosion such as:

- To distribute cuttings in space to guarantee continuity.
- To limit the surface cutting width according to slope.
- To increase the time interval between two consecutive cuttings.
- To perform cuttings avoiding an overlap with periods of maximum precipitation.

- To implement some practical procedures to significantly mitigate the impact of coppicing.

In the present paper we aim to explore this last point, not discussed by Iovino (2007), investigating how to reduce soil erosion by modifying the geometry of SA. The novelty of the manuscript is in the presentation of a new method for determining the geometry of coppicing. Here we show the theoretical framework, while an experimental research is already in progress and will be discussed in future papers. The final goal will be to observe how much the model differs from reality. In this way the model could be improved and calibrated using experimental data.

Materials and Methods

The proposed theoretical model: Bands of standards

After a cutting, erosion usually occurs inside a forest patch. The erosion is more intense as the patch is longer in the downslope direction, the slope is greater, and the forest cover is diminished (Borrelli et al. 2017a). In view of this, we propose a new method of SA related to coppices located in high slope areas, where, typically, cuttings occur with the longer side parallel to the steepest slope direction.

The proposed method is a coppice with bands of standards (Banded Standards Method, BSM), instead of SSM or GSM (Figure 2.1). It consists of leaving standards stripes perpendicular to the steepest slope direction, instead of leaving standards that are scattered all over the area. The proposed method aims in creating a barrier for surface runoff. Indeed, after a traditional coppicing, the residual forest cover ranges between 10% and 20% and the effect of standards on surface runoff is very limited because of their spread diffusion. The same percentage of standards, but clustered in bands parallel to contour lines, could be more efficient with a positive effect on soil erosion due to the cutting geometry.

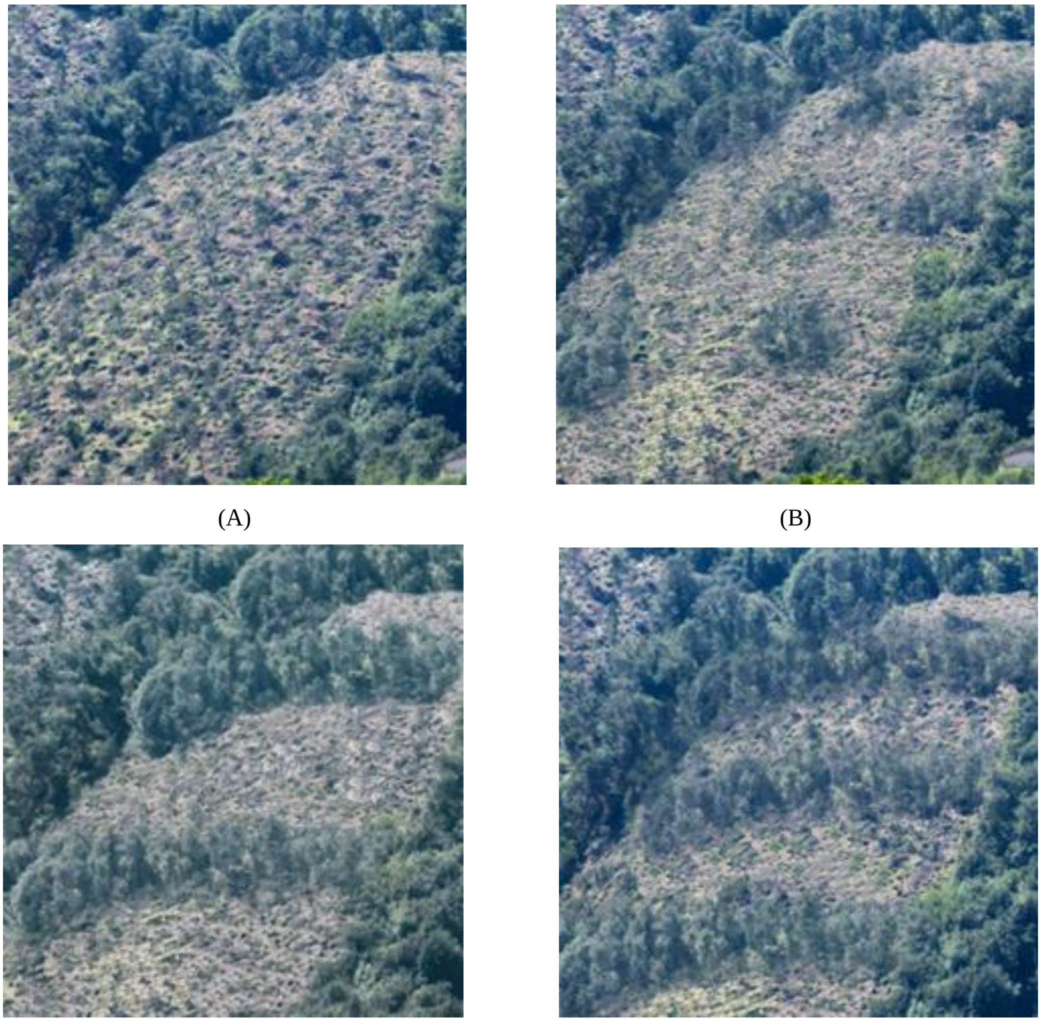

Figure 2.1. Rendering of different types of standards arrangement (SA). (A) Coppice with SSM; (B) Coppice with GSM; (C) Coppice with BSM, two bands; (D) Coppice with BSM, three bands.

Site description

The study site has been selected due to its representativeness for the Central Apennine forests where there are frequent degraded coppices that should be left to natural evolution and, instead, continue to be regularly cut. The investigated area pertains to Colle Tavola hill (Municipality of Rieti, Figure 2.2), it is characterized by an average elevation of 970 m, an average slope of 55%, and it is south-east oriented.

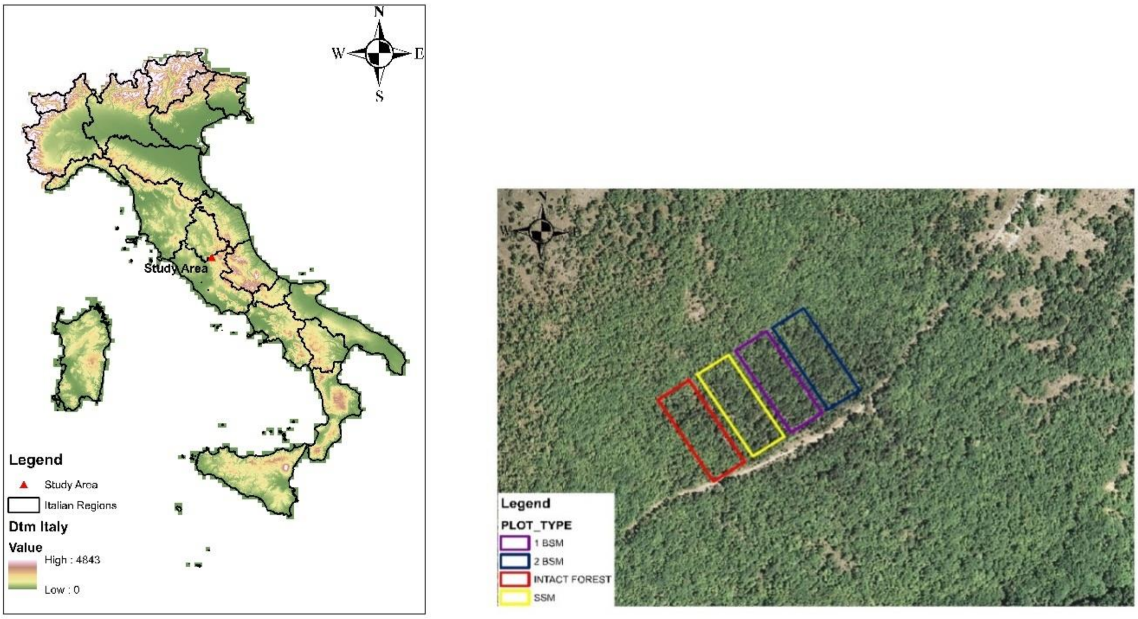

(A) (B)

Figure 2.2. Study site localization. (A) national level. (B) local level.

Regarding the climate, temperature and rainfall data were retrieved from Colli sul Velino meteorological station, in proximity of the selected area. Bagnouls-Gaussen diagram, shown in Figure 2.3, defines the climate as typically Mediterranean, with dry summer and rainfall concentrated during autumn. This circumstance is noteworthy because regional laws prescribe that coppicing cutting to be carried out during autumn and winter periods, i. e. during the vegetation dormant season.

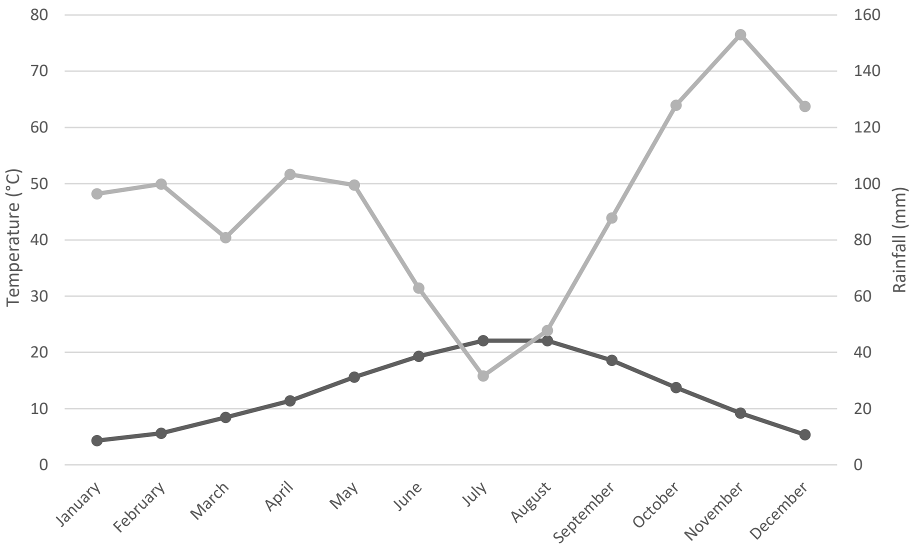

Figure 2.3. Bagnouls-Gaussen diagram of the study area.

Whit respect to geology, the geomorphological setting of the area is characterized by the outcropping of layers of micritic limestones (Facies *Maiolica* Auct.), sometimes densely stratified, fractured and weathered, with the presence of a fault, surveyed just few dozen meters downslope and out of the investigated area. Both surface and subsurface runoff flow from the top of Colle Tavola hill in south-east direction, where the fault line and the gully represent, respectively, the permeability threshold/spring of a perched aquifer and the local base level for runoff. The rock mass quality, after a geological-technical survey, can be expressed as "fair" (Beniawski 1976; Amanti and Pecci 1995).

The soils belong to unit H4e of the Lazio region Soil Map (Napoli et al. 2019) and, precisely, they are *Rendzic Leptosols*. These soils, originated from marl and limestone substrate on steep slopes (> 35%), are very thin and generally thicker from the top to the bottom of the hillslope, as in the case of the investigated area where the soil depth ranges between 10 and 25 cm. Soils tend to be sandier on their surface, and more clayey in the underlying horizons. In the same way, the soil pH is neutral on the top, and slightly alkaline in depth. Typically, the skeleton is quite abundant, with coarse fragments which are strongly calcareous on the upper level and become lesser calcareous at lower layers. These soils are usually well-drained. The laboratory analysis gave the following average values: pH from 7.2 to 7.8; sand 66.05%; silt 16.025%; clay 17.925%; Total Organic Carbon (TOC) 9.9 %; Soil Organic Matter (SOM) 17.1%. In such geo-pedological conditions, the soil is preserved only thanks to the forest cover. In case of forest coppicing soil, accelerated erosion occurs and even irreversible deforestation is possible. In that case, re-forestation becomes the unique solution for the vegetation recovery.

Concerning the vegetation type, the forest could be included into *Cyclamino hederifolii-Quercetum ilicis*. The forest is located on a gradient where *Quercus ilex* L. and *Q. pubescens* Willd. tend to cross each other. In particular, these plant communities, present on hills and mountains of Central Apennine, are relic of past hotter climate conditions, so they are quite different from the typical Mediterranean *Q. ilex* forests, lacking the most thermophilic species (Cianfaglione 2015). Moreover, morphology, spatial structure and dynamics of the studied community are strongly determined by the coppice degenerative or regressive effects (Pedrotti 2013).

The canopy covers around 85% of the surface, consisting mainly of *Q. ilex*, with a large participation of *Q. pubescens*. The canopy composition is completed by *Ostrya carpinifolia* Scop., some maple species (*Acer opalus* Mill., *A. campestre* L., *A. monspessulanum* L.), *Fraxinus ornus* L., *Carpinus orientalis* Mill., *Juniperus deltoides* R.P.

Adams, *Aria edulis* (Willd.) M.Roem. and *Ilex aquifolium* L., this last with sporadic individuals. Plant species nomenclature follows the "Plants of the World" Kew Science database (*http://powo.science.kew.org/*) and syntaxonomical nomenclature follows the prodrome of the vegetation of Italy (*http://www.prodromo-vegetazione-italia.org*). Trees have a maximum age of about thirty years, approximately. Their average diameter is 8 cm, with maximum diameters equal to 17 cm. The average height of the canopy is 6 m, with a maximum height of dominant trees of about 12 m. The largest trees are mostly *Quercus ilex*, and they correspond to the standards left during the last cutting.

Stand structure

For this research, inside the study site, a 3000 m^2 plot (30 m according to the contour lines and 100 m according to the steepest slope direction) has been delimited. The forest canopy covers around 85% of the plot. Within this plot the plants were distinguished into stumps (with shoots), standards and shoots. Then, species, types, position, and diameters of all the plants were detected. For all the stumps, the number of shoots has been counted and their diameters were measured. Using Lidar data (*http://www.pcn.minambiente.it/mattm/visualizzazione-metadati/?keyword=&rid=&paged_e=12*), the average height of the trees has been first calculated and then validated in the field using a Nikon Forestry Pro hypsometer. Since the crowns of the trees intersect each other, it is impossible to detect the crown area of single trees. So, this value has been estimated by dividing the total canopy area by the number of stems, also taking into account the number of standards with respect to the total number of plants. The results were validated by comparison with some plants of a recently coppiced stand.

Soil erosion calculation

Erosion has been estimated in four different situations: intact forest (case 1), forest with SSM (case 2), forest with one band of standards (1BSM, case 3), and forest with two bands of standards (2BSM, case 4).

Due to its easy employment, in terms of calculation and reduced requirement of input data (Benavidez et al. 2018), in order to estimate the soil erosion we used the Universal Soil Loss Equation - USLE (Wischmeier and Smith 1978). USLE is one of the most common equation used for erosion amount assessment (Van Der Knijff et al. 1999; Diodato 2004; Grauso et al. 2015), and is expressed as it follows:

$$A = R \times K \times L \times S \times C \times P \quad (1)$$

where:

A = Annual soil erosion (t/ha/year),

R = Rainfall erosivity factor (MJ*mm/ha/h/year),

K = Soil erodibility factor (t*h/MJ/mm),

L = Length factor (-),

S = Slope factor (-),

C = Soil coverage factor (-),

P = Erosion control measures factor (-).

The R factor for a given considered period is obtained by summing, for each rainstorm, the product of total storm energy (E), expressed in MJ/ha, and the maximum 30-minute intensity (I_{30}), expressed in mm/min, (Van Der Knijff et al. 1999). Because of the difficulty to get such high-resolution data, during the years several empirical formulas have been proposed as alternative, aiming to express R factor using monthly or annual cumulative rainfall values. Among them, we adopted the Torri formula (Torri et al. 2006), as expressed below:

$$R = (3.08 \times P) - 944 \quad (2)$$

With P = total annual rainfall (mm).

It is noteworthy that more accurate estimations could be obtained using the formulas based on the six hours rainfall amount with 2 years return period. Previous eq. (2) has been chosen because of its simplicity and because it has been developed for the Italian climate. The total annual rainfall has been calculated thanks to the data collected from the Colli sul Velino raingauge station.

The K factor is soil erodibility factor. It takes into account the soil properties during a rainfall event, and it has been retrieved, starting from the soil analysis of the study area, with KUERY 1.5 software (Borselli et al. 2012). The software uses an algorithm that calculates K factor values: after having defined the climate type and the rock fragment volume, it is possible to calculate K factor value from the basic information of the soil analysis (percentages of loam, sand, clay, and organic material).

L and S factors measure the influence of the topography on the soil erosion. Longer and steeper is the hillside, higher is the erosion. L and S Factors were assessed using the Morgan formula (Morgan 2001).

$$LS = LxS = \left(\frac{l}{22}\right)^{0.5} (0.065 + 0.045s + 0.0065s^2) \quad (3)$$

$$L = \left(\frac{l}{22}\right)^{0.5} \quad (4)$$

$$S = (0.065 + 0.045s + 0.0065s^2) \quad (5)$$

Where:

l is the runoff length (m) and s is the hillside slope (%). Slope data were taken from slope Lidar map of the study area.

C factor is related to the capacity of vegetation cover to mitigate soil erosion. In this study, we used, respectively, data from Wischmeier and Smith Manual (Wischmeier and Smith 1978) to asses C factor in a "not disturbed forest" situation (trees inside the study area has an average age of 30 years) and in a "just logged forest" situation (forest with a 20-40% canopy cover). Although there are different and more sophisticated methods to calculate C factor such as using NDVI or Corine Land Cover, for this theoretical model we preferred to adopt the original Wischmeier and Smith formulation, because of its simplicity and its wide use.

Finally, P factor is related to the cultural practices aiming to reduce the soil erosion. Since in forestry this factor is typically not used, we used P factor equal to 1 as mentioned in the Wischmeier and Smith Manual (Wischmeier and Smith 1978) even if it is possible that our practice can have also an effect on this factor, but this is impossible to check until field studies will progress.

Results

Stand structure and bands design

As results from the field surveys, 424 plants were counted: 383 stumps with 3-4 shoots each and 41 standards. All the results are reported in Table 2.1.

The Forest Management Plan of the Rieti Municipality, having jurisdiction over the study area, imposes to preserve 90 standards per hectare at the end of each rotation. One third of these trees should have an age equal to or greater than twice the rotation period that is 24 years. So, this is the number of trees to be counted in order to build the bands. Considering the plot of 3000 m^2, after the cutting there should be 27 standards, 9 of them with an age equal to twice the rotation. Multiplying the number of plants by their crown areas it has been found out that they should occupy 156m^2. Therefore, inside the plot it would be possible to make one 150 m^2 band, 5 m long according to the steepest slope direction, 30 m large according to the contour lines, and distant 50 m from the next band upward and downward according the steepest slope direction. As an alternative, it would be possible to make two bands having 2.5 m long in the steepest slope direction, 30 m large according to the contour lines, and distant 33 m each one in the steepest slope direction. Figure 2.4 shows the theoretical map of the plot in the four mentioned cases where the larger and thicker circles represent the standards. Regarding 1BSM (case 3), the band was put in the middle of the plot (50m far from upper and lower sides), meanwhile for 2BSM (case 4) the plot was divided in three zones, putting the two bands at 33 and 66 m from uphill.

Table 2.1. Case study field survey results

	STUMPS	SHOOTS	STANDARDS	STEMS
N	383	1693	41	1734
N/ha	1283	5643	137	5780
N/stump	-	4.42	-	-
Diameter (cm)	-	6.72	17	7
Height (m)	-	6.1	9.2	-
Crown area (m^2)	-	9688	372	10061
Crown area/tree (m^2)	-	5.72	9.1	5.8

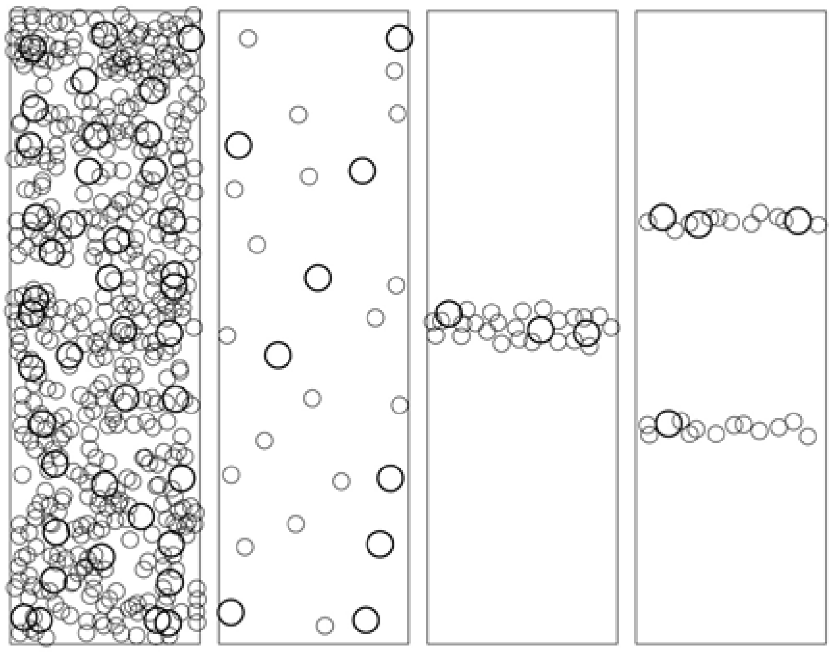

Figure 2.4. Coppicing methods from left to right: intact forest (case 1), SSM (case 2), 1BSM (case 3), 2BSM (case 4).

USLE factors values

L and S factors

As we mentioned before, L and S factors depend on the runoff length of the study area and on its slope. In case 1 (intact forest), computing L factor, we considered the length of our area as 100 m, so L = 2.126. The same result was also obtained for case 2 (SSM). Since the bands should create a barrier for the surface runoff, regarding case 3 (1BSM) and case 4 (2BSM), we choose to consider the length of the study area as 50 m for case 3 and 33 m for case 4. We obtained L factor values of 1.503 for case 3 and of 1.227 for case 4. The investigated study area has an average slope equal to 72%, and since the silvicultural operation will not affect the slope of the hillside, the S factor value does not change for all the cases. The obtained value is equal to 37.

C factor

C factor is one of the most variable factors in the USLE equation. It depends on the land use and on the land cover. In forestry environment C factor depends on the forest type, canopy, and stage (age). For our study we choose to use C factor values related to mature dense forest for case 1, while for all the other cases we assumed C factor values related to forest with 20% of area covered by canopy. So, for case 1 we used the C value of 0.0005 and for the other cases a C value of 0.009 (Wischmeier and Smith 1978). As aforementioned, for the C values estimation we used the USLE original tables.

K factor and R factor

K and R factors do not change depending on the coppicing methods because they refer to soil and rainfall. They are respectively equal to 0.016 t*h/MJ/mm for K, and 2533.7 MJ*mm/ha/h/year for R.

P factor

As it was mentioned before we set a P factor value equal to 1 for each study case.

Applying the USLE equation, we got an annual average soil erosion value of 1.6 $t*ha^{-1}*y^{-1}$ for case 1, a value of 28.9 $t*ha^{-1}*y^{-1}$ for case 2 (SSM), a value of 20.4 $t*ha^{-1}*y^{-1}$ for case 3 (1BSM) and finally a value of 16.7 $t*ha^{-1}*y^{-1}$ for case 4 (2BSM) (Table 2.2). Figure 2.5 offers an immediate information about the influence that the coppicing method has on the soil erosion. As we can observe from Table 2.2 and from Figure 2.5a every time that a forest is logged, independently from the chosen silvicultural method, the soil erosion rate strongly increases. Indeed, the soil erosion increase is about 1718% between case 1 and 2, about 1186% between case 1 and 3 and, finally, about 950% between case 1 and 4 (Table 2.3, Figure 2.5b).

Concluding, we calculate the soil erosion reduction percentage between the traditional coppicing method (SSM) and the proposed methods (1BSM, 2BSM). The soil erosion rate reduction between SSM and 1BSM is 29%, while between SSM and 2BSM is 42% (Table 2.3, Figure 2.5c).

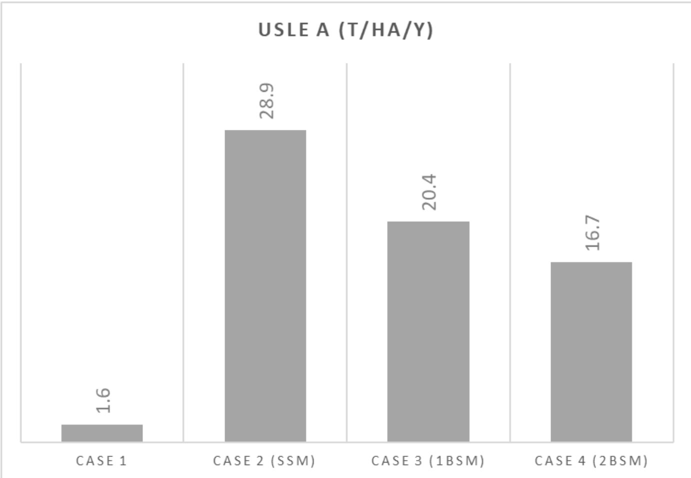

(A)

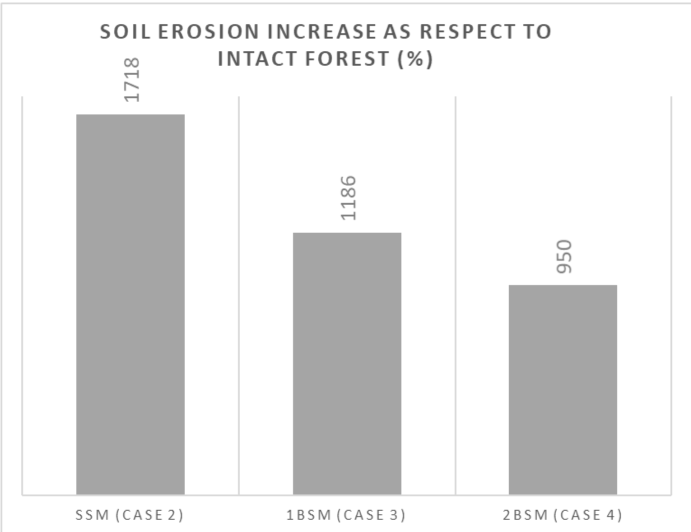

(B)

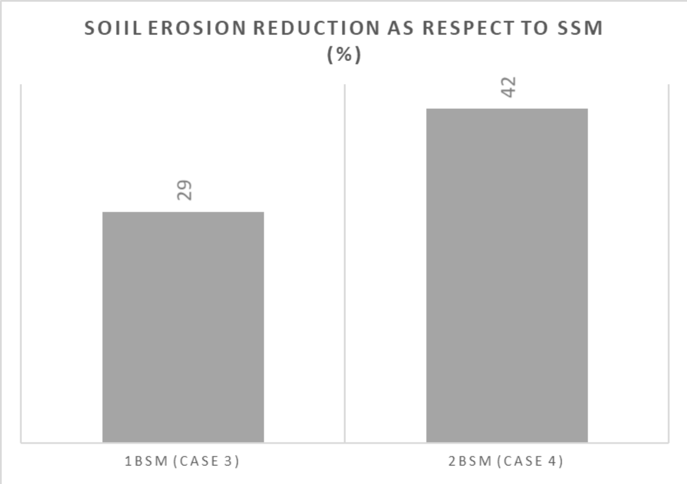

(C)

Figure 2.5. (A) Annual soil erosion; (B) percentage increases of soil erosion for cases 2-3-4 as respect to case 1 (intact forest); (C) percentage decreases of soil erosion for cases 3-4 as respect to case 2 (SSM).

Table 2.2. USLE calculation results

	USLE FACTORS VALUES, **INTACT FOREST (CASE 1)**	USLE FACTORS VALUES, **SSM (CASE 2)**	USLE FACTORS VALUES, **1BSM (CASE 3)**	USLE FACTORS VALUES, **2BSM (CASE 4)**
L FACTOR	2.13		1.5	1.23
S FACTOR	37			
C FACTOR	0.0005	0.009		
K FACTOR	0.016			
P FACTOR	1			
R FACTOR	2533.70			
USLE A (t/ha/y)	1.6	28.9	20.4	16.7

Table 2.3. Variations in soil erosion due to the proposed coppicing methods

	SSM (CASE 2)	**1BSM (CASE 3)**	**2BSM (CASE 4)**
ANNUAL MEAN SOIL EROSION (t/ha/y)	28.9	20.4	16.7
SOIL EROSION INCREASE AS RESPECT TO INTACT FORES (%)	1718	1186	950
SOIIL EROSION REDUCTION AS RESPECT TO SSM (%)	-	29	42

Discussion

In Italy, the relationship between silviculture and soil erosion has not been fully explored up to now. Even the guidelines for the evaluation and the mitigation of hydrogeological risk, published by ISPRA (the Italian national institute for protection and research of the environment), are extremely scarce in the topic (Bazzoffi et al. 2013). As concerns the coppice with standards, comparisons on the amount of soil erosion associated with the traditional SSM and more recent GSM have not even been performed.

Regarding the method here proposed (BSM), it is important to say that, in the past, there were few scientific articles (characterized by a limited diffusion) that proposed to leave the standards in stripes along the contour lines (Del Favero 2001; Bernetti and La Marca 2010). Such articles refer to the possibility of using this method only for the reduction of the damages due to rocks falling after a cutting, circumstance that indeed the stripes of standards could avoid or mitigate. Unfortunately, none of the aforementioned works regards soil erosion neither tries to calculate the amount of soil erosion as a result of this type of arrangement.

However, the results of our conceptual model seem to confirm the validity of this approach and justify the field experiments, in order to verify the theoretical model. In fact, the reduction of erosion in the examined investigated area varies from 29% to 42% depending on the number of bands left on the field. It is important to mention also that the method presented here acts, substantially, only in the Factor L, diminishing the length of the hillslope that is exposed to the erosive process.

In addition, C Factor has its impact on the reduction of soil erosion, that here we did not calculate. It is evident that if trees are not present on the ground, the rainfall can directly fall on the soil surface creating soil erosion. In a forest, the C factor can be approximated with the capacity that the trees have, thanks to their canopies and ground cover (litter, organic residues etc.), to absorb the rainfall impact and to diminish the splash effect. Regarding C Factor, with the theoretical method that we used, it was impossible to distinguish between the two types of cutting (SSM or BSM), because of the same number of trees left, with same age and same canopy. This is the reason why the C factor has the same value in both cases. It is clear that a forest canopy formed by the intersection of multiple tree crowns, as in BSM, even if it consists in the same number of elements with equal dimensions, will intercept a bigger rainfall volume in comparison with the sum of the single crowns of the scattered trees. Moreover, in this model, we are aiming to implement another practical solution that will help reducing soil erosion. When a coppice logging is carried out, after the extraction of tree trunks, typically, forest workers leave bundles of twigs in windrows along the steepest slope direction because this disposition is easier for their work. This material can be left in site for a natural degradation, sometimes enhancing the risk of forest fires, or it can be removed or chipped.

If such material would be placed near the bands of standards, following the contour lines, a natural weir would be created, creating a natural barrier to overland flow, limiting the soil erosion and enhancing the growth of new plants. This was demonstrated inside Majella National Park, using wood barriers inside pine-beech forest (Figure 2.6).

(A)

(B)

Figure 2.6. Examples of coppice with bundles of twigs in windrows and natural regeneration by seed (A) Coppice with bundles of twigs in windrows along the steepest slope direction; (B) Natural regeneration by seed along a logs weir.

In any case, leaving unaltered the number and the type of standards and changing only their positioning inside the logged area, the BSM will not affect the wood extraction. In fact, every forest operation (logging and extraction) would not be complicated.

In addition, this silvicultural operation would bring other numerous ecological, technical, and economical advantages. On the ecological point of view, there would be a significant reduction on the loss of biodiversity, both vegetal and animal. Because of the wide exposure of the bare soil, every time that a coppice is logged with the traditional SSM, the conservation of nemoral flora, linked to a more evolved forest succession, is irreparably lost. The plant community regresses towards the pioneer stages and the vegetation cycle starts again from zero. Some species could also definitely disappear. Baragatti et al. (2002; 2004) compared the composition of the flora and the vegetation dynamics inside different Turkey oak (*Quercus cerris* L.) coppices with different typologies and densities of SA: with no standards, with a limited number of scattered standards (50 plants/ha), with a high number of scattered standards (140 plants/ha) and, finally, with standards disposed in groups (GSM). The results of the study showed that the coppice with GSM is the one that can assure both the greater floristic and vegetational diversity and the conservation of all the nemoral species, thus confirming even for the coppice the Peterken (1999) models on the relationships between forest area size and biodiversity. In our proposed method, leaving unaltered the floristic composition of the stripes, so that they can be considered as small groups, the result should be similar.

The perspective for the fauna component is not different. Most of vertebrate or invertebrate animals can continue to find shelter and refuge (home, alimentation, and reproduction) inside and along the standard stripes where the vegetation is still undisturbed. With reference to Italian coppices, this has been demonstrated using GSM by Capizzi and Luiselli (1996) for rodents, and by Battisti and Marini (2018) for the ornithofauna, that seems to be particularly sensible to the forests changing, both in species richness and in individual numbers. As concerns the invertebrates, many insects' species benefit from the forest cutting thanks to the pioneer herbaceous flora that grows in the soil with no trees, but, on the other hand, there will be less species related to the mature stage of the forest (Greatorex-Davies and Marrs 1992; Buckley and Mills 2018). The coppice with BSM allows the creation of habitats useful to the conservation and the increase of biodiversity in both senses. Finally, the bands of standards permit the conservation of the biotic component that lives in the soil (fungi, bacteria, nematodes, and so on) that for long time has not been considered but nowadays it has been proved to be essential for the entire life on planet, which it is revealing more and more its symbiotic nature (Sheldrake 2020).

The BSM, in comparison with SSM and GSM, can work exactly as an ecological corridor that crosses the logged surface and connects the undisturbed parts of the forest. In this way, it guarantees the continuity of animal movement inside the forest and the vegetal species gene flux (Battisti and Romano 2007).

Moreover, this silvicultural model improves the forest natural regeneration by seed because the shadow of adult trees reduces the competition between pioneer herbaceous plants and seedlings and improves the natural processes of seedling mycorrhization (Figure 2.6b).

Another positive effect of BSM is given by the reduction of the wind effect. Plants in group can better withstand the wind (and snow) pressure and they can protect from the wind action the young suckers and shoots. The BSM, in fact, constitute real windbreaks, able to reduce the wind speed and therefore the damages that it can produce, both directly, as mechanical damages, and indirectly, through the increase of evapotranspiration in countries with drier climate (Cleugh 1998).

Forests have an ecological role on the planet that is often overlooked or underestimated. We refer to the production of liquid water through the interception of droplets of condensed water vapour contained in the air (Sheil 2009, 2014; Santamarta-Cerezal et al. 2012; Ellison et al. 2017; Jarimi et al. 2020;). The intensity of such process depends on the site characteristics, but it is also proportional with the density of trees, their height, and their position. For these reasons, the BSM, in addiction to acting as a windbreak, can increase the capacity to capture atmospheric water that will improve the water availability in the coppice stand and consequently the soil fertility. This process can be crucial in the future considering the climate change context and an always more frequent aridity.

In addition, at silvicultural level, the BSM could offer many advantages. Shoots which resprout from the stumps after the cutting would not suffer the shadow created by the standards (the shadow is concentrated only along the stripes) so that their volume increase would be higher and faster. In such circumstance the foresters could avoid searching compromises on the number of standards per hectare, circumstance that up to now has not unique solution (La Marca 1991). Eventually there should be evaluation only for the sciaphilous species, but in this case some standards could also be left scattered in the logged surface to permit a better shadowing for that kind of plants. Conversely, the reciprocal proximity of the standards inside the bands will create conditions of major competition for the sunlight encouraging a higher and straighter height growth of the stems. For the same reason, in the stems we will observe a lower number of knots and in general less flaws so that a better technological quality and a resulting greater economic value could be retrieved (Bernetti et al. 2012).

This model will also help the conversion from coppice to high forest, as it happens in mixed conversion systems. The conversion could proceed on both sides of the bands and could interest the edges of the forest that are connected by the stripes, proceeding in concentric polygons. This solution belongs to forest restoration approaches in which the width of the bands, or in general the size of the areas covered by trees, is proportional to the success of the operations (Londe et al. 2021). Lastly, this approach could foster the new proposal about the so called "tree-oriented silviculture" (Bastien and Wilhelm 2000, 2003; Manetti et al. 2016).

Moreover, the bands hide better the view of the bare areas simulating a seamless covering of the slopes with a real improvement at the landscape level. Indeed, the reduction of the impact on the landscape is one of the reasons why some authors (ODARC 2004; Fiorucci 2009) are trying to promote the diffusion of GSM coppice instead of the traditional approach (SSM).

Finally, a particular case is represented by forest fires that are often followed by significant erosive phenomena on the steepest sides of mountains (Coschignano et al. 2019). Usually, a typical practice to limit soil erosion after fires is creating fascines along the contour lines. The stripes of standards, even if the upper part of the plant is burned, are living fascines that can ensure a greater soil retention and a better plants recovery or regeneration after a potential fire. They can therefore be effective against accelerated and extended erosive phenomena by reducing the risk coefficient and the need for emergency actions.

Conclusions

The coppice system with bands of standards (BSM), here presented, is very simple and the first simulation seems to be encouraging. It consists of leaving standards stripes perpendicular to the steepest slope direction, instead of the scattered ones all over the area, in order to make a barrier for surface runoff. Application of USLE equation showed that with respect to the scattered standards method (SSM), the BSM is able to reduce soil erosion amount in the range 29%-42%.

It must be underlined that this model can be assimilated to a clearcut on small surfaces logging method (Perrin 1954; Bernetti et al. 2012), and it is exactly like this. It is a simple coppice on small areas represented by the division of a large surface using a certain number of stripes of trees drawn along the hillslope contour lines, with the aim for the stripes to absorb all the runoff coming from the upper coppiced area. In some cases, this model could be a variation of the shelterwood system that is a silvicultural method in which cutting surfaces are alternated with untreated ones. The BSM, anyway, reflects the proposal of Buckley et al. (2018), and of the references cited therein, that on steeper terrain always recommend logging on very small surfaces, not wider than 0.5 ha.

The model was here presented and discussed from a theoretical point of view, and in the further step of the research, the effectiveness of the proposed system will be validated through field experiments keeping into account different environments and species. In particular, the best geometric layout of standards that may include linear bands, sinuous, discontinuous, alternate in groups, and so on will be investigated. The core of the experimental field campaign will be to assess whether these bands are able to absorb all the runoff coming from the upper coppiced area, confirming or not the theoretical model.

In order to avoid the not negligible damage caused by soil erosion, the introduction of bands of standards system can be an effective method to reduce drawbacks, conserve nemoral biodiversity and encourage forest restoration.

Authors' Contributions

Conceptualization: BS, TA, AP; Data curation: PS, AP; Formal analysis: PS, AP; Funding acquisition: BS, MP; Investigation: BS, PS, KC, MP; AP; Methodology: BS, PS, AP; Project administration: BS; Software: PS; Supervision: BS, AP; Writing - original draft: BS, PS, KC, MP, AP; Writing - review and editing: PS, FV.

Acknowledgements

This research has been financed by the Department for Regional Affairs and Autonomies (DARA), Presidency of the Council of Ministers, Rome. Number of Grant DARA-DAFNE 40506. We thank the Municipality of Rieti for having granted a parcel of its forest property to carry out the research.

Conflict of Interests

The authors declare that there are no conflicts of interest related to this article.

References

1. Altieri V, De Franco S, Lombardi F, Marziliano PA, Menguzzato G, Porto P (2018). The role of silvicultural systems and forest types in preventing soil erosion processes in mountain forests: a methodological approach using cesium-137 measurements. Journal of Soils Sediments 18(12):3378-3387. https://doi.org/10.1007/s11368-018-1957-8
2. Amanti M, Pecci M (1995). Proposta di una scheda per la raccolta e l'informatizzazione dei dati utili alla classificazione e caratterizzazione degli ammassi rocciosi. [Proposal for the creation of a database for the collection and computerisation of data for the classification and characterisation of rock masses]. Atti IV Convegno dei giovani ricercatori in geologia applicata, Riccione, Quaderni di geologia applicata, 1, 1-8, Pitagora Editrice, Bologna, Italy.
3. Amorini E, Bruschini S, Cutini A, Di Lorenzo MG, Fabbio G (1998). Intensity of standard release and shoots dynamics in a Turkey oak (Quercus cerris L.) coppicies. First contribution. Annali Istituto Sperimentale Selvicoltura Arezzo 27(1996):105-111.

4. Baragatti E, Frati L, Chiarucci A (2002-2004). Cambiamenti nella diversità della vegetazione in seguito a diversi tipi di matricinatura in boschi di cerro. [Changes in vegetation diversity as a result of different types of coppicing in turkey oak forests]. Annali Istitituto Sperimentale Selvicoltura 33:39-50.
5. Bastien Y, Wilhelm GJ (2000). Une sylviculture d'arbres pour produire des gros bois de qualité. [A tree silviculture to produce high quality wood]. Revue Forestière Française 5:407-424.
6. Bastien Y, Wilhelm GJ (2003). Selvicoltura d'albero: un approccio per la produzione di legname con buone caratteristiche e di grandi dimensioni. [Tree silviculture: an approach to produce good quality and dimension wood]. Sherwood–Foreste e Alberi Oggi 86:5-13.
7. Battisti C, Marini F (2018). Structural changes in bird communities before and after coppice management practices: a comparison using a diversity/dominance approach. Israel Journal of Ecology and Evolution 64:16-24. https://doi.org/10.1163/22244662-20181033
8. Battisti C, Romano B (2007). Frammentazione e connettività. Dall'analisi ecologica alla pianificazione ambientale. [Fragmentation and connectivity. From the ecological analysis to the environmental planification]. Città Studi Edizioni, Torino, pp 467.
9. Bazzoffi P, Ciccarese L, De Meo A, Di Leginio M, Fumanti F, Guerra P, … Trigila A (2013). Linee guida per la valutazione del dissesto idrogeologico e la sua mitigazione attraverso misure e interventi in campo agricolo e forestale. [Guidelines for the evaluation of the Hydrogeological risk and its mitigation trough measures and intervention in agriculture and forest field]. ISPRA. Manuali e Linee Guida 85/2013.
10. Benavidez R, Jackson B, Maxwell D, Norton K (2018). A review of the (Revised) Universal Soil Loss Equation ((R)USLE): With a view to increasing its global applicability and improving soil loss estimates. Hydrology and Earth System Sciences 22(11):6059-6086. https://doi.org/10.5194/hess-22-6059-2018
11. Bernetti G, Del Favero R, Pividori M (2012). Selvicoltura produttiva. Manuale pratico. [Productive silviculture. Practice manual]. Edagricole, Bologna, pp 225.
12. Bernetti G, La Marca O (2010). Il bosco ceduo nella realtà italiana. [Coppice forest in the italian reality]. Lettura tenuta il 21 ottobre 2010. Atti dei Georgofili, pp 44.
13. Bianchi L, Giovannini G (2006). Observations on the felling of standards in oak coppices, Central Italy. Forest 3(3):397-406. https://doi.org/10.3832/efor0390-0030397
14. Bieniawski ZT (1976). Rock mass classification in rock engineering. Proceedings Symposium Exploration for Rock Engineering. Johannesburg. Balkema 1:97-106.
15. Borrelli P, Panagos P, Märker M, Modugno S, Schütt B (2017a). Assessment of the impacts of clear-cutting on soil loss by water erosion in Italian forests: First comprehensive monitoring and modelling approach. Catena 149:770-781. https://doi.org/10.1016/j.catena.2016.02.017
16. Borrelli P, Robinson DA, Fleischer LR, Lugato E, Ballabio C, Alewell C, … Panagos P (2017b). An assessment of the global impact of 21st century land use change on soil erosion. Nature Communications 8(1):2013. https://doi.org/10.1038/s41467-017-02142-7
17. Borselli L, Torri D, Poesen J, Iaquinta P (2012). A robust algorithm for estimating soil erodibility in different climates. Catena 97:85-94. https://doi.org/10.1016/j.catena.2012.05.012
18. Bottacci A (2018). Il TUFF, la gestione attiva dei boschi e le generazioni future. [TUFF, active forest management and future generations]. Italia Forestale e Montana 73:4-5.
19. Buckley P, Mills J (2018). Conservation of Coppice and High Forest Management within the Natura 2000 Network – A Review. Chapter 4. In: Unrau A, Becker G, Spinelli R, Lazdina D, Magagnotti N, Nicolescu VN, Buckley P, Bartlett D, Kofman PD (Eds). Coppice Forests in Europe. Albert Ludwig University of Freiburg, pp 110-135.
20. Buckley P, Suchomel C, Moos C, Conedera M (2018). Prevention of Soil Erosion and Rockfall by Coppice and High Forest – A Review. Chapter 4. In: Unrau A, Becker G, Spinelli R, Lazdina D, Magagnotti N, Nicolescu VN, Buckley P, Bartlett D, Kofman PD (Eds). Coppice Forests in Europe. Albert Ludwig University of Freiburg, pp 139-151.
21. Capizzi D, Luiselli L (1996). Ecological relationships between small mammals and age of coppice in an oak-mixed forest in central Italy. Revue d'Écologie 51:277-291.

22. Ceccherini G, Duveiller G, Grassi G, Lemoine G, Avitabile V, Pilli R, Cescatti A (2020). Abrupt increase in harvested forest area over Europe after 2015. Nature 583:72-77. https://doi.org/10.1038/s41586-020-2438-y
23. Cianfaglione K (2015). On the potential of Quercus pubescens Willd. and other species of Quercus in the Camerino syncline (Central Italy). In: Box EO and Fujiwara K (Eds). Warm-temperate Deciduous Forests Around the Northern Hemisphere. Geobotany Studies. Basics, Methods and Case Studies. Springer Nature, Switzerland, pp 165-174. https://doi.org/10.1007/978-3-319-01261-2_9
24. Clauser F (1989). Povertà del bosco ceduo. [Poverty of coppice forest]. In: Biondi E (Ed). Il Bosco nell'Appennino: 83-98. Centro Studi Valleremita, Fabriano.
25. Cleugh HA (1998). Effects of windbreaks on airflow, microclimates and crop yields. Agroforest Systems 41:55-84.
26. Corona P, La Marca O, Schirone B (1986). Ricerche sull'ottimizzazione della intensità di matricinatura nei cedui di cerro:I – Il ceduo composto a maturità. [Research on the optimization of the intensity of the release of standards in turkey oak coppice: I-mature mixed coppice]. Annali Accademia Italiana Scienze Forestali 35:123-158.
27. Coschignano G, Nicolaci A, Ferrari E, Cruscomagno F, Iovino F (2019) Evaluation of hydrological and erosive effects at the basin scale in relation to the severity of forest fires. iForest-Biogeosciences and Forestry 12:427-434. https://doi.org/10.3832/ifor2878-012
28. Del Favero R (2001). Progetto Boschi del Parco Regionale dei Colli Euganei. [Project Forests of the Colli Euganei regional park]. Progetto Leader II – G.A.I. Patavino. Parco Regionale dei Colli euganei, Este (Padova).
29. Desiato F, Fioravanti G, Fraschetti P, Perconti W, Piervitali E (2015). Il Clima Futuro in Italia: Analisi delle proiezioni dei modelli regionali. [Future Climate in Italy: Analysis of the projections of regional model]. Edizione 2015. ISPRA, Stato dell'Ambiente 58/2015.
30. Di Fernando S, Marchetti A, Migliore M, Napoli R, Paolanti M, Pennelli B (2019). Atlante dei Suoli della Regione Lazio. [Latium region Atlas of soils]. Arsial, Regione Lazio, ISBN 978-88-904841-2-4.
31. Diodato N (2004). Estimating RUSLE's rainfall factor in the part of Italy with a Mediterranean rainfall regime. Hydrology and Earth System Sciences 8(1):103-107. https://doi.org/10.5194/hess-8-103-2004
32. EEA - European Environment Agency (2017). Climate Change Adaptation and Disaster Risk Reduction in Europe. EEA: Kongens Nytorv, Denmark 15:1-171.
33. Ellison D, Morris CE, Locatelli B, Sheil D, Cohen J, Murdiyarso D, … Sullivan CA (2017). Trees, forests, and water: Cool insights for a hot world. Global Environmental Change 43:51-61. https://doi.org/10.1016/j.gloenvcha.2017.01.002
34. Eurostat-European Statistical Office (2020). Eurostat. Retrieved 2021 February 14 from https://ec.europa.eu/eurostat/web/energy/data/energy-balances
35. Fiorucci E (2009) Le matricine nei boschi cedui: le attuali regole di rilascio sono ancora valide? [Standards in coppice forests: current rules are still valid?]. Forest@-Journal of Silviculture and Forest Ecology 6:56-65.
36. Garfì G, Veltri A, Callegari G, Iovino F (2006). Effetti della ceduazione sulle perdite di suolo in popolamenti di castagno della Catena Costiera Cosentina (Calabria). [Effect on the soil loss after coppicing in chestnut populations of the Cosentino Coast Chain (Calabria)]. L'Italia Forestale e Montana 6:507-531.
37. Grauso S, Verrubbi V, Zini A, Peloso A, Crovato C, Sciortino M (2015). Soil Erosion Estimate in Southern Latium (Central Italy) Using Rusle and Geostatistical Techniques. ENEA Technical Reports, RT/2015/22/ENEA.
38. Greatorex-Davies JN, Marrs RH (1992). The quality of coppice woods as habitats for invertebrates. In: Buckley GP (Ed). Ecology and Management of Coppice Woodlands. Springer, Dordrecht, pp 271-296.
39. Grohmann F, Savini P, Frattegiani M (2002). La matricinatura per gruppi. [Grouped Standards method]. Sherwood 80:25-29.

40. Iovino F (2007). Analisi dell'uso del suolo e linee operative di gestione forestale sostenibile per mitigare la vulnerabilità del territorio di Pizzo d'Alvano (Campania). [Use of soil analysis and operative guidelines for a sustainable forest management in Pizzo D'Alvano area (Campania)]. Quaderni del Laboratorio di Cartografia Ambientale e Modellistica Idrogeologica, Università della Calabria, Dipartimento Difesa del Suolo. Volume 2, pp 64.
41. Iovino F (2009). Ruolo della selvicoltura nella conservazione del suolo. [Silviculture role on the conservation of soil]. In: Atti del Terzo Congresso Nazionale di Selvicoltura (Taormina, 16-19 Ottobre 2008). Accademia Italiana di Scienze Forestali, Firenze, pp 425-436.
42. Jarimi H, Powell R, Riffat S (2020). Review of sustainable methods for atmospheric water harvesting. International Journal of Low-Carbon Technologies 15(2):253-276. https://doi.org/10.1093/ijlct/ctz072
43. La Marca O (1991). Studi e ricerche sull'ottimizzazione della matricinatura nei boschi cedui. [Study and research on the optimization of the release of standards in coppice forest]. Italia Forestale e Montana 2:118-132.
44. La Marca O, Marzialiano PA, Scotti R (1996). Effect of standard density on coppice structure development: evaluation 14 year after coppicing in a Turkey oak experimental trial. Annali Istituto Sperimentale Selvicololtura, Arezzo 27:161-166.
45. La Marca O, Mattioli M, Iorio G (1987). Ricerche sull'ottimizzazione della intensità di matricinatura nei cedui di cerro: II – Il soprassuolo arboreo nei primi due anni del ciclo produttivo. [Research on the optimization of the intensity of the release of standards in turkey oak coppice: The tree stand in the first two years of the production cycle]. Annali Accademia Italiana Scienze Forestali 36:3-33.
46. Londe V, Messias TBMC, Caldas de Sousa H (2021). Vegetation restoration is associated with increasing forest width. New Forests 52:129-144. https://doi.org/10.1007/s11056-020-09786-2
47. Manetti MC, Becagli C, Sansone D, Pelleri F (2016). Tree-oriented silviculture: a new approach for coppice stands. iForest-Biogeosciences and Forestry 9:791-800. https://doi.org/10.3832/ifor1827-009
48. Morgan RPC (2001). A simple approach to soil loss prediction: A revised Morgan-Morgan-Finney model. Catena 44(4):305-322. https://doi.org/10.1016/S0341-8162(00)00171-5
49. ODARC (2004). Guide pratique pour l'exploitation des forêts de chêne vert en Corse. [Practical guide for the exploitationof the holm oak forests in Corsica]. Office Développement Agricole Rural de Corse, Bastia, France pp 40.
50. Pedrotti F (2013). Plant and vegetation mapping. Springer, Dordrecht, pp 249.
51. Perrin H (1954). Sylviculture. [Silviculture. Ed. Ecole Nationale des Eaux et Forêts. Trad. ital. Selvicoltura, 1986. Accademia Italiana di Scienze Forestali. Firenze.
52. Peterken GF (1999). Applying natural forestry concepts in a intensively managed landscape. Global Ecology and Biogeography 8:321-328. https://doi.org/10.1046/j.1365-2699.1999.00140.x
53. Piussi P (2000). Selvicoltura generale. [General silviculture]. UTET, Torino.
54. Plant of the World http://powo.science.kew.org/
55. Searchinger TD, Beringer T, Holtsmark B, Kammen DM, Lambin EF, Lucht W, ... van Ypersele JP (2018). Europe's renewable energy directive poised to harm global forests. Nature Communications 9:1-4.
56. Sheil D (2009). How forests attract rain: an examination of a new hypothesis. BioScience 59:341-347. https://doi.org/10.1525/bio.2009.59.4.12
57. Sheil D (2014). How plants water our planet: advances and imperatives. Trends in Plant Science 19(4):209-211. https://doi.org/10.1016/j.tplants.2014.01.002

PAPER REFERENCE:

Schirone, B., Salvaneschi, P., Cianfaglione, K., Pecci, M., Andrisano, T., Vessella, F., & Petroselli, A. (2021). A proposal for modifying coppicing geometry in order to reduce soil erosion in the forest areas. *Notulae Botanicae Horti Agrobotanici Cluj-Napoca*, *49*(2), 12325.
https://doi.org/10.15835/nbha49212325

3. Comparative Evaluation of the Rainfall Erosivity in the Rieti Province, Central Italy, Using Empirical Formulas and Stochastic Rainfall Generator (research article).

Andrea Petroselli[1], Ciro Apollonio[2],*, Davide Luciano De Luca[3], Pietro Salvaneschi[2], Massimo Pecci[4], Tatiana Marras[2] and Bartolomeo Schirone[2]

1 Department of Economics, Engineering, Society and Business Organization (DEIM), Tuscia University, 01100 Viterbo, Italy; petro@unitus.it
2 Department of Agriculture and Forest Sciences (DAFNE), Tuscia University, 01100 Viterbo, Italy; salvaneschi@unitus.it (P.S.); tatianamarras@unitus.it (T.M.); schirone@unitus.it (B.S.)
3 Department of Informatics, Modelling, Electronics and System Engineering, University of Calabria, 87036 Arcavacata di Rende, Italy; davide.deluca@unical.it
4 Dipartimento per gli Affari Regionali e le Autonomie, Presidenza del Consiglio dei Ministri, 00100 Roma, Italy; m.pecci@palazzochigi.it
* Correspondence: ciro.apollonio@unitus.it

Abstract

Soil erosion caused by intense rainfall events is one of the major problems affecting agricultural and forest ecosystems. The Universal Soil Loss Equation (USLE) is probably the most adopted approach for rainfall erosivity estimation, but in order to be properly employed it needs high resolution rainfall data which are often unavailable. In this case, empirical formulas, employing aggregated rainfall data, are commonly used. In this work, we select 12 empirical formulas for the estimation of the USLE rainfall erosivity in order to assess their reliability. Moreover, we used a Stochastic Rainfall Generator (SRG) to simulate a long and high-resolution rainfall time series with the aim of assessing its application to rainfall erosivity estimations. From the analysis, performed in the Rieti province of Central Italy, we identified three equations which seem to provide better results. Moreover, the use of the selected SRG seems promising and it could help in solving the problem of hydrological data scarcity and consequently guarantee major accuracy in soil erosion estimation.

Keywords: soil erosion; soil loss; rainfall erosivity; R-factor; Rieti province; synthetic rainfall generator; USLE

Introduction

Soil erosion caused by intense rainfall events is recognized as one of the major problems affecting agricultural and forest ecosystems [1]. Heavy rainfall can indeed provoke phenomena such as shallow landslides, soil loss, pollution of water bodies and can decrease crop productivity [2]. Studies on soil erosion, aiming to select solutions for limiting the soil loss, are hence crucial for conserving and protecting the environment [3]. Since the first decades of the last century, they have increased in number and variety and, in recent years, the soil loss due to rainfall erosivity has been systematically analyzed [4].

Many mathematical models of soil erosion have been developed by the scientific community. One pivotal contribution can be represented by the studies of Wischmeier and Smith [5,6], which gave birth to the worldwide known Universal Soil Loss Equation (USLE), later rearranged in the revised USLE (RUSLE) [7,8]. USLE and its modifications are probably the most adopted approaches to estimate soil erosion.

The soil erosion caused by heavy rainfall occurs with the detachment of soil particles due to the impact of the raindrops and the subsequent downslope transport of the detached material [9]. This is a complex phenomenon that is a combination of different rainfall characteristics, such as intensity and duration, mass and diameter of rainfall drops, plus other factors depending on soil properties, e.g., topographic characteristics, and agroforestry practices.

Concerning rainfall erosivity, USLE expresses the impact of rainfall on soil loss using a rainfall erosivity factor, R. In the original formulation, the R-factor has been defined as the summation of the total storm energy (E) of an erosive rainfall event multiplied by the corresponding maximum rainfall intensity calculated at 30 min resolution (I30) within a certain period, for instance, one year [10]. The original method requires the use of continuous long-term and high-resolution rainfall data for its proper application, but unfortunately this kind of information is usually difficult to obtain due to the commonly reduced number and unequal spatial distribution of rain gauge stations where pluviographic data are available [11]. A second drawback is represented by the common lack of long-term high-resolution rainfall data [12], leading to a low availability of accurate R-factor values for many countries [13].

In order to overcome such drawbacks, the original R-factor calculation is often replaced by the use of empirical formulas, where simple pluviometric information, such as annual, monthly or daily rainfall amounts are present [14–16]. However, empirical equations should be applied with caution, because they are usually based on regressions among locally measured data and cannot be applied in larger areas [17]. Moreover, such formulas could not capture the high rainfall intensities, which usually occur at very short time scales and have a significant influence on rainfall erosivity [12]. Indeed, hydrological estimation measures in small and ungauged basins represent a challenging and open research topic for hydrologists [18].

Consequently, in this context of uncertainty, the use of Stochastic Rainfall Generators (SRG) appears helpful for a more in-depth analysis of rainfall-related processes, mainly for obtaining long rainfall time series which are representative of rainfall fields at hydrological spatial and temporal scales. The use of a SRG for rainfall-related processes analyses has been successfully tested in a wide variety of climatic conditions [19–23]. However, some works [24,25] showed that R-factors calculated using synthetic rainfall series often need to be calibrated due to systematic discrepancies of real R-factor values. Thus, we believe that the use of SRG should be more deeply investigated with the aim to assess their application to rainfall erosivity estimation.

Considering all the aforementioned, the aims of the manuscript are as follows:

1. To apply to a selected case study corresponding to the Rieti province, in Central Italy, a selection of empirical formulas for the estimation of the rainfall erosivity using the USLE approach, in order to assess the uncertainty in the rainfall erosivity estimation due to the specific empirical formula. The most appropriate empirical formulas will be assessed using a proposed index of reliability. It is noteworthy that the Rieti province, characterized by a mountainous environment and a rainy climate, is lacking an official R-factor map and an official rainfall erosivity estimation.
2. To apply, in one rain gauge station of Rieti province, a new and recently developed SRG, parsimonious in terms of input parameters. The application of the SRG allows the synthetic generation of a high-resolution time series that can be used for estimating the rainfall erosivity, employing the same empirical formulas of previous point 1), or using the original USLE formulation. Such application will allow assessment if the proposed SRG can be a suitable alternative for the estimation of soil erosion in case of rainfall data scarcity.

It is important to underline that the novelty of this work is represented by the use of the proposed SRG for rainfall erosivity estimation, and by the introduction of the index of reliability that gives the possibility to choose the most appropriate formula for each selected case study. Moreover, the definition of rainfall erosivity maps for the province of Rieti can be very important for land panning and management. Knowing the areas where a great R-factor value is supposed to be, can be helpful in localizing areas prone to soil erosion and hydro-geological risk.

The present manuscript is organized as follows: in Section 2, materials and methods are described. In particular, the paragraph describes the selected case study, reports the investigated formulas, and illustrates the proposed SRG. In Section 3, results are presented and discussed, while in Section 4 the conclusions are reported.

Materials and Methods

Study Area

The selected study area, shown in Figure 3.1, is the Rieti province, located in the Lazio region of Central Italy. The study area has an extension equal to 2749 km^2 and it includes 73 municipalities with a total number of inhabitants greater than 155,000. The landscape, vegetation and climate are vary extremely, for instance the elevations range from 25 to almost 2500 m a.s.l.. Typical alluvial valleys, such as the Tiber River and Velino River valleys are present; however, high mountains, such as Terminillo (2217 m) and Monte Navegna (1508 m), that are part of the Apennines, are also visible.

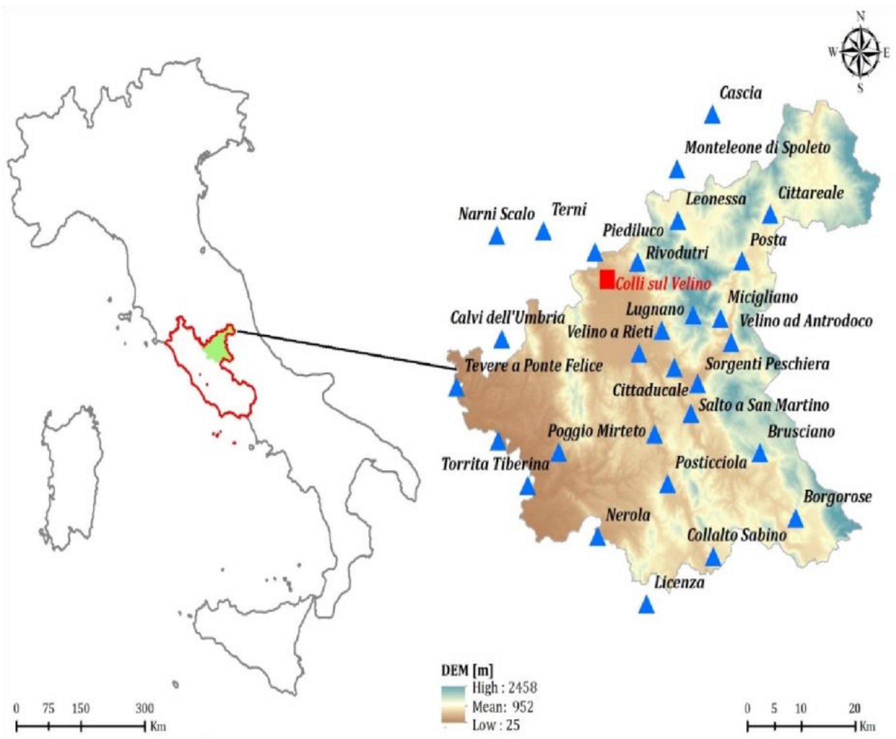

Figure 3.1. Study area localization. Left: Italy (grey border), Lazio region (red border), Rieti province (filled green). Right: Rieti province digital elevation model (DEM) with rain gauge stations (blue triangles) and Colli sul Velino rain gauge station (red square).

Climate and Vegetation of the Study Area

The Rieti province belongs to the Italian temperate eco-regional division [26]. This division embraces the northern and inner part of the Italian peninsula, including the main orographic chains of the Alps and the Apennines. It is characterized by a temperate climate, with annual medium temperatures above 5 °C and 4–8 months with medium temperatures below 10 °C. The mountain sectors above 1500 m present a prolonged winter season. Annual thermal excursion is marked. The minimum temperatures of the coldest month

(January) are always below 3 °C, not excluding the possibility of frosts, while the maximum temperatures exceed 30 °C in the warmest months (July and August) at hilly elevations. Annual precipitation ranges almost everywhere from 800 mm up to over 2000 mm, so the pluviometric regime can be considered as Continental (with a winter minimum) or Apenninic (with a summer minimum and two maxima in autumn and spring). In the summer season, the aridity period is generally not remarkable and, in any case, shorter than 2 months.

With specific reference to the Rieti province, the annual precipitation ranges from 1200 to 1600 mm, with October, November, and December being the rainiest months [27]. Rainfall has two maxima, the main one in autumn and the second in late spring [28]. The summer aridity period is limited to the months of July and August [27]. Figure 3.2 confirms the descripted monthly trend. The winter season generally lasts 140 days, covering part of spring [28]. Snow falls generally on hills and mountains, rarely on the valley where it is instead possible to have some foggy days, especially during spring and autumn.

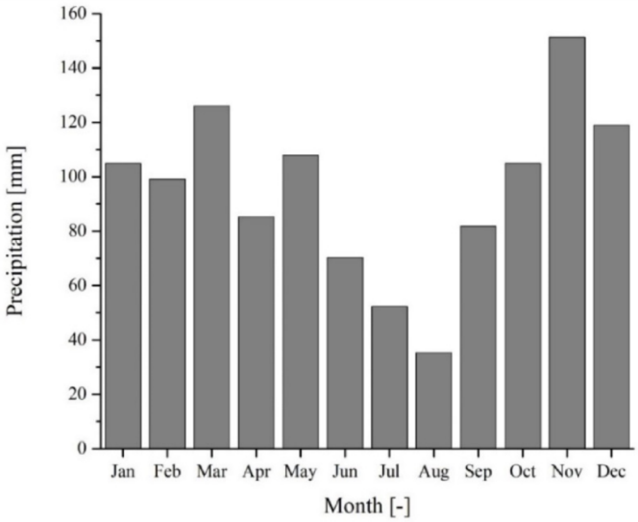

Figure 3.2. Observed precipitation data in Rieti province from 2008 to 2018.

Regarding the rainfall data, all the rain gauge stations located inside the selected case study area, and in the immediate external proximity, have been identified from the regional hydrographic offices. Rain gauge stations used in the present work have been selected with the compromise of having both a great number of stations, in order to accurately describe the spatial rainfall distribution, and an adequate number of observed years of rainfall data, in order to accurately characterize the temporal rainfall distribution. In doing so, we selected 30 rain gauge stations, shown in Figure 3.1, characterized by a continuous daily rainfall data availability ranging from 2008 to 2018, for a total of 11 years. Although we are aware that 11 years is not a great number for an accurate statistical rainfall estimation, it is noteworthy that the data scarcity is a common problem for researchers and practitioners, leading often to analyze a limited number of rainfall data for similar applications. Some examples can be found in Diodato and Bellocchi [4] and in Porto [29], which analyzed stations with only 4 or 5 years of data for a rainfall erosivity estimation employing the USLE formulation.

The majority (19) of the rain gauge stations here selected are located in Lazio region, Rieti province. Five rain gauge stations are located in Lazio region, Roma province, and the remaining six rain gauge stations are located in Umbria region, in the provinces of Perugia and Terni. From the retrieved daily data, it was possible to calculate the USLE R-factor according to the methodologies presented in the following paragraphs.

The complex landscape of the Rieti province with river valleys characterized by the presence of different lakes (the largest lakes are represented by the Ripasottile Lake, located in the Rieti Plain and about 2 km long, and the Salto Lake in the Salto Valley, about 10 km long, and the surrounding Appenninic chains (Monti Reatini, mountains of Salto and Turano valleys, Monti Sabini)) lead to a great variability in habitats and vegetation patterns. River and lake vegetation in the valleys cohabit with extensive crops, mainly maize and cereal cultivation [30], and olive trees on hills. With specific reference to the forest vegetation, it appears similar to a mosaic due to the local variations in terms of altitude, rainfall, temperature and sun exposure. The huge variation in altitude has influenced the distribution of agricultural, silvicultural, and breeding activities during time, and indirectly that of forests.

In relation to the altitude, it is possible to identify at least 15 different forest types. Among them, the most important are beech forests (Fagus sylvatica), chestnuts forests

(Castanea sativa), deciduous oak forests (Quercus cerris, Q. robur and Q. pu-bescens) and evergreen oak forests (Quercus ilex).

USLE R-Factor Original Calculation

Wischmeier [31] was the first to introduce a rainfall erosion index for the soil erosion calculation, paving the way for the USLE - Universal Soil-Loss Equation [5,6]. USLE is one of the most used empirical equations to calculate the theoretical soil erosion in a determinate area, mainly because of its easy employment in terms of calculation and reduced requirement of input data [32]. Since its development, this equation was subject to different modifications and improvements, mainly made to allow its use in GIS environments. It is for this reason that the RUSLE (Revised Universal Soil Loss Equation) [7] was developed. The original USLE equation is expressed as follows:

$$A = R \times K \times LS \times C \times P \tag{1}$$

where A is the annual soil erosion (t * ha^{-1} * $year^{-1}$), R is the rainfall erosivity factor (MJ * mm * ha^{-1} * h^{-1} * $year^{-1}$), K is the soil erodibility factor (t * ha^{-1} * [MJ * (ha * mm)$^{-1}$ * ha^{-1}]* $year^{-1}$), LS is the product between length (L) and slope (S) factors (dimensionless), C is the soil coverage and management factor (dimensionless) and P is the support practice factor (dimensionless).

The rainfall erosivity factor represents the erosivity power that rainfall has on the soil in a determinate area. In its first formulation, the R-factor was defined as the summation of the total storm energy (E) of an erosive rainfall event multiplied by the corresponding rainfall maximum intensity over a time span of 30 min (I30) within a certain time period, for instance one year [10]. It was expressed as follows:

$$R = \frac{\sum_{i=1}^{j} (EI_{30})_i}{N} \tag{2}$$

where: $EI_{30} = E \times I_{30}$; $E = 916 + 331 \cdot \log_{10}(I)$, with I being the rainfall intensity (in* h^{-1}); $(E_{I30})_i$ is related to storm i-th and j is the total number of storms in an N-year period. It is noteworthy that units of Equation (2) are imperial (R is expressed in 100 foot-ton * in * $acre^{-1}$ * h^{-1} * $year^{-1}$) and that results should be multiplied by 17.02 to convert in metric units (R expressed in MJ * mm * ha^{-1} * h^{-1} * $year^{-1}$).

As it can be noted from Equation (2), the USLE R-factor calculation using the original formulation is possible only if high resolution (at 30 min) rainfall data are available. Due to data scarcity and inaccuracy of old rain gauge stations, many authors elaborated alternative approaches for R-factor estimation, proposing different empirical formulas that are reported in the following paragraph.

Alternative Approaches for USLE R-Factor Calculation

When high resolution rainfall data are not available, alternative approaches can be used for calculating rainfall erosivity. Almost all these approaches make use of monthly and yearly cumulative rainfall data, or the Modified Fournier Index [33,34]. From an extensive literature analysis, we identified 12 empirical formulas, listed in Table 3.1, that have been often applied in Mediterranean countries and in semiarid areas.

Table 3.1. Rainfall erosivity equations used in this work.

ID	Equation	Source
R1	$R = 0.302 \times MFI^{1.93}$ where: $MFI:\ Modified\ Fournier\ Index,\ MFI = \sum_{i=1}^{12} \frac{p_i^2}{P}$ p_i is the average monthly precipitation and P is the average annual precipitation.	[35]
R2	$R = \{(4.17 \times MFI) - 152\} \times 17.02$ where: $MFI:\ Modified\ Fournier\ Index,\ MFI = \sum_{i=1}^{12} \frac{p_i^2}{P}$ p_i is the average monthly precipitation and P is the average annual precipitation.	[34]
R3	$R = 38.46 + 3.48 \times P$ where: P is the average annual precipitation.	[36]
R4	$R = 587.8 - 1.219P + 0.004105P^2$ where: P is the average annual precipitation.	[37]
R5	$R = 0.0483 \times P^{1.61}$ where: P is the average annual precipitation.	[37]
R6	$R = 0.739 \times MFI^{1.847}$ where: $MFI:\ Modified\ Fournier\ Index,\ MFI = \sum_{i=1}^{12} \frac{p_i^2}{P}$ p_i is the average monthly precipitation and P is the average annual precipitation.	[37]
R7	$R = 3.82 \times MFI^{1.41}$ where: $MFI:\ Modified\ Fournier\ Index,\ MFI = \sum_{i=1}^{12} \frac{p_i^2}{P}$ p_i is the average monthly precipitation and P is the average annual precipitation.	[38]
R8	$R = 0.092 \times P^{1.5}$ where: P is the average annual precipitation.	[39]
R9	$R = 4.04 * P - 965.53$ where: P is the average annual precipitation.	[39]
R10	$R = 3.08 \times P - 944$ where: P is the average annual precipitation.	[40]
R11	$R = \sum_{1}^{12} Ei_{30}$ where: $EI_{30} = 7.05 {*} RAIN_{10} - 88.92 {*} DAYS_{10}$ $DAYS_{10}$ = sum of the days in a month where it rained more than 10 mm. $RAIN_{10}$ = mean monthly precipitation in those months where it rained more than 10 mm in a day.	[41]
R12	$R = \sum_{1}^{12} Ei_{30}$ where: $Ei_{30} = 6.56 \times RAIN_{10} - 75.09 \times DAYS_{10}$ $DAYS_{10}$ = sum of the days in a month where it rained more than 10 mm. $RAIN_{10}$ = mean monthly precipitation in those months where it rained more than 10 mm in a day.	[42]

The use of the 12 investigated empirical formulas allowed the calculation of rainfall erosivity for all the selected rain gauge stations using the daily data recorded in the period 2008–2018, assessing the uncertainty in the rainfall erosivity estimation due to the specific applied formulation.

From the values of rainfall erosivity estimated at the rain gauge stations, it was possible to create rainfall erosivity GIS maps, using the software ArcMap 10.6 and a Kriging interpolation. This allowed us to create rainfall erosivity maps of the province of Rieti for all the empirical analyzed formulas.

The Stochastic Rainfall Generator (SRG)

Many works (see [43], for a list of references) highlighted the capacity of a specific class of SRGs, i.e., the Poisson cluster models, to satisfactorily reproduce observed summary statistics, such as mean, variance, skewness, proportion of dry/wet periods, and k-lag autocorrelation values, of the continuous rainfall process at several fine time scales. Poisson cluster models mainly comprise of Neyman–Scott and Bartlett–Lewis families, which perform equally well [43]. In this context, the most adopted shape for a rain cell in literature, i.e., the rectangular one, is considered in this work and then the Neyman–Scott Rectangular Pulses (NSRP, [43]) are adopted.

The NSRP model is based on the following assumptions from (a) to (d) (see Figure 3.3): (a) the inter-arrival time between the origins of two consecutive storms is assumed as an independent and identically distributed random variable, and it follows an exponential distribution; (b) each storm includes a number of rain cells (also indicated as bursts or pulses). Such a number is set as geometrically distributed, with the goal of having at least one burst for each storm. Each burst origin occurs, from the associated storm origin, after a waiting time, which is assumed as an exponentially distributed variable; (c) each burst has a rectangular shape, with an intensity and a duration that are both considered as exponential distributed; and (d) the total precipitation intensity at time t is then calculated as the sum of the intensities that are related to the active bursts at time t, starting from rainfall intensities, the aggregated process, i.e., the rainfall height cumulated at the desired temporal resolution, can be calculated.

The model has a set of parameters that are usually calibrated by minimizing an objective function, which is defined as the sum of residuals between the considered statistical properties of the observed data at chosen resolutions and their theoretical expressions. The statistical properties are typically referred to as a high-resolution continuous time series. However, continuous high-resolution data sets are very short or absent in many locations, with respect to Annual Maximum Rainfall (AMR) with different durations that usually are available with an adequate sample size. For this reason, the possibility to calibrate the model using only AMR data [43–45] and basic statistics, such as cumulate values for monthly or annual rainfall, has been adopted here. Such choice allows for a better reconstruction of extreme events, which are of main interest in many hydrological studies, for instance in the case of soil erosion caused by intense rainfall events.

Moreover, De Luca et al. [46,47] proposed a parsimonious modelling of seasonality, which was adopted in this work. The goal is to avoid an over parameterization by using monthly or seasonal parameter sets. In detail, due to the fact that the information regarding the seasonality of the rainfall process during the year is lost with the use of an AMR series, a simple goniometric series can be defined for any summary statistic of interest for the model.

In conclusion, the NSRP model is calibrated here by selecting the set of parameters, which optimizes the reproduction of mean values for hourly/multi-hourly AMR, plus the cumulative values for the annual rainfall. Then, validation is carried out by comparing the sample and theoretical Amount-Duration-Frequency (ADF) curves for hourly and multi-hourly rainfall heights.

The described NRSP model has been applied in one of the previously described rain gauge stations, i.e., Colli sul Velino station (see Figure 3.1). The choice of such a station is due to the availability of both daily rainfall data and AMR rainfall data for different durations, a circumstance that allows the comparison of modeled and observed rainfall data not only for daily durations, but also for sub-daily durations. The comparison will allow an assessment if the proposed SRG can be a suitable alternative for the estimation of rainfall erosivity.

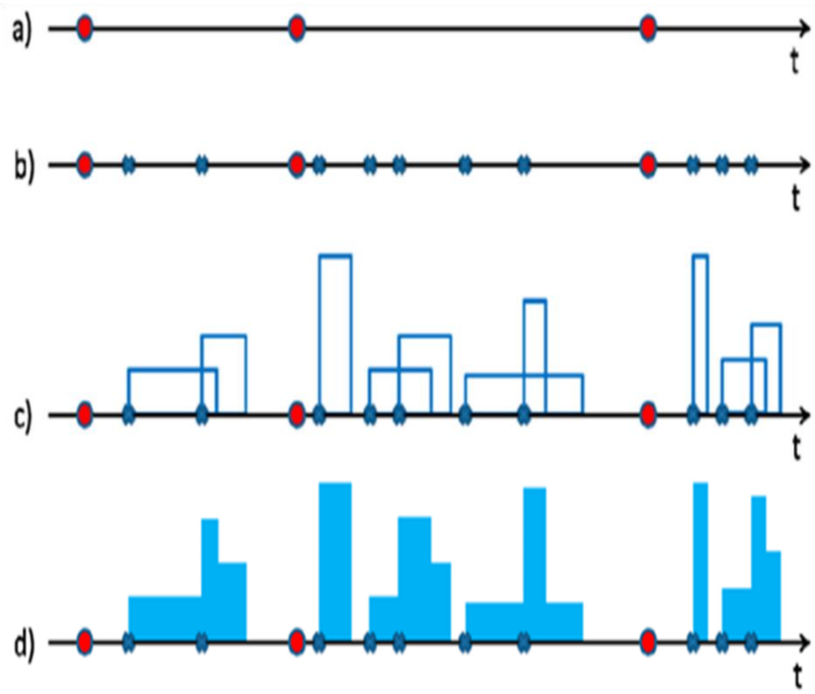

Figure 3.3. Representation of the (NSRP) stochastic process for at-site rainfall modeling (from [43]): (**a**) occurrences of storms; (**b**) for each storm, determination of the number of pulses and their temporal occurrences; (**c**) estimation of intensity and duration for all the pulses; (**d**) calculus of total intensity at time t.

Results and Discussion

Analysis of Rainfall Erosivity in Rieti Province

Rainfall erosivity has been calculated using 12 empirical formulas (Table 3.1). After having calculated, for every single year the rainfall erosivity values, the mean, maximum and minimum values for each equation were examined for the whole period. The average rainfall erosivity values have been reported in Figure 3.4, where rain gauge stations are numbered in order of decreasing observed yearly cumulative rainfall value.

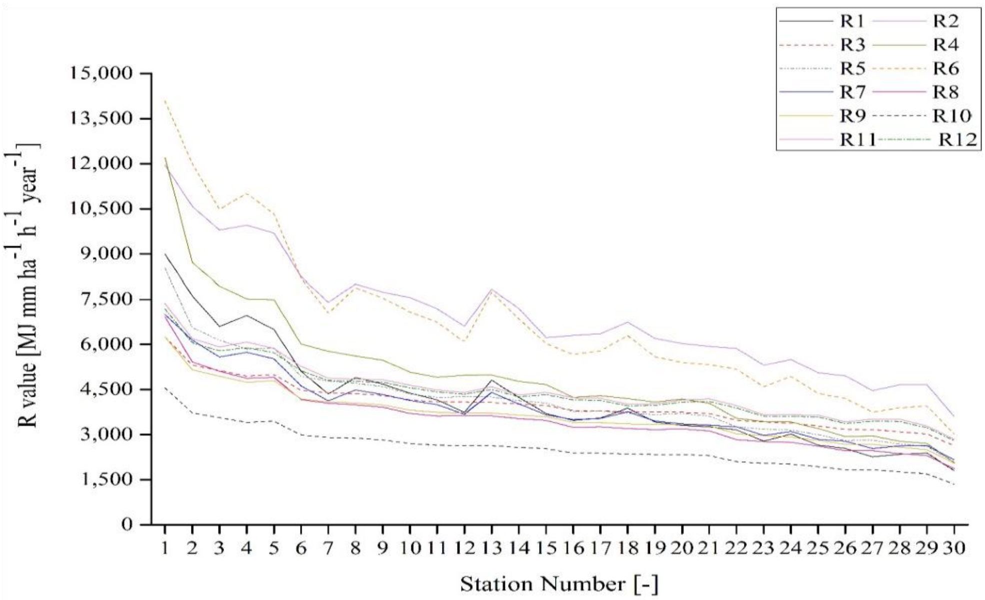

Figure 3.4. Average rainfall erosivity values obtained with the selected 12 formulas for each Rain gauge station. The stations were numbered in order of decreasing observed yearly cumulative rainfall value.

It is interesting to note the spatial geomorphological characteristics of the study area. In Figure 3.5, the rainfall erosivity maps obtained with the 12 investigated empirical formulas are shown. As it is possible to see, even if the maximum rainfall erosivity values vary a lot between all the maps, these are always located in the Monte Terminillo area, where the highest mountains of the province are located. It is also interesting to note that other high mountains are located in the South East part of the Rieti province, but not so high rainfall erosivity values have been obtained for such stations.

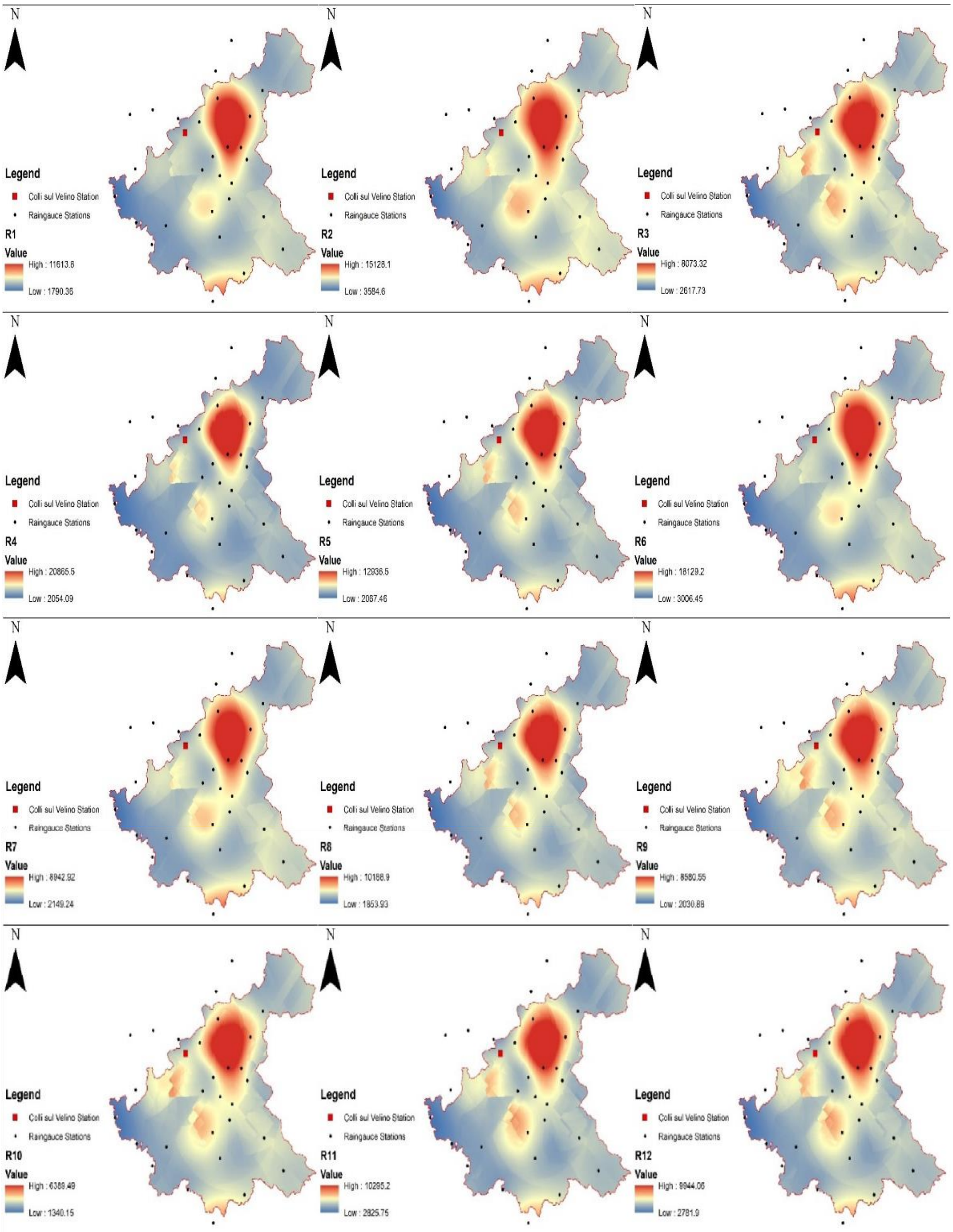

Figure 3.5. Rainfall erosivity maps created using the 12 equations. All the values are expressed in MJ * mm * ha^{-1} * h^{-1} * $year^{-1}$.

Finally, Figure 3.6 shows the minimum, average, and maximum rainfall erosivity values for all the formulas investigated, considering all years from 2008 to 2018. As it possible to see, there are not big differences between the average values of all the formulas. Only R2, R6, and R10 are quite different, with R2 and R6 having a higher value than the mean, and

R10 a lower value than the mean. Concerning the minimum rainfall erosivity values, they too are similar, and the differences are negligible.

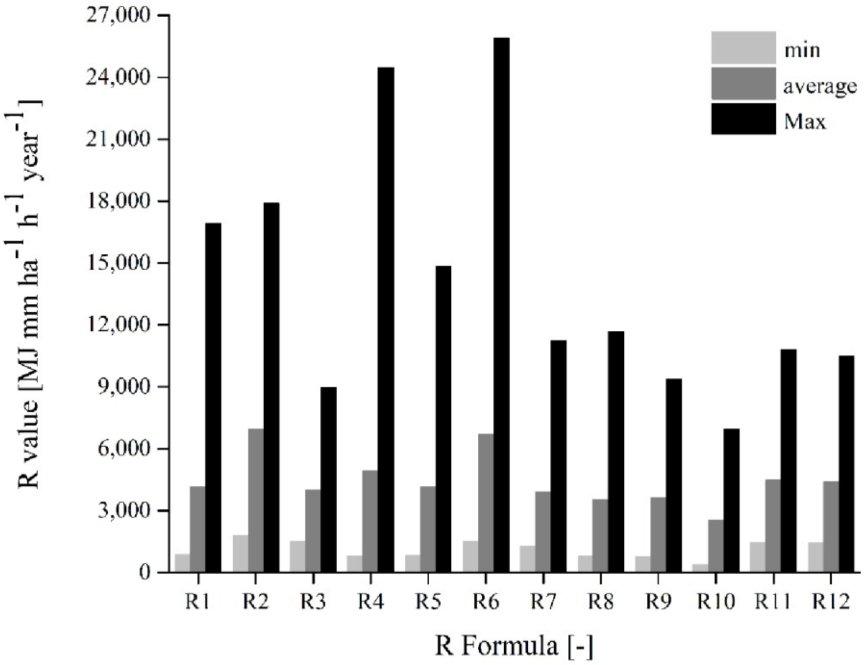

Figure 3.6. Minimum, average, and maximum rainfall erosivity values obtained with the 12 selected formulas.

Even if the average and minimum values are similar, we can observe strong differences between all the formulas in the maximum rainfall erosivity values. Here the difference of the values can vary from about 8000 MJ * mm * ha^{-1} * h^{-1} * year^{-1}), that is the lowest maximum value (R10), to more than 24,000 MJ * mm * ha^{-1} * h^{-1} * year^{-1}) for R4 and R6 formulas.

The rain gauge station that generated the maximum rainfall erosivity values is the Monte Terminillo station (Station number 18 in Figure 3.4), in the year 2010. In the year 2010, it is possible to see that 14 of the rain gauge stations produced their rainfall erosivity maximum values.

The rainfall erosivity equations that generated the maximum values are R4 and R6, both coming from Renard and Freimund's research [37]. The first one utilizes the annual mean precipitation, the second one the Modified Fournier Index (MFI), and both are exponential equations. It is interesting to note that R5, that comes from the same research, does not have such a high maximum rainfall erosivity value. Indeed, the maximum value for this equation is almost 15,000 MJ * mm * ha^{-1} * h^{-1} * year^{-1}), while R4 and R6 present a 25,000 MJ * mm * ha^{-1} * h^{-1} * year^{-1}) value.

From the aforementioned analysis, it is not possible to individuate a reference equation to estimate the rainfall erosivity, probably because too few rainfall data are available. In fact, the sample of data at our disposal is not "hydrologically" significant.

In order to overcome the scarce availability of rainfall data and to individuate a reference equation for rainfall erosivity, an additional analysis has been conducted, using 50 years of synthetic rainfall time series generated for Colle sul Velino rain gauge station (Station number 13 in Figure 3.4). The rain gauge station choice is based on the considerations seen in Figure 3.5, where it appears evident that Colli sul Velino station could be considered representative of the whole study area, considering both the average rainfall erosivity values and the precipitation data.

Analysis of the Synthetically Generated Rainfall Time Series

By employing the proposed NSRP model, 50 years of synthetic rainfall time series at 30 min resolution have been generated for Colli sul Velino raingauge station. As previously mentioned, for the selected station, both daily both AMR rainfall data for the durations D of 1, 3, 6, 12, and 24 h are available. Before employing the synthetic rainfall time series for the R-factor estimation, a comparison analysis with observed rainfall data is desirable in order to verify if the synthetic rainfall series can be representative of the case study rainfall field. For the sake of brevity, and since the focus is here on the soil erosion due to extreme rainfall events, the comparison is performed by analyzing the corresponding AMR for the recorded rainfall durations.

In Figure 3.7 the relationships between the return period (Tr) and the observed AMR in terms of cumulative rainfall values (hp) are shown. The return period has been estimated according to the Weibull empirical cumulative distribution [48]. As it can be seen from Figure 3.7, the NSRP application is characterized by good performances. In particular, for D = 1 h we have a slight overestimation for Tr lower than 5 years, and then the differences decrease for higher Tr. For D = 3 h and D = 6 h we have a slight overestimation, for Tr lower than 2 years, and a slight underestimation for Tr higher than 3 years, then the differences decrease for higher Tr. For D = 12 h we have a moderate underestimation for Tr higher than 3 years. Finally, for D = 24 h we have a moderate underestimation for Tr higher than 3 years; however, the differences decrease for higher Tr.

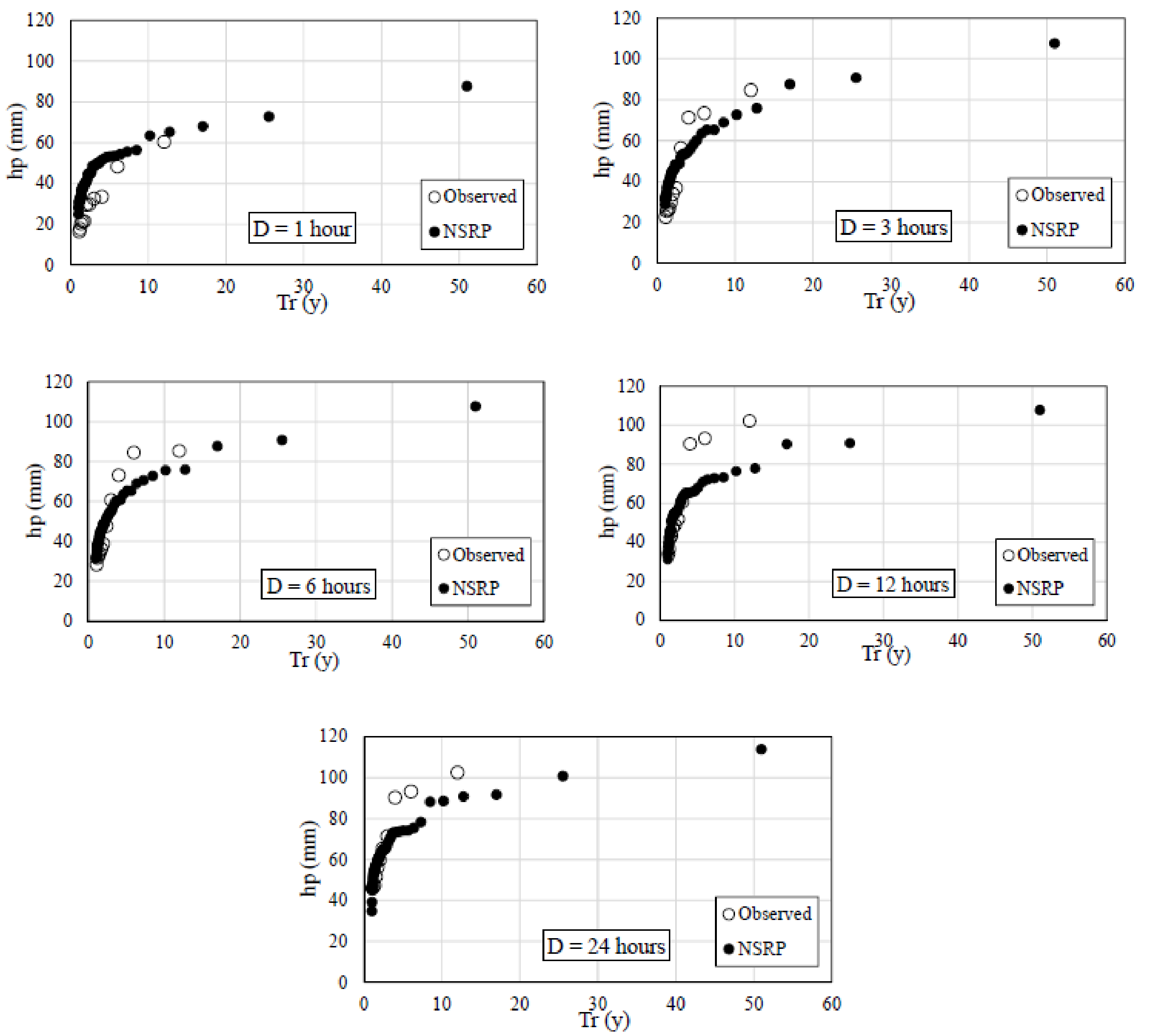

Figure 3.7. Relationships, for different rainfall durations (D), among return periods (Tr) and cumulative values of annual maxima rainfall (hp).

Looking at Figure 3.7, the best performances of the model are obtained for D = 1, 3 and 6 h. Since a short duration (e.g., a few hours) rainfall is generally characterized by a high rainfall intensity, and since we are focusing here on soil erosion caused by extreme rainfall events, the obtained results seem to justify the use of the synthetic rainfall time series for R-factor calculation.

Comparison between Rainfall Erosivity Values Using Observed and Modelled Rainfall for the Station "Colli sul Velino"

Using the investigated 12 equations, a comparison between rainfall erosivity values obtained using synthetically generated and observed rainfall data has been conducted, in order to identify the most reliable equation to calculate rainfall erosivity in the study area.

Figure 3.8 shows, for all equations, the variability of R-factor for the Colli sul Velino rain gauge station. In the graph, average values of 12 simulated and observed data are shown, where the red line represents the average of 12 values obtained considering the synthetically generated rainfall data, while the black dashed line represents the average of 12 values obtained considering the observed data.

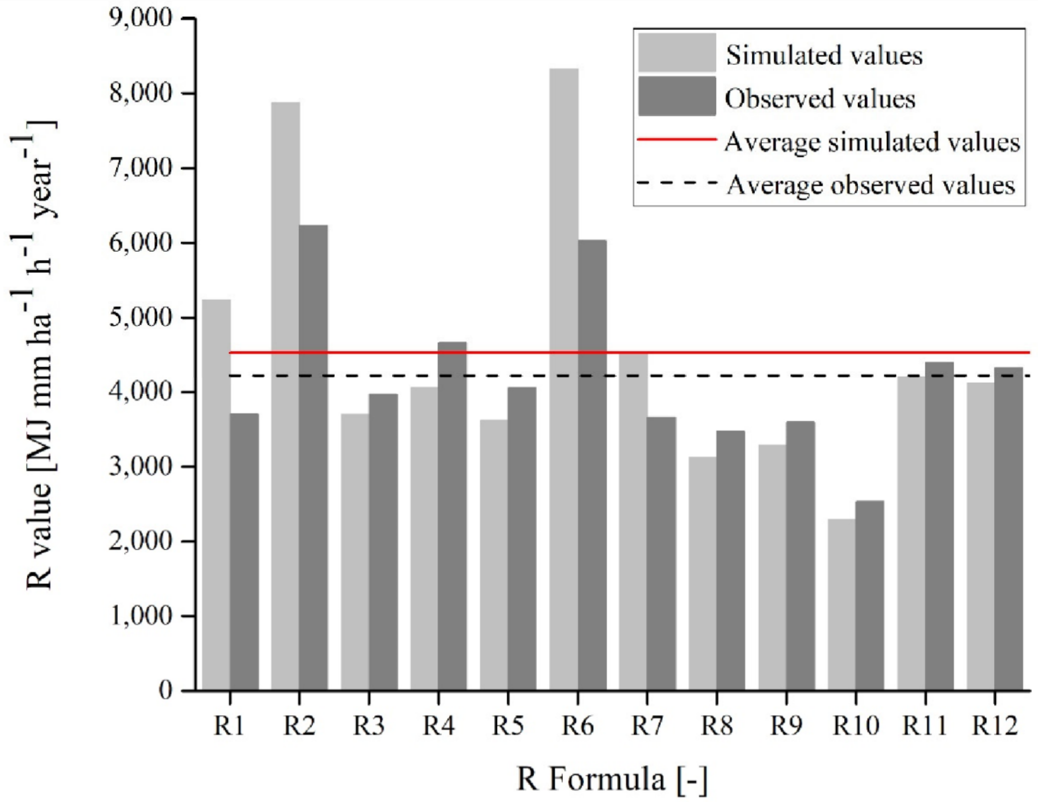

Figure 3.8. Rainfall erosivity value obtained with the 12 investigated equations, respectively, with simulated and observed rainfall data set. The red line represents the average of 12 values obtained considering the synthetically generated rainfall data, while the black dashed line represents the average of 12 values obtained considering the observed data.

The dimensionless ratio between the rainfall erosivity value and its average value has been calculated for the simulated and observed rainfall data set. Through this dimensionless ratio, it was possible to establish, with the procedure described below, the degree of reliability of each equation.

The equation reliability degree can be high, medium or low. In particular, if the equation presents at least one of the following characteristics it will be assigned a low degree of reliability:

- Both values of columns 4 and 5 of Table 3.2 differ from the unitary value by +/−15%;

• Only one of the columns 4 and 5 of Table 3.2 differs from the unitary value by +/−15% and these values are opposite (for example one greater than the unitary value and the other smaller).

Table 3.2. Equation reliability degree based on rainfall erosivity values using simulated and observed rainfall for rain gauge station Colli sul Velino.

Equation	Rainfall Erosivity Value-Simulated	Rainfall Erosivity Value-Observed	Ratio with Average Value-Simulated	Ratio with Average Value-Observed	Equation Reliability Degree
No.1	5238.92	3704.38	1.16	0.88	Low
No.2	7875.30	6232.32	1.74	1.48	Low
No.3	3700.09	3967.76	0.82	0.94	Medium
No.4	4061.81	4671.93	0.90	1.11	Medium
No.5	3624.35	4055.61	0.80	0.96	Medium
No.6	8329.25	6031.61	1.84	1.43	Low
No.7	**4531.35**	**3663.48**	**1.00**	**0.87**	**High**
No.8	3125.44	3470.80	0.69	0.82	Low
No.9	3286.59	3597.43	0.73	0.85	Low
No.10	2296.75	2533.66	0.51	0.60	Low
No.11	**4208.30**	**4403.50**	**0.93**	**1.04**	**High**
No.12	**4115.87**	**4329.42**	**0.91**	**1.03**	**High**

The degree of reliability is evaluated as "medium" if the following conditions are met:

• Only one of the columns 4 and 5 of Table 3.2 differs from the unitary value by +/−15%, but these values are both greater or smaller than the unitary value;

• Both the values of columns 4 and 5 of Table 3.2 differ from the unitary value by less than +/−15% and these values are opposite (for example one greater than the unit and the other smaller).

Finally, the degree of reliability is rated "high" if the following conditions are met:

• Both the values of columns 4 and 5 of Table 3.2 differ from the unitary value by less than +/−15%, but these values are both greater or smaller than the unitary value;

• Both the values of columns 4 and 5 of Table 3.2 differ from the unitary value by less than +/−10% and these values are opposite (for example one greater than the unit and the other smaller).

From the data reported in Table 3.2 we can conclude that:

(i) the dimensionless ratio between rainfall erosivity values obtained using simulated rainfall and their average values only three times greater than 1 (equations no. 1-2-6), while the same ratio calculated with observed rainfall data is five times greater than 1 (equations no. 2-4-6-11-12). In general, in 8 times out of 12, the analysis on the observed rainfall data returns higher rainfall erosivity values; this aspect could be due to the larger sample data considered by modelled analysis.

(ii) Equations no. 11 and 12 [41,42], both validated for Mediterranean zones, confirm a high reliability degree for the observed data set that, as said, is very small.

(iii) Equation no. 7 [38] provides the better result for the synthetic data set. This demonstrates the adequacy of Yu and Rosewell's equation for estimating the R-factor, one of the most used in international literature.

Conclusions

Intergovernmental Panel on Climate Change (IPCC) reports have shown higher precipitation projections, increasing the risk of soil loss by water runoff in the next century.

Therefore, evaluation of the rainfall erosivity is an important task, the determination of which affects the correct evaluation of soil erosion. In this paper, rainfall erosivity variability in the Rieti province of Central Italy has been investigated, analyzing 12 empirical formulas, suggested by literature, and using rainfall daily data observed from 2008 to 2018.

Starting from these premises, this work describes the efforts made to develop a methodology for rainfall erosivity evaluation in the case of ungauged or scarcely gauged areas. In fact, despite the fact that in the literature there are several equations to estimate rainfall erosivity, these two conditions represent a strong constrain to individuate the more reliable approach.

Results of numerical tests carried out for the Colli sul Velino rain gauge station were presented and discussed. In particular, the observed rainfall data were compared with numerical results obtained using a synthetic rainfall generator model developed by De Luca et al. [44–48]. Some peculiar features were observed.

The results reported in Figure 3.8 show consistent behavior across the three equations. In particular, it is interesting to note that equation no. 7 [38] represents one of the most used and one of oldest available in the literature. Particularly important are two other equations (no. 11 and 12) [41,42] that were developed for a Mediterranean habitat.

In our opinion, the use of a synthetic rainfall time series could help in solving the problem of hydrological data scarcity and consequently, guarantee major accuracy in estimating the R-factor for soil erosion evaluation.

Moreover, the availability of other rainfall data and the installation of new rain gauge stations in the Rieti province will make an upgrade of this work possible that could be seen as an interesting initial shift in the Lazio region's soil loss management, which is still grounded in merely theoretical approaches.

Author Contributions: Conceptualization, A.P.; methodology, all authors; software, D.L.D.L.; writing— original draft preparation, A.P., D.L.D.L., C.A. and P.S.; writing—review and editing, all authors. All authors have read and agreed to the published version of the manuscript.

Funding: The Department for Regional Affairs and Autonomies (DARA), Presidency of the Council of Ministers, Rome (Italy), has co-financed this research. Number of Grant: DARA-DAFNE 40506.

Conflicts of Interest: The authors declare no conflict of interest.

References

1. Beguería, S.; Serrano-Notivoli, R.; Tomas-Burguera, M. Computation of rainfall erosivity from daily precipitation amounts. *Sci. Total Environ.* **2018**, *637–638*, 359–373. [CrossRef] [PubMed]
2. Xin, Z.; Yu, X.; Li, Q.; Lu, X.X. Spatiotemporal variation in rainfall erosivity on the Chinese Loess Plateau during the period 1956–2008. *Reg. Environ. Chang.* **2011**, *11*, 149–159. [CrossRef]
3. Apollonio, C.; Petroselli, A.; Tauro, F.; Cecconi, M.; Biscarini, C.; Zarotti, C.; Grimaldi, S. Hillslope Erosion Mitigation: An Experimental Proof of a Nature-Based Solution. *Sustainability* **2021**, *13*, 6058. [CrossRef]
4. Diodato, N.; Bellocchi, G. MedREM, a rainfall erosivity model for the Mediterranean region. *J. Hydrol.* **2010**, *387*, 119–127. [CrossRef]
5. Wischmeier, W.H.; Smith, D.D. *Predicting Rainfall-Erosion Losses from Cropland East of the Rocky Mountains. Guide for Selection of Practices for Soil and Water Conservation*; Agriculture Handbook No. 282; US Department of Agriculture: Washington, DC, USA, 1965.
6. Wischmeier, W.H.; Smith, D.D. *Predicting rainfall-erosion losses: A Guide to Conservation Farming*; Agricultural Handbook 537; US Department of Agriculture: Washington, DC, USA, 1978; pp. 1–151.
7. Renard, K.G.; Foster, G.R.; Weesies, G.A.; McCool, D.K.; Yoder, D.C. *Predicting soil erosion by water: A guide to conservation planning with the Revised Universal Soil Loss Equation (RUSLE)*;

Agriculture Handbook No. 703; United States Department of Agriculture: Washington, DC, USA, 1997; p. 404.
8. Foster, G.R. *User's Reference Guide. Revised Universal Soil Loss Equation Version 2 (RUSLE2)*; National Sedimentation Laboratory, USDA-Agricultural Research Service: Washington, DC, USA, 2004; p. 418.
9. Lim, Y.S.; Kim, J.K.; Kim, J.W.; Park, B.I.; Kim, M.S. Analysis of the relationship between the kinetic energy and intensity of rainfall in Daejeon, Korea. *Quat. Int.* **2015**, *384*, 107–117. [CrossRef]
10. Brown, L.C.; Foster, G.R. Storm erosivity using idealized intensity distribution. *Trans. ASAE* **1978**, *30*, 379–386. [CrossRef]
11. Cecílio, R.A.; Moreira, M.C.; Pezzopane, J.E.M.; Pruski, F.F.; Fukunaga, D.C. Assessing rainfall erosivity indices through synthetic precipitation series and artificial neural networks. *An. Acad. Bras. Ciências* **2013**, *85*, 1523–1535. [CrossRef]
12. Panagos, P.; Ballabio, C.; Borrelli, P.; Meusburger, K.; Klik, A.; Rousseva, S.; Tadic´, M.P.; Michaelides, S.; Hrabalíková, M.; Olsen, P.; et al. Rainfall erosivity in Europe. *Sci. Total Environ.* **2015**, *511*, 801–814. [CrossRef]
13. Isikwue, M.; Ocheme, J.; Aho, M. Evaluation of rainfall erosivity index for Abuja, Nigeria using Lombardi method. *Niger. J. Technol.* **2015**, *34*, 56. [CrossRef]
14. Yu, B.; Hashim, G.M.; Eusof, Z. Estimating the R-factor with limited rainfall data: A case study from Peninsular Malaysia. *J. Soil Water Conserv.* **2001**, *56*, 101–105.
15. Davison, P.; Hutchins, M.G.; Anthony, S.G.; Betson, M.; Johnson, C.; Lord, E.I. The relationship between potentially erosive storm energy and daily rainfall quantity in England and Wales. *Sci. Total Environ.* **2005**, *344*, 15–25. [CrossRef] [PubMed]
16. Capolongo, D.; Diodato, N.; Mannaerts, C.M.; Piccarreta, M.; Strobl, R.O. Analyzing temporal changes in climate erosivity using a simplified rainfall erosivity model in Basilicata (southern Italy). *J. Hydrol.* **2008**, *356*, 119–130. [CrossRef]
17. Gioia, A.; Lioi, B.; Totaro, V.; Molfetta, M.G.; Apollonio, C.; Bisantino, T.; Iacobellis, V. Estimation of Peak Discharges under Different Rainfall Depth–Duration–Frequency Formulations. *Hydrology* **2021**, *8*, 150. [CrossRef]
18. Grimaldi, S.; Nardi, F.; Piscopia, R.; Petroselli, A.; Apollonio, C. Continuous hydrologic modelling for design simulation in small and ungauged basins: A step forward and some tests for its practical use. *J. Hydrol.* **2021**, *595*, 125664. [CrossRef]
19. Ritschel, C.; Ulbrich, U.; Névir, P.; Rust, H.W. Precipitation extremes on multiple timescales—Bartlett–Lewis rectangular pulse model and intensity–duration–frequency curves. *Hydrol. Earth Syst. Sci.* **2017**, *21*, 6501–6517. [CrossRef]
20. van Vliet, M.T.H.; Blenkinsop, S.; Burton, A.; Harpham, C.; Broers, H.P.; Fowler, H.J. A multi-model ensemble of downscaled spatial climate change scenarios for the Dommel catchment, Western Europe. *Clim. Chang.* **2012**, *111*, 249–277. [CrossRef]
21. Blenkinsop, S.; Harpham, C.; Burton, A.; Goderniaux, P.; Brouyère, S.; Fowler, H.J. Downscaling transient climate change with a stochastic weather generator for the Geer catchment, Belgium. *Clim. Res.* **2013**, *57*, 95–109. [CrossRef]

22. Forsythe, N.; Fowler, H.J.; Blenkinsop, S.; Burton, A.; Kilsby, C.G.; Archer, D.R.; Harpham, C.; Hashmi, M.Z. Application of a stochastic weather generator to assess climate change impacts in a semi-arid climate: The Upper Indus Basin. *J. Hydrol.* **2014**, *517*, 1019–1034. [CrossRef]
23. Jones, P.D.; Harpham, C.; Burton, A.; Goodess, C.M. Downscaling regional climate model outputs for the Caribbean using a weather generator. *Int. J. Climatol.* **2016**, *36*, 4141–4163. [CrossRef]
24. Yu, B. An assessment of uncalibrated CLIGEN in Australia. *Agric. For. Meteorol.* **2003**, *119*, 131–148. [CrossRef]
25. Zhang, Y.-G.G.; Nearing, M.A.; Zhang, X.-C.C.; Xie, Y.; Wei, H. Projected rainfall erosivity changes under climate change from multimodel and multiscenario projections in Northeast China. *J. Hydrol.* **2010**, *384*, 97–106. [CrossRef]
26. Blasi, C.; Capotorti, G.; Copiz, R.; Guida, D.; Mollo, B.; Smiraglia, D.; Zavattero, L. Classi-fication and mapping of the ecoregions of Italy. *Plant Biosyst.* **2014**, *148*, 1255–1345. [CrossRef]
27. Bartolucci, F. Contributo alla conoscenza della flora dei monti carseolani (settore laziale): Monte Navegna (LAzio, Rieti). *Inf. Bot. Ital.* **2006**, *38*, 3–35.
28. Anderlini, M.; De Santoli, L.; Fraticelli, F. Distributed Energy Generation: Case Study Of A Mountain School Campus In Italy. *WIT Trans. Ecol. Environ.* **2013**, *73*, 537–549.
29. Porto, P. Exploring the effect of different time resolutions to calculate the rainfall erosivity factor R in Calabria, southern Italy. *Hydrol. Process.* **2016**, *30*, 1551–1562. [CrossRef]
30. Mensing, S.A.; Schoolman, E.M.; Tunno, I.; Noble, P.J.; Sagnotti, L.; Florindo, F.; Piovesan, G. Historical ecology reveals landscape transformation coincident with cultural development in central Italy since the Roman Period. *Sci. Rep.* **2018**, *8*, 2138. [CrossRef]
31. Wischmeier, W.H. A rainfall erosion index for a Universal Soil-Loss Equation. *Soil Sci. Soc. Am. Proc.* **1959**, *23*, 246–249. [CrossRef]
32. Benavidez, R.; Jackson, B.; Maxwell, D.; Norton, K. A review of the (Revised) Universal Soil Loss Equation ((R)USLE): With a view to increasing its global applicability and improving soil loss estimates. *Hydrol. Earth Syst. Sci.* **2018**, *22*, 6059–6086. [CrossRef]
33. Fournier, F.G.A. *Climat et Erosion: La Relation Entre L'érosion du Sol par L'eau et les Précipitations Atmosphériques*, 1st ed.; PUF: Paris, France, 1960.
34. Arnoldus, H.M.J. An approximation of the rainfall factor in the Universal Soil Loss Equation. In *Assessment of Erosion*; John Wiley and Sons Ltd.: Hoboken, NJ, USA, 1980; pp. 127–132.
35. Arnoldus, H.M.J. Methodology used to determine the maximum potential average annual soil loss due to sheet and rill erosion in Morocco. *FAO Soils Bull.* **1977**, *34*, 39–48.
36. Lo, A.; El-Swaify, S.A.; Dangler, E.W.; Shinshiro, L. Effectiveness of EI30 as an erosivity index in Hawaii. *Soil Conserv. Soc. Am.* **1985**.
37. Renard, K.G.; Freimund, J.R. Using Monthly Precipitation Data to Estimate the R Factor in the Revised USLE. *J. Hydrol.* **1994**, *157*, 287–306. [CrossRef]
38. Yu, B.; Rosewell, C.J. Technical notes: A robust estimator of the R-factor for the universal soil loss equation. *Trans. ASAE* **1996**, *39*, 559–561. [CrossRef]

39. Ferrari, R.; Pasqui, M.; Bottai, L.; Esposito, S.; Di Giuseppe, E. Assessment of soil erosion estimate based on a high temporal resolution rainfall dataset. In Proceedings of the 7th European Conference on Applications of Meteorology (ECAM), Utrecht, Netherlands, 12–16 September 2005; pp. 12–16.
40. Torri, D.; Borselli, L.; Guzzetti, F.; Calzolari, M.C.; Bazzoffi, P.; Ungaro, F.; Bartolini, D.; Salvador Sanchis, M.P. Italy. In *Soil Erosion in Europe*; Wiley: Chichester, UK, 2006; pp. 245–261.
41. De Santos Loureiro, N.; De Azevedo Coutinho, M. A new procedure to estimate the RUSLE EI30 index, based on monthly rainfall data and applied to the Algarve region, Portugal. *J. Hydrol.* **2001**, *250*, 12–18. [CrossRef]
42. Ferreira, V.; Panagopoulos, T. Seasonality of Soil Erosion Under Mediterranean Conditions at the Alqueva Dam Watershed. *Environ. Manag.* **2014**, *54*, 67–83. [CrossRef] [PubMed]
43. Burton, A.; Fowler, H.J.; Blenkinsop, S.; Kilsby, C.G. Downscaling transient climate change using a Neyman-Scott rectangular pulses stochastic rainfall model. *J. Hydrol.* **2010**, *381*, 18–32. [CrossRef]
44. De Luca, D.L.; Galasso, L. Calibration of NSRP Models from Extreme Value Distributions. *Hydrology* **2019**, *6*, 89. [CrossRef]
45. De Luca, D.L.; Petroselli, A.; Galasso, L. Modelling Climate Changes with Stationary Models: Is It Possible or Is It a Paradox? In *Numerical Computations: Theory and Algorithms. NUMTA 2019*; Lecture Notes in Computer Science (Including Subseries Lecture Notes in Artificial Intelligence and Lecture Notes in Bioinformatics); Springer: Cham, Switzerland, 2020; Volume 11974, pp. 84–96.
46. De Luca, D.L.; Petroselli, A.; Galasso, L. A transient Stochastic Rainfall Generator for climate changes analysis at hydrological scales in Central Italy. *Atmosphere* **2020**, *11*, 1292. [CrossRef]
47. De Luca, D.L.; Petroselli, A. STORAGE (STOchastic RAinfall GEnerator): A user-friendly software for generating long and high-resolution rainfall time series. *Hydrology* **2021**, *8*, 76. [CrossRef]
48. Recanatesi, F.; Petroselli, A.; Ripa, M.N.; Leone, A. Assessment of stormwater runoff management practices and BMPs under soil sealing: A study case in a peri-urban watershed of the metropolitan area of Rome (Italy). *J. Environ. Manag.* **2017**, *201*, 6–18. [CrossRef] [PubMed]

PAPER REFERENCE

Petroselli, A., Apollonio, C., De Luca, D. L., Salvaneschi, P., Pecci, M., Marras, T., & Schirone, B. (2021). Comparative Evaluation of the Rainfall Erosivity in the Rieti Province, Central Italy, Using Empirical Formulas and a Stochastic Rainfall Generator. *Hydrology*, *8*(4), 171. https://doi.org/10.3390/hydrology8040171

4. Assessing the efficiency of two silvicultural approaches for soil erosion mitigation thanks to a novel monitoring apparatus (research article submitted)

Pietro Salvaneschi[1], Antonio Pica[2], Ciro Apollonio[1], Teodoro Andrisano[3], Massimo Pecci[4], Andrea Petroselli[1] and Bartolomeo Schirone[1]

[1]DAFNE Department, Tuscia University, 01100 Viterbo, Italy

[2]DEB Department, Tuscia University, 01100 Viterbo, Italy

[3] Maiella National Park, Via Badia 28, 67039 Sulmona, Italy

[4] Department of Regional Affairs and Autonomies (DARA) – Presidency of the Council of Ministers, Via della Stamperia 8, 00186 Rome, Italy

Abstract

Soil erosion and hydrogeological risk are critical phenomena gaining increased recognition within the scientific community. Although these occurrences are naturally occurring, human activities can exacerbate their impacts. For example, deforestation consistently amplifies soil erosion. This study examines two distinct forest management strategies aimed at addressing soil erosion: the Banded Standards Method (BSM) and the Scattered Standards Method (SSM). We conducted a field experiment in two test areas located in central Italy, with one area employing the BSM and the other implementing the SSM. Two soil erosion plots were established, representing prototypes of a novel erosion monitoring apparatus called the Natural Erosion Trap (NET), or Diabrosimeter, specifically designed for forest environments. At regular intervals, particularly after significant storm events, sediment and leaf litter accumulated within the erosion plots were collected, dried, and weighed to quantify erosion rates and assess the efficacy of the silvicultural methods under investigation. The results revealed a 30.72% reduction in the eroded material with BSM compared to SSM, underscoring BSM's ability to mitigate potential hazards and preserve environmental integrity.

Keywords: Soil erosion; Watershed management; Forest management; Soil conservation; Experimental plots; silvicultural treatment.

Introduction

Soil erosion and hydrogeological risk represent critical phenomena garnering increasing attention from the scientific community [1–3] as well as international and national regulatory bodies [4–6], owing to their profound ramifications on human livelihoods, infrastructure integrity, and ecological balance [7,5,8,9]. While both phenomena are inherently natural, anthropogenic activities often exacerbate their severity [10–15]. For instance, deforestation invariably triggers soil erosion, and contingent upon the geomorphological characteristics of the affected area, may precipitate hydrogeological instability [16–18]. Over time, numerous empirical investigations have been undertaken to understand soil erosion dynamics [19]. Pioneering work in this domain was conducted by Wischmeier and Smith [20,21], who, following years of experimental research, formulated the Universal Soil Erosion Equation (USLE).

This equation remains the cornerstone in soil erosion modelling, notably in its revised iteration, the Revised Universal Soil Loss Equation (RUSLE) [22,23]. Indeed, the genesis of this formula stemmed from extensive experimental endeavours predominantly within agricultural contexts [24]. The widespread adoption of the USLE (or RUSLE) framework for regional applications underscores its enduring utility [25].

To determine the equation, the researchers devised experimental plots with cemented sides terminating in water and sediment collectors, representing a widely employed setup in experimental fields. A comprehensive review revealed that the majority of such experiments have been conducted within agricultural contexts [26,27]. However, investigations into soil erosion estimation within forested areas utilizing experimental plots remain relatively scarce, with only a limited number of studies examining the effects of logging on soil dynamics [28,29,17]. In recent years, the predominant approach in natural environment research pertaining to soil erosion has shifted towards modelling within a Geographic Information System (GIS) framework, leveraging the Revised Universal Soil Loss Equation (RUSLE) [30–35].

Nevertheless, a significant challenge in such modelling approach lies in the scarcity of detailed input data. Notably, commonly utilized digital elevation models, typically with a resolution of 30 meters, lack representation of soil microtopography, potentially leading to oversimplified terrain characterization and erroneous erosion estimations. Consequently, the paucity of experimental studies on forest soil erosion primarily stems from the logistical challenges associated with constructing experimental plots. Notably, conventional plot construction techniques [20,21,36] are associated with notable environmental impacts, including substantial soil disturbance, introduction of artificial elements incongruent with natural settings, and significant financial outlay.

Italy stands out as one of Europe's most hydrologically vulnerable nations, with 94% of its administrative regions grappling with various forms of hydrological instability according to the ISPRA Report on hydrogeological instability [37]. This predicament is poised to exacerbate in the coming years, particularly under the specter of climate change, which forecasts a marked reduction in average rainfall alongside an uptick in extreme weather events, potentially escalating the frequency and severity of hydrological disturbances such as floods [6,38].

Italy's geographical landscape is characterized by 41.6% hilly terrain, 35.2% mountainous regions, and a mere 23.2% flat land, predominantly occupied by urban settlements. Natural ecosystems, including forests, are predominantly situated in hilly and mountainous terrains. Consequently, owing to the Mediterranean precipitation patterns prevalent in the country, Italy witnesses a notably higher average annual soil erosion rate within forested areas compared to other European regions, as elucidated by Borrelli et al. [17]. Specifically, Italian forest ecosystems exhibit an average annual soil erosion rate of 0.33 t/ha/yr, surpassing the rates observed in Mediterranean forests (0.18 t/ha/yr) and other European counterparts (0.003 t*ha−1*yr−1).

Given the substantial proportion (42.3%) of Italian forest cover comprising coppice forests, which inherently engender greater soil erosion compared to high stand forests, it becomes imperative to devise silvicultural strategies aimed at mitigating post-harvest soil erosion and subsequent hydrological instability. In pursuit of this objective, we investigate the efficacy of the Banded Standards Method (BSM), a silvicultural coppice method hypothesized by Del Favero [39] and conceptually scrutinized by our research team [40].

The primary distinction between the two coppice forest management techniques lies in the arrangement of the trees that remain in the forest after logging, known as standards. In the Scattered Standards Method (SSM), these standards are dispersed throughout the logged area. This method ensures that the trees are evenly spread, providing a more uniform structure to the forest after logging operations. In contrast, the BSM arranges the standards in a band or stripe that runs parallel to the contour lines of the terrain. This technique creates a more organized and systematic layout, concentrating the remaining trees in specific areas and following the land's natural topography.

The BSM can make forest management practices, such as replanting and maintenance, more efficient due to the organized layout of the standards. By following the contour lines, this method can also help in reducing soil erosion and managing water flow more effectively, as the trees act as barriers to slow down runoff. This approach can be particularly advantageous in areas prone to erosion or with uneven terrain. Because of the band of standards that act as ecological corridor, this method can also bring to a reduction of loss of animal and plant biodiversity and can ensure the conservation of gene flows. Those stripes can act also as wind barriers so they can reduce the wind effect followed by the logging, and finally they hide better the view of the bare areas simulating a seamless covering of the slopes with a real improvement at the landscape level.

To evaluate the viability of the BSM, we conducted a field experiment wherein two test areas were established: one employing the conventional SSM, typical in Italian coppice forest management, and the other implementing the BSM.

The experiment was carried out within a mixed coppice forest situated in the Maiella National Park. After logging activities, two soil erosion plots were installed, each covering one of the logged areas. These soil erosion plots represent prototypes of a novel erosion monitoring apparatus termed Natural Erosion Traps (NET) or Diabrosimeter, specifically designed for forest environments. At regular intervals, and particularly following significant storm events, sediment and leaf litter accumulated within the erosion plots were collected, dried, and weighed to quantify erosion rates and assess the efficacy of the silvicultural methods under investigation.

Materials and Methods

Study area

The study area (Figure 1) is situated within the "Gole di Popoli" in the Municipality of Popoli, in the Abruzzo Region (central Italy). The site is part of the Maiella National Park and of the State Natural Reserve “Mt. Rotondo”(42°11'20.78"N; 13°50'57.24"E). The altitudinal range of the area spans from 308 m to 332 m above sea level, characterized by an average slope of 48.5%, moderate ruggedness, and predominant northeast-facing aspect. Geophysical data obtained from Geoportale Abruzzo [41] indicate that the study area exhibits typical physiographic features and lithological composition consistent with sloping terrain containing valleys and calcareous substrates. Specifically, the area is typified by Middle-Late Jurassic limestones and calcarenites, with radiolarian and filaments-like remains [42].

As for the climatic aspects , the area can be classified in the temperate macroclimate, temperate oceanic submediterranean bioclimate with upper subhumid ombrotype, and upper mesotemperate thermotype [43]. According to the Köppen-Geiger climate classification, the study area has a temperate climate with hot summers and no dry seasons (symbol Cfa) [44]. The average annual rainfall is 719.6 mm, with an average of 86 rainy days in a year [45].

The maximum collected rainfalls are 36.4 mm (1h) and 177.4 mm (24h). The rainiest seasons are spring (April) and autumn (October, November, and December).

The minimum rainfall is in July (25.8 mm). The average daily temperature is 13.5°C, with average maximum temperatures exceeding 30.0°C in summer months (absolute maximum 45.0°C) and average minimum temperatures ranging between 0.1°C and 0.8°C during the coldest months (absolute minimum -17.0°C). All climatic data refer to the thermopluviometric station of Popoli (UTM WGS84: 32T 899738.33E, 4678532.80N), for the period 1951-2000 [45] (Figure 2).

According to the phytosociological classification, the study area is covered by a mixed deciduous broadleaf forest dominated by *Quercus pubescens* Willd. belonging to the plant association *Roso sempervirentis-Quercetum virgilianae* with elements of Mediterranean sclerophyllous vegetation (*Quercus ilex* L., *Viburnum tinus* L., *Ruscus aculeatus* L., *Smilax aspera* L., etc.) of the class *Quercetea ilicis* [46,47].

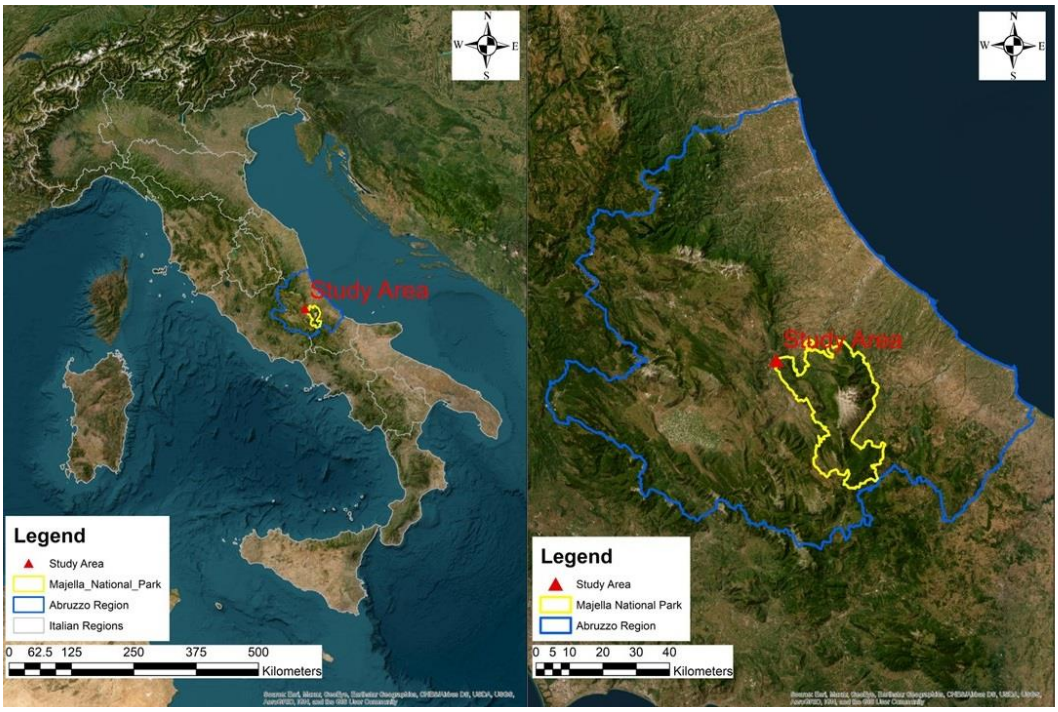

Figure 1. The figure represents the location of the study area. On the left its location on a national scale, while on the right on a regional scale. In blue color is highlighted the Abruzzo Region, in yellow is highlighted the contour of the Maiella National Park and, in red the study area. The image on the right is a satellite orthophoto of the Region.

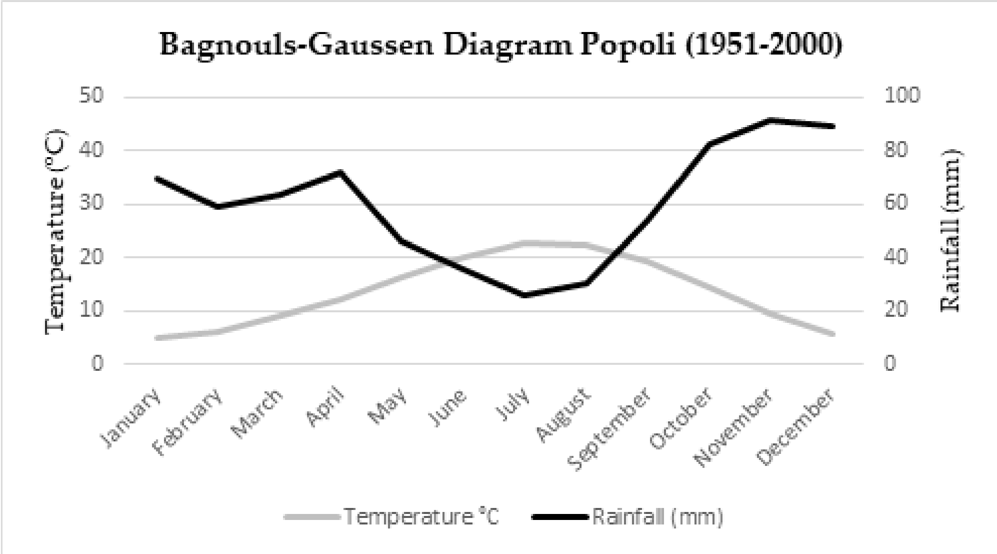

Figure 2. Bagnouls-Gaussen diagram of the study area, during the period 1951-2000.

Silvicultural treatment

The forest underwent coppicing using the "coppice with standards" method. In one plot, standards were released onto the ground utilizing the SSM, the most prevalent technique in coppicing. Conversely, the other plot employed the BSM as proposed by Schirone et al. [40]. This method involves releasing standards in stripes perpendicular to the steepest slope direction, thereby altering conventional coppicing geometry. It was specifically designed to manage steep coppice forests and mitigate soil erosion following logging activities.

A field campaign was conducted in the logged area to assess the main characteristics of vegetation within the two plots. Data on the number of plants categorized into standards and stumps, the number of shoots, and their respective diameters (DBH) were collected (Table 1). The mean height of the trees, determined through direct measurement of selected logged trees, was recorded at 14 meters (Table 1). Plot 1 (P1) corresponds to the area where SSM was implemented, while Plot 2 (P2) represents the BSM plot. The average diameter of Plot P1 was 7.76 cm, the one in Plot P2 was 8.58 cm and their mean was 8.17 cm. The diameter was calculated at the breast height (1.30m) for each standard and shoot with a diameter superior to 3 cm. All the standards, stumps, and shoots were counted. By summing the number of the standards with the number of the shoots we obtained the total number of stems present in the two plots. Finally, the results were compared in hectares and then summed. Plot P1 resulted to have 88 standards (1760/ha), 65 shoots (1300/ha) for a total of 153 stems, (3060/ha). Plot P2 resulted to have 79 standards (1580/ha), and 69 shoots (1380/ha) for a total of 148 stems, (2960/ha). The sum of the two plots was 167 standards (1670/ha), 134 shoots (1340/ha), and in total 301 stems (3010/ha).

Table 1. Summary of the principal characteristics of the 2 plots and in total. The first two lines show the average diameter (DBH) and height of the standing trees, and the other lines represent data on the number of plants, in their categories., the results were reported both, as they were counted and compared to hectares. Finally, the basal area and the volume of the trees inside the plots.

	Plot P1 (SSM)		Plot P2 (BSM)		Total	
	N	**N/ha**	**N**	**N/ha**	**N**	**N/ha**
Average diameter (DBH)	7.76		8.58		8.17	
Average height (m)	13.60		13.70		13.65	
Standards	88	1760	79	1580	167	1670
Stumps	29	580	28	560	57	570
Shoots	65	1300	69	1380	134	1340
Stems	153	3060	148	2960	301	3010

The coppice cutting of the two plots was carried out Between the end of September and the end of October 2022, by releasing 140 standards per hectare. Given that each plot was 500 square meters, 7 trees (standards) were left in each plot (see Figure 3).

In the first plot (SSM), the standards were dispersed throughout the study area, ensuring the representation of each species within the plot. The species, diameter (DBH) and height of these standards are detailed in Table 2. In the second plot (BSM), the standards were strategically positioned to form a single stripe (band) in the middle of the area, running parallel to the shorter side and approximately 25 meters from both the base and the top of the plot. The two plots were modelled in three dimensions using the LiDAR module of the iPhone 14 pro combined with PolyCam app [48], and the resulting models are included in the supplementary materials (Figure S1, Figure S2). Species differentiation was not considered; instead, standards were selected solely for inclusion in the designated band of standards (refer to Table 2). For this reason, in Plot P2, only two species remained (*Quercus pubescens* Wild. and *Fraxinus ornus* L.), while in Plot P1 4 (*Quercus pubescens* Wild., *Quercus ilex* L., *Ostrya carpinifolia* Scop., and *Acer monspessulanum* L.) (Table 2). Brushwood resulting from limbing activities was piled on the upper side of the standards band to further mitigate water runoff and act as a barrier against rocks of varying sizes, reducing the risk of hazards to humans.

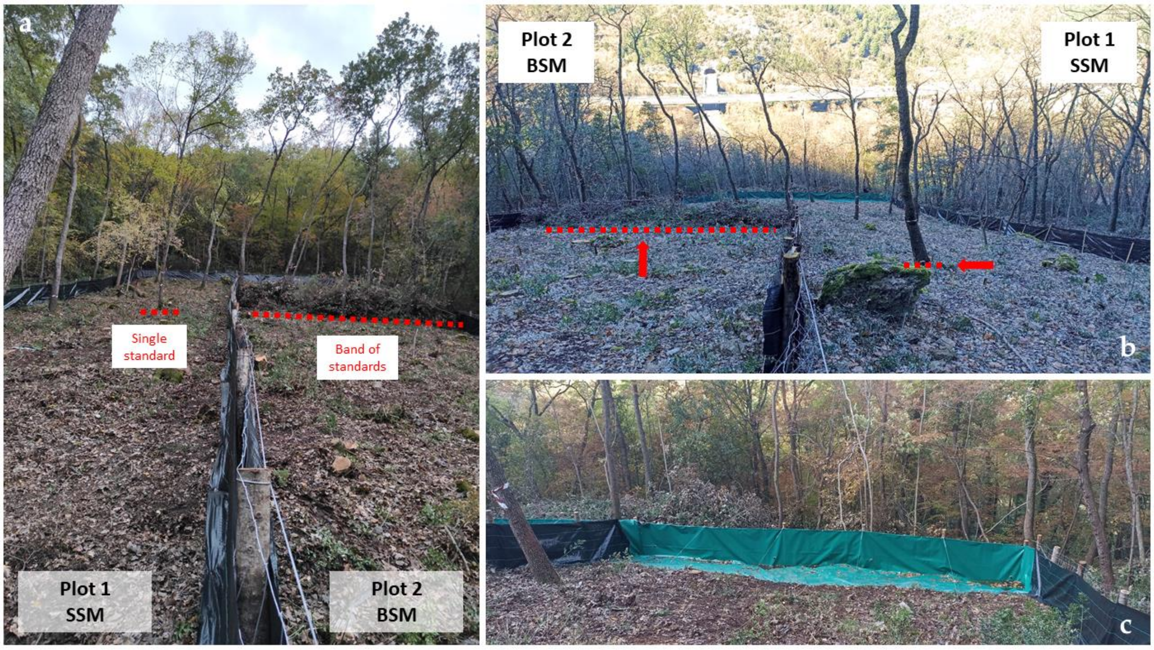

Figure 3. Views of silvicultural treatments applied in the study area: (a) from the bottom with Plot P1 on the left employs the Scattered Standards Method (SSM), while Plot P2 on the right uses the Banded Standards Method (BSM); (b) from the top with plot P2 (BSM) on the left and plot P1 (SSM) on the right. In plot P1, the typical standards disposition is visible, while in P2, the band of standards and the bundles of twigs are positioned on the base of them; (c)detailed view from above of the PVC collector installed at the bottom of the cut area.

Table 2. This table summarizes the main characteristics of the standards left after logging. Species, diameter (DBH), and height are noted. In particular, on the left are represented the standards inside Plot P1 (SSM), and on the right those in Plot P2 (BSM).

Plot P1 (SSM)			**Plot P2 (BSM)**		
Species	**DBH (cm)**	**h (m)**	**Species**	**DBH (cm)**	**h (m)**
Quercus pubescens	20	13.5	*Quercus pubescens*	17	13.5
Quercus pubescens	23.5	14	*Quercus pubescens*	13	13
Quercus pubescens	21	12.6	*Quercus pubescens*	15	14
Quercus ilex	14.5	14.4	*Quercus pubescens*	13	14.4
Ostrya carpinifolia	15.75	13.5	*Quercus pubescens*	17	13.5
Acer monspessulanum	27.5	14	*Quercus pubescens*	23	14
*Acer monspessulanum**	23-31.5	13.5	*Fraxinus ornus*	9	13.5

*bicormic

Hydrological and geological data

Recognizing that soil erosion within a specific area is influenced significantly by both the rainfall regime and soil properties [21], we conducted thorough analyses on these factors. For the rainfall regime assessment, we utilized data obtained from a rain gauge station of the Abruzzo Hydrological Centre (Centro Funzionale e Ufficio Idrologia, Idrografico, Mareografico - Agenzia di Protezione Civile della Regione Abruzzo) situated near the study area.

Our examination focused on the daily rainfall and temperature readings recorded at the station, spanning from November 2022 to December 2023. Furthermore, we employed the 2023 dataset to construct the 2023 Bagnouls-Gaussen diagram (Figure 2), enabling us to grasp the climatic variances between 2023 and the data averages spanning 1951 to 2000 [45].

In terms of soil analysis, a comprehensive field campaign was undertaken, during which we collected four soil samples from each plot. With the utmost care, the initial 20 cm were extracted through samplings at a distance of 12.5 m in a 30x30 cm plot. These samples were subsequently subjected to analysis to determine key soil parameters, including texture, Total Organic Carbon (TOC), and Soil Organic Matter (SOM). The findings of these soil analyses are presented in Table 3.

Table 3. Summary of soil analysis. The results are shown in percentage (%). The samples were taken every 10/15 m, from the bottom to the top of the plots, in the central part of them.

			Plot P1 (SSM)		
Sample	**1**	**2**	**3**	**4**	**Mean**
%					
Sand	70.0	71.5	71.5	87.7	75.2
Silt	13.2	21.0	6.9	8.2	12.3
Clay	16.8	7.5	21.6	4.1	12.5
TOC	5.0	5.7	4.3	3.8	4.7
SOM	8.5	9.8	7.3	6.6	8.0
			Plot P2 (BSM)		
Sample	**1**	**2**	**3**	**4**	**Mean**
%					
Sand	71.7	62.6	79.5	94.4	77.1
Silt	11.6	23.4	14.0	5.6	13.7
Clay	16.7	14.0	6.5	0.0	9.3
TOC	5.0	4.7	6.4	3.9	5.0
SOM	8.7	8.1	11.1	6.7	8.7

Experimental plot

Following the logging activities, we introduced a novel erosion control mechanism known as the Natural Erosion Trap (NET) or Diabrosimeter. This choice stemmed from the necessity for a larger plot compared to the traditional Wischmeier soil erosion plots, measuring 22.13 meters in length and 1.83 meters in width [49]. The forested study area demanded a larger footprint than agricultural settings due to the general high biodiversity, the presence of trees and their expansive canopies, which significantly influence erosion dynamics. Thus, there was a clear need for a solution that could be easily installed and removed, had minimal environmental impact, could adapt to various terrains including protected areas, and effectively mitigate risks associated with falling rocks within the study site.

The NET prototype was meticulously engineered to intercept water runoff, sediment, rocks, and organic debris. Its adaptable design facilitates deployment across diverse environmental conditions, accommodating variable slopes, and allowing customization in terms of shape and size to meet specific research objectives (see Figure 4).

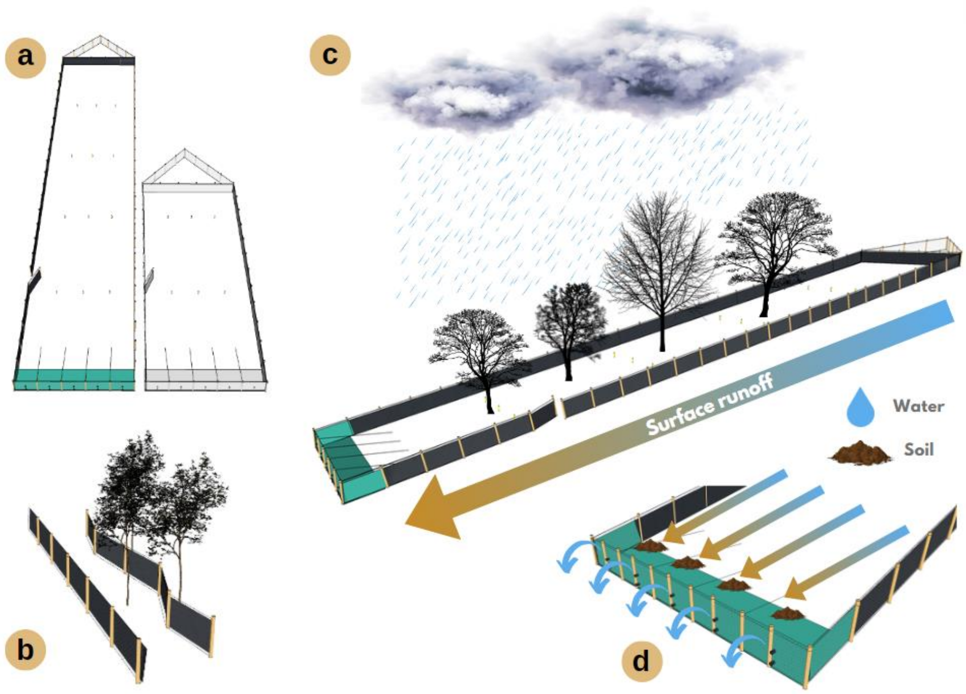

Figure 4. Features and operation of the NET erosion plot prototype: (a) plot length can be modulated; (b) plot perimeter can be easily adjusted to suit different environmental conditions; (c) the system operates by channeling surface runoff towards the base of the plot following rainfall events; (d) the collector receives water and eroded soil, with the soil settling while the water flows through nozzles.

The initial prototype we constructed features a rectangular configuration, with its shorter sides aligned parallel to contour lines and the longer sides perpendicular to these lines. Divided into two primary sections, the first serves as a protective barrier, effectively isolating the plot from its surroundings, while the second functions as the primary collection unit.

The protective barrier comprises a sturdy metallic mesh to shield the plot from external rockfall and other debris, complemented by a mulching film that serves to prevent ingress of water and sediment. This fencing component spans three sides of the plot, encompassing the top and longer edges.

Meanwhile, the collector section incorporates a reinforcing net structure along with a heavy-duty 900g/m^2 waterproof PVC tarpaulin, acting as the sediment collection apparatus. Both sections are affixed to wooden poles positioned along the perimeter at regular intervals, approximately two meters apart.

For installation, the fencing component is vertically embedded into the soil, while the collector's net is similarly inserted vertically. The PVC tarpaulin is partially secured horizontally to the soil, with its upper section buried about 10cm deep and the remainder fixed in conjunction with the net.

Additionally, the vertical section of the collector can accommodate nozzles, facilitating either water runoff collection or functioning as a relief valve (refer to Figure 5).

The vertical section of the collector effectively intercepts water and assorted sediments, while the horizontal component facilitates the flow of water and sediment toward the vertical portion. The robust fencing and the substantial PVC tarpaulin ensure that even sizable rock fragments are impeded, safeguarding the system from damage. Various methods exist for sediment retrieval, contingent upon forest type and topography. Options include employing nozzles connected to tubing and tanks for sediment and water collection, or alternatively, blocking the nozzles and utilizing a pump to extract water and sediment into tanks. In the absence of water, sediment can be directly retrieved from the collector. Additionally, depending on research objectives, pegs can be installed using the soil erosion pegs method depicted in Figure 5 [50–52].

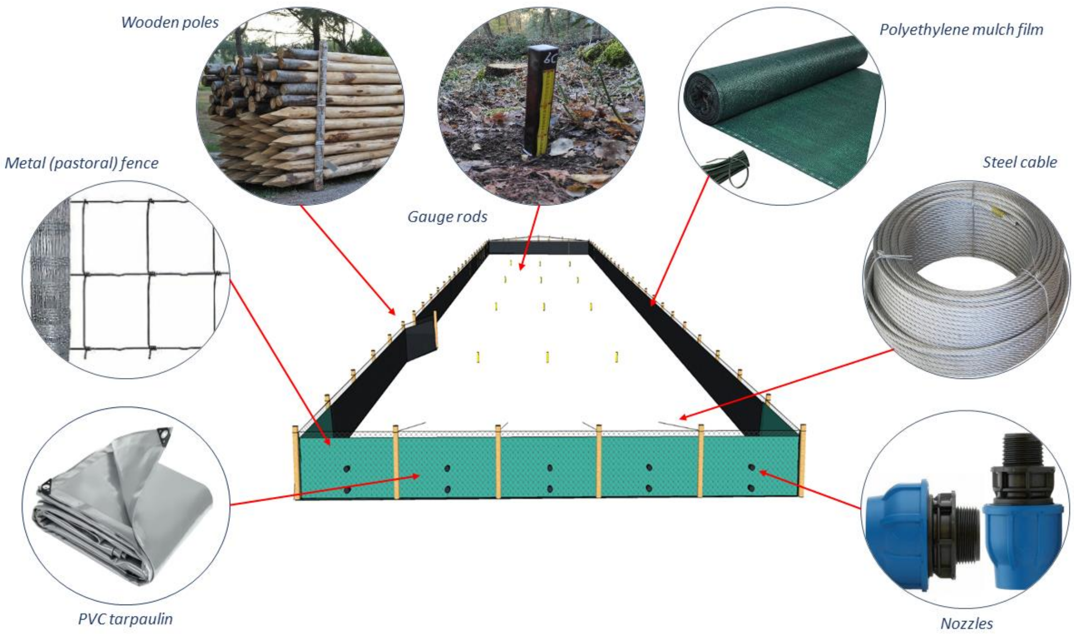

Figure 5. Overview of the erosion plot prototype elements.

Collection and analysis methodologies

The research team manually conducted the removal of sediments and leaves accumulated by the two NETs over the period from November 2022 to December 2023. This task typically involved two operators. The first operator accessed the site via a side entrance positioned in the middle of the left long side of the plot, cautiously minimizing ground disturbance while navigating along the perimeter to reach the collector. Meanwhile, the second operator remained outside the plot.

The picking process unfolded systematically, progressing from left to right in a prescribed sequence. Initially, surface materials, predominantly dead leaves, were gathered and placed into numbered bags. Next, residual water accumulated within the collector was suctioned out using a pump and stored in numbered tanks. Subsequently, sediment accumulated at the bottom of the collector was retrieved and stored in numbered containers. This sequence was repeated for the adjacent experimental plot, adhering to the same operational protocol.

Once the sediment, residual water, and leaves were removed from the plots, they were transported to the laboratory for further analysis. Initial processing involved cleaning the leaves to eliminate any adhering sediment, also to prevent potential fermentation within the bags. This cleaning procedure entailed soaking the leaves in water, followed by thorough cleaning, drying, and subsequent weighing after each collection.

Regarding sediment analysis, samples collected directly from the plots were naturally dried or oven-dried as appropriate. Sediment suspended in water tanks underwent a decanting process to separate the solid components, after which it was dried and combined with other sediment samples. Subsequent differentiation classified sediment into gravel (particles with a diameter greater than 2 mm) and fine sediment (particles with a diameter less than 2 mm, including sand, loam, and clay), achieved through the use of pedological sieves. The weights of the two sediment types were recorded and summed for each plot.

Results and discussion

The two NETs plots commenced operations effectively from November 4th, 2022, continuing until December 14th, 2023, spanning approximately 13 months. To ensure a meaningful comparison between the two plots and to accurately convert erosion results into square meters and hectares, we initially determined their respective areas and slopes. Plot P1 (SSM) exhibited a mean slope of 47.1% and covered an area of 373 m^2, while Plot P2 (BSM) featured a mean slope of 49.03% and occupied an area of 435 m^2. The combined average slope for both plots was calculated at 48.17%. As for leaf collection, we conducted multiple weightings throughout the year, whereas sediment weight measurements were undertaken only three times during the entire year.

Since the initial leaf collection, a notable disparity became evident between the two plots. Plot P1, managed using the SSM method, amassed a greater quantity of leaves compared to Plot P2, where the BSM method was applied. Plot P1 accumulated a total leaf weight of 6.4 kg, whereas Plot P2 amassed 3.8 kg.

These findings, however, did not factor in the variation in slope between the two plots. To address this, we adjusted the results proportionally considering the slope. Consequently, the weighted leaf mass of Plot P1 experienced a slight increase, rising from 6.4 kg to 6.6 kg, while Plot P2 saw a decrease, dropping from 3.8 kg to 3.7 kg. Subsequently, we divided the adjusted sum by the respective plot areas, revealing soil loss rates of 0.018 kg/m^{2}for Plot P1 (SSM) and 0.008 kg/m^2 for Plot P2 (BSM). Notably, the BSM method exhibited a 55.5% reduction in leaf loss compared to the SSM method (Table 4).

Table 4. Weighing results of the leaves collection. The first column shows the total rainfall that led to leaves loss. The second and third column show the results for plot P1 and plot P2, respectively. Each weight is associated with the date of collection.

		Plot P1	**Plot P2**
Collecting Date	**Total rainfall (mm)**	**Weight (g)**	
15/12/2022	240.6	1011	464.8

19/01/2023	56.4	632.7	588.6
16/02/2023	94.6	303.4	249.2
22/02/2023	0.2	330.6	159.6
08/03/2023	26	127.9	66.5
21/04/2023	132.8	766.1	399.5
05/05/2023	97.8	189.9	101.7
28/08/2023	117	391.3	225.1
28/10/2023	96	712	421.1
14/11/2023	42	273.3	126.8
14/12/2023	71.6	1670.9	947.7
Total (g)	-	6409.1	3750.6
Total (kg)	-	6.4	3.8
Plot Slope (%)	-	47.1	49
Mean Slope (%)	-	48.2	48.2
Total considering Slope	-	6.6	3.7
Area m^2	-	373.1	434.8
Total kg/m^2	-	**0.018**	**0.008**

After that first process of weighting, we looked on the rainfall that generated the leaves loss. Thanks to the data provided by the rain gauge of the Abruzzo Hydrological Centre (Centro Funzionale e Ufficio Idrologia, Idrografico, Mareografico - Agenzia di Protezione Civile della Regione Abruzzo), we could correlate the leaves loss inside the two plots with the rainfall that generated that loss. As evident, there exists a substantial correlation between rainfall, seasonal variations, and leaf loss. Particularly during November and December, an important leaf loss is observed, closely associated with both rainfall and the seasonal shedding typical of broadleaf forests. Despite potentially lower rainfall levels during this period compared to others, the majority of leaf shedding occurs, as exemplified by the January collection which yielded more leaves than that of February 16th. This trend persists throughout the year, with consistent leaf loss occurring even during periods of relatively lower total rainfall. Consequently, there is a continual loss of organic matter throughout the year, emphasizing the ongoing impact of leaf shedding on forest ecosystems (Table 5 and Figure 6).

As for Table 5, it is clear, looking to Table 5 and Figure 6, that the Plot P2 decrease the loss of leaves, letting think that this plot has a blocking effect on the leaves, so it could reduce the Organic Matter loss.

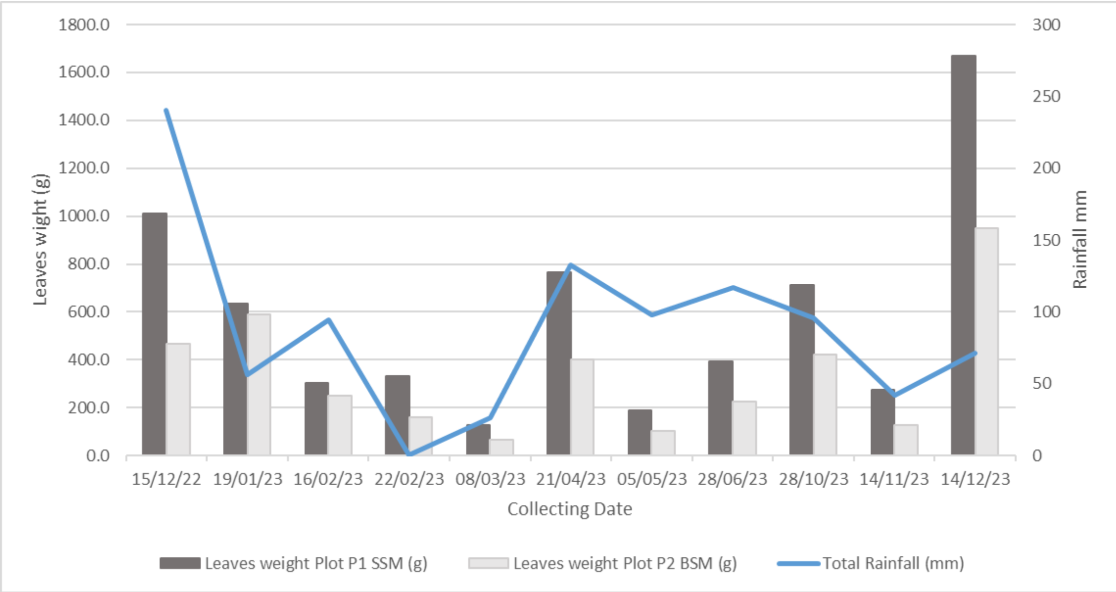

Figure 6. Relationship between rainfall and leaves loss, and the difference of leave loss between the two plots. Plot P1 is represented by the dark grey column, while the plot P2 by the light grey column.

Regarding the sediment collected by the two erosion plots, we faced limitations in conducting the same procedure as for the leaves. We could only conduct three weightings throughout the year, allowing us to establish correlations with rainfall and seasonal variations. Recognizing the significance of differentiating sediment types—rock fragments which, depending on their size, can pose risks to human health, while fine sediment affects only soil fertility—we initially categorized the collected sediment into gravel (with a diameter larger than 2 mm) and fine sediment (including sand, loam, and clay).

The results of this differentiation revealed that in Plot P1 (SSM), we collected 4508.1 g of gravel and 3698.4 g of fine sediment, while in Plot P2 (BSM), we collected 3486.2 g of gravel and 5039 g of fine sediment. Similar to the leaves, we adjusted the collected sediment weights based on slope and area to obtain values in kg/ha.

For Plot P1 (SSM), erosion rates were calculated at 123.5 kg/ha for gravel and 101.3 kg/ha for fine sediment, totaling 224.8 kg/ha. In Plot P2 (BSM), erosion rates were 78.8 kg/ha for gravel and 113.9 kg/ha for fine sediment, with a total erosion of 192.6 kg/ha. Notably, the BSM method exhibited lower erosion rates overall, with a 19% decrease in total soil erosion. While gravel erosion consistently favored Plot P1, fine sediment erosion initially favored Plot P2, though this trend equalized over the year. The final weighing showed a decrease in fine sediment erosion in Plot P2, attributed to its enhanced anti-erosive capacity one-year post-logging, suggesting better forest recovery and subsequent erosion mitigation. The results show promising differences.

For a better comprehension of the results, Table 5 shows the plot P1 and P2 results.

Table 5. Sediment weight of the Plot P1 (SSM) and Plot P2 (BSM).

	Sediment Weight Plot P1 SSM			**Sediment Weight Plot P2 BSM**		
Collecting Date	**Gravel**	**Fine Sediment**	**Total**	**Gravel**	**Fine Sediment**	**Total**
28/08/2023	4241.35	3202.96		3381	3672.6	
28/10/2023	195.7	234.4		66.4	245.4	
14/12/2023	71	261		38.8	121	
Total (g)	4508.1	3698.4	8206.4	3486.2	5039	8525.2
Slope (%)	47.13	47.13		49.03	47.13	
Mean Slope (%)	48.17	48.17		48.17	48.17	
Total with slope (g)	4607.5	3780	8387.5	3425	4950.6	8375.6
Area	373	373		435	435	
Total g/ha	123493.1	101312.5	224805.6	78772	113859.9	192631.9
Total kg/ha	**123.5**	**101.3**	**224.8**	**78.8**	**113.9**	**192.6**
%	**55**	**45**		**41**	**59**	

Apart from mitigating leaf and soil loss, the BSM method demonstrated effectiveness in averting large rock displacement. While Plot P1 experienced no obstructions from rocks, Plot P2 intercepted numerous rocks successfully. By integrating standards with bundled twigs, the method effectively prevented the movement of six rocks, collectively weighing 90.35 kg. Notably, these blocked rocks encompassed varying weights, including heavy ones, underscoring the method's pivotal role in ensuring human safety.

The results underscore the method's ability to address broader concerns beyond soil erosion. By obstructing rocks, the BSM method mitigates potential hazards and preserves environmental integrity, demonstrating its versatility across diverse terrains. Its successful application in Plot P2 highlights its adaptability to challenging conditions, validating its efficacy in sustainable land management. Continued research and implementation of the BSM method offer promise in mitigating soil erosion and enhancing environmental resilience. Integrating findings from this study into land management practices can inform the development of more robust erosion control strategies, ensuring the long-term health and sustainability of ecosystems globally. The ability of the BSM method to effectively block rocks complements its other benefits, making it a comprehensive solution for mitigating various forms of land degradation and promoting ecosystem health.

After converting all measurements to tons per hectare (t/ha), we conducted a comprehensive analysis of sediment accumulation in two plots, P1 and P2, showed in Table 6.

Table 6. Resume of the total sediment collected by the two erosion plots.

Sum of the sediments		
	Plot P1	**Plot P2**
Leaves	175.58	84.75
Sediment	224.8	192.6
Total kg/ha	400.37	277.35
Total t/ha	0.40	0.28
Rocks t/ha		2.07
Absolute total	0.4	2.35
Percentage decrease		30.72%

The sediment amassed in P1 totaled 0.40 t/ha, while P2 accumulated 0.28 t/ha. This calculation revealed a noteworthy 30.72% reduction in erosion for P2 compared to P1, indicating a potentially more effective erosion control strategy in the latter. Additionally, we assessed the impact of rock barriers installed in the area.

The weight of rocks obstructed by these barriers was quantified at 2.07 t/ha. Had the barriers not been in place, the erosion rate in P2 would have surged to 2.35 t/ha. This figure is staggering, representing a 487.5% increase over P1's erosion rate and 739.3% increase over the actual erosion rate in P2. The results indicate that there are encouraging differences.

The comparison between P1 and P2 highlights the effectiveness of such treatments, emphasizing the importance of implementing sustainable land management practices to combat erosion effectively.

This study not only provides valuable insights into erosion dynamics but also emphasizes the need for proactive measures to address soil erosion. Further research and implementation of erosion control strategies are warranted to mitigate the adverse effects of erosion on land and ecosystems worldwide.

From our experience, we can infer that within coppice forests in sloping areas, especially where there is a significant risk to human health (such as the presence of large rocky boulders), it might be prudent to employ our silvicultural model, known as the BSM. The data collected during the initial year of experimentation is preliminary and requires further verification over subsequent seasons, as there are no existing experimental data in the literature for comparison.

Regarding the considered silvicultural aspects, the preliminary results confirm the effectiveness of the BSM as a treatment to mitigate surface soil erosion risk. Our model successfully reduces erosion, particularly concerning large sediment, and prevents the loss of leaves and organic matter. These positive outcomes are attributed to the action of the bands of standards and the bundle of twigs, which act as effective barriers. Additionally, the BSM does not compromise wood production or forest owner profits, while simultaneously improving ecological efficiency. Notably, there are no reported technical inconveniences for forest users, and access methods and extraction procedures remain straightforward.

Regarding leaf loss, the BSM-treated plot shows a great reduction (55%) in litter removal. This finding underscores the influence of coppice management on gradual soil fertility decline. Due to frequent rotations compared to high forest management, the system lacks sufficient time for organic matter mineralization. Moreover, on sloping terrain, a substantial portion of litter is lost due to water erosion.

The NET (Natural Erosion Plot), although still a prototype, demonstrates usefulness and effectiveness. It effectively captures sediment of all types, even in the challenging context of a coppice forest with an average slope of 48%. Its applicability extends to various environments, and with modifications, it could potentially provide run-off data in addition to its existing capabilities.

Conclusions

This paper delves into a comprehensive investigation of two distinct forest management strategies aimed at mitigating soil erosion. Initial observations present promising prospects for erosion reduction, evident in differences in eroded material between the experimental plots. The innovative erosion monitoring system developed deserves attention, although the data collected during the inaugural year of experimentation are preliminary and warrant validation through subsequent seasons, given the absence of comparable experimental data in existing literature.

Examining the silvicultural dimensions under scrutiny, albeit in preliminary stages, the results affirm the efficacy of band of standards method as a viable approach for mitigating soil surface erosion risk in coppice forests.

In particular, two soil erosion plots were established, representing prototypes of a novel erosion monitoring apparatus called the Natural Erosion Trap (NET), or Diabrosimeter, specifically designed for forest environments. At regular intervals, particularly after significant storm events, sediment and leaf litter accumulated within the erosion plots were collected, dried, and weighed to quantify erosion rates and assess the efficacy of the silvicultural methods under investigation. The results revealed a 30.72% reduction in the eroded material with BSM compared to SSM, underscoring BSM's ability to mitigate potential hazards and preserve environmental integrity.

Analysis of materials captured in the traps also reveals a notable presence of microfauna alongside soil and litter, highlighting the occurrence of biological erosion—a phenomenon often overlooked in agricultural studies focusing on soils devoid of natural biological components.

To gather comprehensive scientific information on erosion measurement methods in forest environments and assess the efficiency of the NET erosion plot, further experiments are necessary. These experiments should be conducted in diverse locations, considering different soil types and various forest ecosystems. Overall, considering this research as a preliminary proof, there are compelling reasons to consider strip thinning as part of coppice management.

Patents

Supplementary Materials: The following supporting information can be downloaded at: www.mdpi.com/xxx/s1, Figure S1: A three-dimensional model of Plot P1 is shown.; Figure S2: A three-dimensional model of Plot P2 is shown.

Author Contributions (Acronyms as it follows: Pietro Salvaneschi: P.S., Antonio Pica: A.PC., Ciro Apollonio: C.A., Teodoro Andrisano: T.A., Massimo Pecci: M.P., Andrea Petroselli: A.PT, Bartolomeo Schirone: B.S.): Ideation, B.S; Conceptualization, C.A., A.PC., P.S. T.A. and B.S.; data gathering and field investigation, A.PC., P.S., and T.A.; methodology, C.A., P.S., M.P. and B.S.; data processing, A.PC. and P.S.; writing—original draft preparation P.S., A.PC., A.PT., B.S. and C.A.; figures and tables, P.S. and A.PC.; writing—review and editing of the final document by all authors; funding acquisition, B.S. and C.A.. All authors have read and agreed to the published version of the manuscript.

Funding: This research was funded by the Maiella National Park Authority. Also, this study was carried out within the Agritech National Research Center and received funding from the European Union Next-GenerationEU (PIANO NAZIONALE DI RIPRESA E

RESILIENZA (PNRR) – MISSIONE 4 COMPONENTE 2, INVESTIMENTO 1.4 – D.D. 1032 17/06/2022, CN00000022). This manuscript reflects only the authors' views and opinions, neither the European Union nor the European Commission can be considered responsible for them.

Data Availability Statement: Data are available on request to Authors.

Acknowledgments: The authors gratefully acknowledge: the Maiella National Park for authorizations; the Abruzzo Region that owns the forest, which granted the area for the study and authorized the cutting; the Carabinieri Biodiversity Department of Pescara, whose forestry workers carried out the cutting of the plots, and for the support received during the performed tests by in particular Lt. Col. Cristina Di Tommaso and Dr. Roberto Fracasso.

Conflicts of Interest: The authors declare no conflict of interest.

References

1. Yang, D.; Kanae, S.; Oki, T.; Koike, T.; Musiake, K. Global Potential Soil Erosion with Reference to Land Use and Climate Changes. Hydrol. Process. 2003, 17, 2913–2928, doi:10.1002/hyp.1441.
2. Alewell, C.; Borrelli, P.; Meusburger, K.; Panagos, P. Using the USLE: Chances, Challenges and Limitations of Soil Erosion Modelling. Int. Soil Water Conserv. Res. 2019, 7, 203–225, doi:10.1016/j.iswcr.2019.05.004.
3. Kumar, M.; Sahu, A.; Sahoo, N.; Dash, S.; Raul, S.K.; Panigrahi, B. Global-Scale Application of the RUSLE Model: A Comprehensive Review. Hydrol. Sci. J. 2022, 67, doi:10.1080/02626667.2021.2020277.
4. Van der Knijff, J.; Jones, R.; Montanarella, L. Soil Erosion Risk Assessment in Italy Available online: https://publications.jrc.ec.europa.eu/repository/handle/JRC19353 (accessed on 22 February 2024).
5. FAO Soil Erosion: The Greatest Challenge for Sustainable Soil Management. 2019.
6. Panagos, P.; Ballabio, C.; Himics, M.; Scarpa, S.; Matthews, F.; Bogonos, M.; Poesen, J.; Borrelli, P. Projections of Soil Loss by Water Erosion in Europe by 2050. Environ. Sci. Policy 2021, 124, 380–392, doi:10.1016/j.envsci.2021.07.012.
7. FAO; ITPS Status of the World's Soil Resources: Main Report. 2015.
8. Wuepper, D.; Borrelli, P.; Finger, R. Countries and the Global Rate of Soil Erosion. Nat. Sustain. 2020, 3, 51–55, doi:10.1038/s41893-019-0438-4.
9. Li, P.; Wu, J.; Zhou, W.; LaMoreaux, J.W. Hazard Hydrogeology; Environmental Earth Sciences; Springer International Publishing: Cham, 2023; ISBN 978-3-031-48426-1.
10. Pimentel, D. Soil Erosion: A Food and Environmental Threat. Environ. Dev. Sustain. 2006, 8, 119–137, doi:10.1007/s10668-005-1262-8.
11. Adornado, H.A.; Yoshida, M.; Apolinares, H.A. Erosion Vulnerability Assessment in REINA, Quezon Province, Philippines with Raster-Based Tool Built within GIS Environment. Agric. Inf. Res. 2009, 18, 24–31, doi:10.3173/air.18.24.

12. Karamage, F.; Shao, H.; Chen, X.; Ndayisaba, F.; Nahayo, L.; Kayiranga, A.; Omifolaji, J.K.; Liu, T.; Zhang, C. Deforestation Effects on Soil Erosion in the Lake Kivu Basin, D.R. Congo-Rwanda. Forests 2016, 7, 281, doi:10.3390/f7110281.
13. Poesen, J. Soil Erosion in the Anthropocene: Research Needs. Earth Surf. Process. Landf. 2018, 43, 64–84, doi:10.1002/esp.4250.
14. Zhao, L.; Hou, R. Human Causes of Soil Loss in Rural Karst Environments: A Case Study of Guizhou, China. Sci. Rep. 2019, 9, 3225, doi:10.1038/s41598-018-35808-3.
15. Borrelli, P.; Alewell, C.; Alvarez, P.; Anache, J.A.A.; Baartman, J.; Ballabio, C.; Bezak, N.; Biddoccu, M.; Cerdà, A.; Chalise, D.; et al. Soil Erosion Modelling: A Global Review and Statistical Analysis. Sci. Total Environ. 2021, 780, 146494, doi:10.1016/j.scitotenv.2021.146494.
16. Kavian, A.; Azmoodeh, A.; Solaimani, K. Deforestation Effects on Soil Properties, Runoff and Erosion in Northern Iran. Arab. J. Geosci. 2014, 7, 1941–1950, doi:10.1007/s12517-013-0853-1.
17. Borrelli, P.; Panagos, P.; Märker, M.; Modugno, S.; Schütt, B. Assessment of the Impacts of Clear-Cutting on Soil Loss by Water Erosion in Italian Forests: First Comprehensive Monitoring and Modelling Approach. CATENA 2017, 149, 770–781, doi:10.1016/j.catena.2016.02.017.
18. Riquetti, N.B.; Beskow, S.; Guo, L.; Mello, C.R. Soil Erosion Assessment in the Amazon Basin in the Last 60 Years of Deforestation. Environ. Res. 2023, 236, 116846, doi:10.1016/j.envres.2023.116846.
19. Apollonio, C.; Petroselli, A.; Tauro, F.; Cecconi, M.; Biscarini, C.; Zarotti, C.; Grimaldi, S. Hillslope Erosion Mitigation: An Experimental Proof of a Nature-Based Solution. Sustainability 2021, 13, 6058, doi:10.3390/su13116058.
20. Wischmeier, W.H.; Smith, D.D. Predicting Rainfall-Erosion Losses from Cropland East of the Rocky Mountains: Guide for Selection of Practices for Soil and Water Conservation; Agricultural Research Service, U.S. Department of Agriculture, 1965;
21. Wischmeier, W.H.; Smith, D.D. Predicting Rainfall Erosion Losses: A Guide to Conservation Planning; Department of Agriculture, Science and Education Administration, 1978;
22. Kinnell, P.I.A. Event Soil Loss, Runoff and the Universal Soil Loss Equation Family of Models: A Review. J. Hydrol. 2010, 385, 384–397, doi:10.1016/j.jhydrol.2010.01.024.
23. Renard, K.G. Predicting Soil Erosion by Water: A Guide to Conservation Planning with the Revised Universal Soil Loss Equation (RUSLE); U.S. Department of Agriculture, Agricultural Research Service, 1997; ISBN 978-0-16-048938-9.
24. Laflen, J.M.; Flanagan, D.C. The Development of U. S. Soil Erosion Prediction and Modeling. Int. Soil Water Conserv. Res. 2013, 1, 1–11, doi:10.1016/S2095-6339(15)30034-4.
25. Petroselli, A.; Apollonio, C.; De Luca, D.L.; Salvaneschi, P.; Pecci, M.; Marras, T.; Schirone, B. Comparative Evaluation of the Rainfall Erosivity in the Rieti Province, Central Italy, Using Empirical Formulas and a Stochastic Rainfall Generator. Hydrology 2021, 8, 171, doi:10.3390/hydrology8040171.
26. Bagarello, V.; Di Piazza, G.V.; Ferro, V.; Giordano, G. Predicting Unit Plot Soil Loss in Sicily, South Italy. Hydrol. Process. 2008, 22, 586–595, doi:10.1002/hyp.6621.
27. Bagarello, V.; Di Stefano, C.; Ferro, V.; Pampalone, V. Using Plot Soil Loss Distribution for Soil Conservation Design. CATENA 2011, 86, 172–177, doi:10.1016/j.catena.2011.03.009.<

28. Stott, T.; Leeks, G.; Marks, S.; Sawyer, A. Environmentally Sensitive Plot-Scale Timber Harvesting: Impacts on Suspended Sediment, Bedload and Bank Erosion Dynamics. J. Environ. Manage. 2001, 63, 3–25, doi:10.1006/jema.2001.0459.

29. An, S.; Zheng, F.; Zhang, F.; Van Pelt, S.; Hamer, U.; Makeschin, F. Soil Quality Degradation Processes along a Deforestation Chronosequence in the Ziwuling Area, China. CATENA 2008, 75, 248–256, doi:10.1016/j.catena.2008.07.003.

30. Fernandez, C.; Wu, J.Q.; McCool, D.K.; Stöckle, C.O. Estimating Water Erosion and Sediment Yield with GIS, RUSLE, and SEDD. J. Soil Water Conserv. 2003, 58, 128–136.

31. Farhan, Y.; Nawaiseh, S. Spatial Assessment of Soil Erosion Risk Using RUSLE and GIS Techniques. Environ. Earth Sci. 2015, 74, 4649–4669, doi:10.1007/s12665-015-4430-7.

32. Ganasri, B.P.; Ramesh, H. Assessment of Soil Erosion by RUSLE Model Using Remote Sensing and GIS - A Case Study of Nethravathi Basin. Geosci. Front. 2016, 7, 953–961, doi:10.1016/j.gsf.2015.10.007.

33. Phinzi, K.; Ngetar, N.S. The Assessment of Water-Borne Erosion at Catchment Level Using GIS-Based RUSLE and Remote Sensing: A Review. Int. Soil Water Conserv. Res. 2019, 7, 27–46, doi:10.1016/j.iswcr.2018.12.002.

34. Eniyew, S.; Teshome, M.; Sisay, E.; Bezabih, T. Integrating RUSLE Model with Remote Sensing and GIS for Evaluation Soil Erosion in Telkwonz Watershed, Northwestern Ethiopia. Remote Sens. Appl. Soc. Environ. 2021, 24, 100623, doi:10.1016/j.rsase.2021.100623.

35. Weslati, O.; Serbaji, M.-M. Spatial Assessment of Soil Erosion by Water Using RUSLE Model, Remote Sensing and GIS: A Case Study of Mellegue Watershed, Algeria–Tunisia. Environ. Monit. Assess. 2023, 196, 14, doi:10.1007/s10661-023-12163-z.

36. Kinnell, P.I.A. A Review of the Design and Operation of Runoff and Soil Loss Plots. CATENA 2016, 145, 257–265, doi:10.1016/j.catena.2016.06.013.

37. Trigila, A.; Iadanza, C.; Lastoria, B.; Bussettini, M.; Barbano, A. Dissesto Idrogeologico in Italia: Pericolosità e Indicatori Di Rischio, 356 2021; 2021; ISBN 978-88-448-1085-6.

38. EEA Climate Change Adaptation and Disaster Risk Reduction in Europe — European Environment Agency Available online: https://www.eea.europa.eu/publications/climate-change-adaptation-and-disaster (accessed on 22 February 2024).

39. Del Favero, R. Progetto Boschi Del Parco Regionale Dei Colli Euganei. Pubblicazione Del Parco Regionale Dei Colli Euganei; Pubblicazione del Parco Regionale dei Colli Euganei: Grafica Atestina. Este (PD), 2001;

40. Schirone, B.; Salvaneschi, P.; Cianfaglione, K.; Pecci, M.; Andrisano, T.; Vessella, F.; Petroselli, A. A Proposal for Modifying Coppicing Geometry in Order to Reduce Soil Erosion in the Forest Areas. Not. Bot. Horti Agrobot. Cluj-Napoca 2021, 49, 12325–12325, doi:10.15835/nbha49212325.

41. Geoportale Abruzzo Carta Dei Suoli Della Regione Abruzzo – ARSSA 2023.

42. ISPRA Istituto Superiore per La Protezione e La Ricerca Ambientale. Carta Geologica d'Italia Alla Scala 1:50.000. Foglio 369 "Sulmona". 2005.

43. Pesaresi, S.; Galdenzi, D.; Biondi, E.; Casavecchia, S. Bioclimate of Italy: Application of the Worldwide Bioclimatic Classification System. J. Maps 2014, 10, 538–553, doi:10.1080/17445647.2014.891472.
44. Peel, M.C.; Finlayson, B.L.; McMahon, T.A. Updated World Map of the Köppen-Geiger Climate Classification. Hydrol. Earth Syst. Sci. 2007, 11, 1633–1644, doi:10.5194/hess-11-1633-2007.
45. Giuliani, D.; Antenucci, F. Valori Medi Climatici Dal 1951 al 2000 Nella Regione Abruzzo. Servizio Presidi Tecnici Di Supporto al Settore Agricolo – DPD023. Ufficio Coordinamento Servizi Vivaistici e Agrimeteo - Scerni (CH). 2017.
46. Pirone, G.; Ciaschetti, G.; Frattaroli, A.R. La caratterizzazione fitosociologica dei boschi in Abruzzo. La Carta Tipologico-Forestale della Regione Abruzzo. Regione Abruzzo, Struttura Speciale di Supporto Sistema Informatico Regionale, Direzione Politiche Agricole e di Sviluppo Rurale, Forestale, Caccia e Pesca, Emigrazione. Volume generale, 49-62. 2009.
47. Pirone, G. Alberi, Arbusti e Liane d'Abruzzo. 2a Edizione. Penne (PE).; 2014;
48. Polycam Available online: https://poly.cam/ (accessed on 3 June 2024).
49. Carollo, F.G.; Serio, M.A.; Pampalone, V.; Ferro, V. The Unit Plot of the Universal Soil Loss Equation (USLE): Myth or Reality? J. Hydrol. 2024, 632, 130880, doi:10.1016/j.jhydrol.2024.130880.
50. Takei, A.; Kobashi, S.; Fukushima, Y. Erosion and Sediment Transport Measurement in a Weathered Granite Mountain Area. 1981.
51. Smith, H.G.; Dragovich, D. Post-Fire Hillslope Erosion Response in a Sub-Alpine Environment, South-Eastern Australia. CATENA 2008, 73, 274–285, doi:10.1016/j.catena.2007.11.003.
52. Borrelli, P. Risk Assessment of Human-Induced Accelerated Soil Erosion Processes in the Intermountain Watersheds of Central Italy. 2011.

5. Popoli study area soil erosion estimation

Introduction

In addition to the experimental field campaign explained in chapter 4, we decided to estimate soil erosion inside the two plots using the RUSLE model (Renard et al, 1997). We estimated soil erosion before and after the logging, to have a better comprehension of the impact of logging in soil erosion terms. We used the results also for a comparison between the erosion collected by our erosion plots (chapter 4, CITAZIONE NUOVO ARTICOLO), and the soil erosion calculated with the RUSLE models.

Before the creation of the model and in order to be able compare the two plots, it has been necessary to obtain the real GPS position and the real surface of the two plots. Those data were essential to the positioning of the two plots in the space and to the evaluation of soil erosion. Infact because of the difficulties related to work in forest environments, the two plots had not the same area, and the same position as predicted at the beginning.

In order to obtain such data, we first create a dense point cloud of the two plots, then from the point cloud a Digital Surface Model, DSM. We used the DSM to obtain the area and a mask of the two plots. The real surface of the plots was used to be able to compare the erosion collected by the erosion plot inside them. The masks were used to extract the soil erosion map of the two plots using the RUSLE model.

The dense point cloud was created by using the Lidar module of the iPhone 14 pro, in combination with the application Pix4dcatch.

Lidar, acronyms of Light Detection and Ranging (Collis, 1966), is a remote sensing method that uses a pulsed light laser to measure variable distances to the Earth (NOOA). The sensor emits light pulses into the surrounding environment. These pulses bounce off surrounding objects and return to the sensor. The sensor uses the time it took for each pulse to return to the sensor to calculate the distance it travelled, knowing the velocity of light, that is constant. Repeating this process millions of times per second, the lidar sensor create a 3d map called lidar point cloud that we used to obtain the real surface of the two plots.

New iPhone pro has a small Lidar sensor integrated on the cameras, and it is beginning to be used by researchers (Mikita et al., 2022; Monsalve et al., 2023; Tatsumi et al., 2023) in order to create dense point cloud.

Once that a field campaign was carried out, where the two plots were filmed using the Pix4dcatch app, the data collected were processed using the software Pix4Dmatic. The results of the process were, as mentioned before, two 3d model and two DSM of the plots, that we used for the estimation of their surface and as masks for the extraction of the soil erosion maps (figure 5.1 A, B). Thanks to the DSM created we could also discover the real area of the two plots that was 373m^2 for the plot P1, the one where the SSM method was done, and 435m^2 for the plot P2, the one where the BSM method was done.

Once this first step was done, we carried out the RUSLE model of the two plots, before and after the logging.

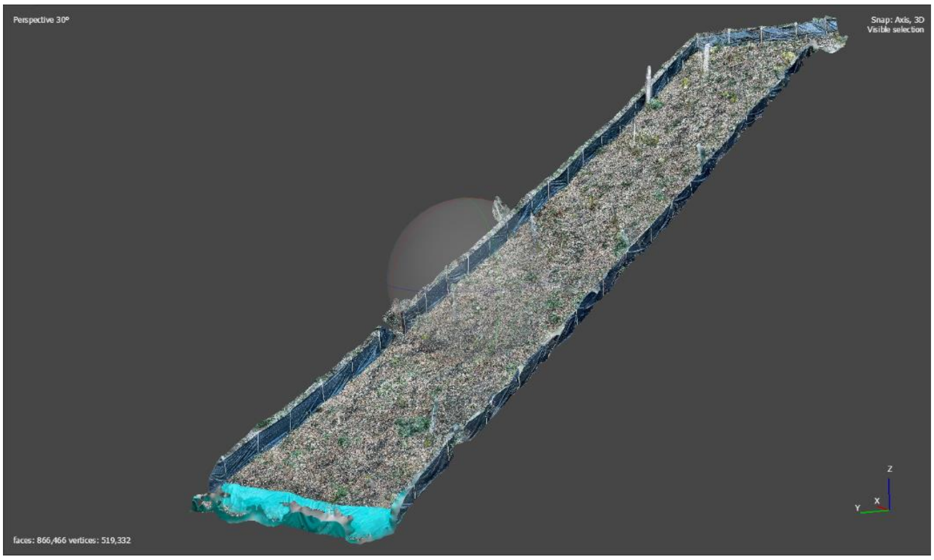

(A)

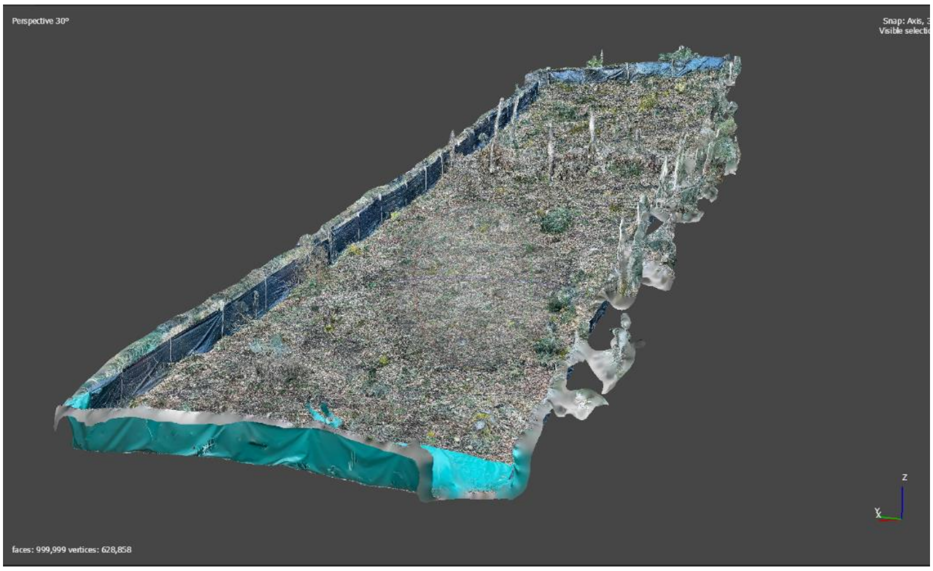

(B)

Figure 5.1. 3d model of the two plots. A: 3d model of plot P1 SSM. B: 3d model of plot P2 BSM.

RUSLE model

The RUSLE model, as the USLE equation (Wischmeier and Smith, 1978), is formed by the product of different factors. The only difference between them is that in the RUSLE, the factors values are substituted by maps representing them.

The RUSLE equation is formulated as follows:

A = LS x R x K x C x P

Where:

A = Annual soil erosion (t/ha/year),

LS= Length slope factor (-),

R = Rainfall erosivity factor (MJ*mm/ha/h/year),

K = Soil erodibility factor (t*h/MJ/mm),

C = Soil coverage factor (-),

P = Erosion control measures factor (-).

LS factor

The LS factor is related to the length and slope of a specific area, Longer and steeper is the study area, bigger will be the soil erosion (Chapter 2, Schirone et al., 2021). The only difference between the LS factor map and the traditional LS factor equation is that the length of the equation is substitute by a map of the Specific Contributing Area, and the slope by a map of the slopes (Hrabalíková and Janeček, 2017).

We choose to use the equation by Moore and Burch (1986) and Moore and Wilson (1992) as follows, according with Hrabalíková and Janeček (2017):

LS = (As/22.13)m $\times$ (sin β /0.0896)n

Where:

As: Specific Contributing Area = Flow Accumulation map (FA) * pixel dimension,

β : Slope map of the study area, slope calculated in radians,

m: factor with values that range from 0.4 to 0.6, we chose 0.4,

n: factor with values that range from 1.22 to 1.30, we chose 1.3.

For the creation of the slope maps and the As (FA map*pixel dimension) maps, we used a Digital Terrain Model (DTM), with a resolution of 1m2, provided by Italian National Geoportal (MASA). The maps realised are maps with different values, each pixel represents a LS factor value.

R factor

The R factor is related to the erosivity power of a rainstorm. It is obtained by summing, for each rainstorm, the product of total storm energy (E), expressed in MJ/ha, and the maximum 30-minute intensity (I30), expressed in mm/min, (Chapter 2, Schirone et al, 2021). Because of the difficulties related to have that kind of data, multiple equations have been created to calculate that factor easily (Chapter 3, Petroselli et al., 2021). According to our research made in the province of Rieti (chapter 3 Petroselli et al, 2021), we chose to use the three equations that fit better in the Province of Rieti, that they could be considerate the three equations that fit better for the internal part of central Italy. After the calculation of the three R factors, we did the mean of them and then we digitalize the result as a raster map with a single value.

The rainfall data were provided by the Abruzzo Hydrological centre (Centro Funzionale e Ufficio Idrologia, Idrografico, Mareografico - Agenzia di Protezione Civile della Regione Abruzzo). Thanks to the data provided we had the possibility to use daily rainfall data of a rain gauge located 3.5km far from the study area. We analysed one year of rainfall data from the 1st of November 2022 to the 31st of October 2023.

The three equation that we used are the following:

1) R factor formula by Yu and Rosewell (1996):

R = 3.82 x MFI1.41

Where:

MFI: Modified Fournier Index MFI = $\sum_{i=1}^{12} \frac{p_i^2}{P}$

pi: average monthly precipitation

P: average annual precipitation.

2) R factor formula by De Santos Loureiro and De Azevedo Coutinho (2001):

R = $\sum_{1}^{12} Ei_{30}$

Where:

Ei30 = 7.05*RAIN10 - 88.92*DAYS10

DAYS10 = sum of the days in a month where it rained more than 10 mm,

RAIN10 = mean monthly precipitation in those months where it rained,

more than 10 mm in a day.

3) R factor formula by Ferreira and Panagopoulos (2014):

$R = \sum_{1}^{12} Ei_{30}$

Where:

Ei30 = 6.56*RAIN10 – 75.09*DAYS10

DAYS10 = sum of the days in a month where it rained more than 10 mm,

RAIN10 = mean monthly precipitation in those months where it rained,

more than 10 mm in a day.

K factor

The K factor is related to the capacity of the soil to be eroded after a rainfall event. The factor was calculated by using the software KUERY 1.5 (Borselli et al. 2012) in application to the soils analyses that we carried out. Indeed, Given the principal soil analysis (percentages of loam, sand, clay, and organic material), the percentage of the rock fragment, and the climate type, the software uses an algorithm to calculate the K factor. We performed soils analyses on 4 soil samples each plot. After that process we calculated all the K factors, and we did the average. creating a mean K factor. Using the values obtained we built a raster map with a single value.

C factor

C factor is related to the capacity of the vegetation cover to mitigate soil erosion. Because there is a correlation between tree canopy and soil erosion, researchers have demonstrated that there is a correlation between the NDVI (Normalized Difference Vegetation Index) and the C factor (Almagro et al, 2019). Between the two more cited equation (Van der Knjiff et al, 1999, Durigon et al, 2014) we chose to use the one by Durigon et al. (2014) as it follows:

$C = 0.1 * \left(\frac{-NDVI+1}{2}\right)$

Where:

NDVI: Normalized Difference Vegetation Index $(\frac{NIR-RED}{NIR+RED})$

NIR: the surface spectral reflectance in the Near-Infrared band

RED: is the surface spectral reflectance in the Red band.

The result of this equation is a map where all the values represent a C factor value.

The calculation of the C factor was possible thanks to the data provided by the ESA Mission SENTINEL 2. This satellite mission provides multispectral images of any location around the world, and it passes over the same place more than once a month, so it is possible to check the past and present changes of a specific area. The satellite images have a resolution of 10m2. Once determined the kind of research to do, is it possible, using the Copernicus web site (https://browser.dataspace.copernicus.eu/), to search for images from the data that the mission was launched till today. It is possible to see a preview of the image and if there are no cloud it is possible to download a pack of images, containing an image for every sensor presents inside the satellite. The NIR and RED images are respectively the B8 sensor and the B4 sensor images. We downloaded a pack of images per moths from November 2021 till November 2023 in order to create two different c factor maps, one with the values after the logging and the other with the value before the logging.

P factor

Finally, the P factor is related to the agricultural procedures done with the aim to reduce the soil erosion. This factor is not considered in natural environments, so we didn't take that factor into account.

Results

RUSLE estimation

LS factor

The LS factor, as mentioned in the previous chapter was calculated using the Moore and Burch (1986) and Moore and Wilson (1992) equation. We started the process by using the DTM provided by the Italian Ministry of the Environment. We use that map to create the Flow Accumulation map, and the slope maps. After these processes we used the FA map to create the L factor part of the equation and the slope map, after that it was converted to radians, to create the S factor part. Once we had the L factor map and the S factor map, we multiplied them together obtaining the map showed in figure 5.2. In the map the LS valued are coloured in different kinds of blue, light blue seems low values of LS, while dark blue represents high values of LS. The two polygons represent the two-erosion plot. As it possible two see, comparing with other areas of the maps, the LS factor of the two plots it is not so high, but are very visible the micro watersheds where the most part of soil erosion will take part. The values of LS factor ranged from 0 to 214.1. As specified before LS factor is dimensionless.

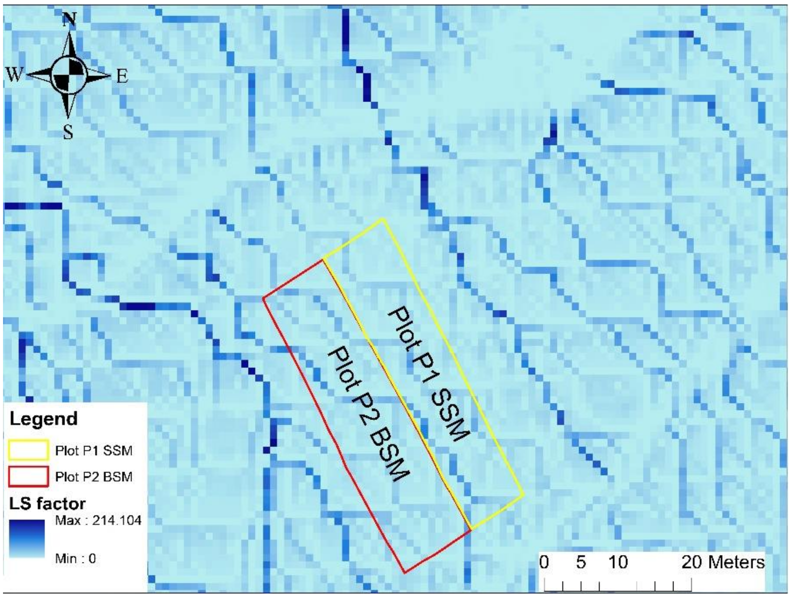

Figure 5.2: The figure shows the LS factor of the study area. From light blue to dark blue the LS factor is increasing. The two polygons represent the two plots, in yellow the plot P1, SSM, in red the plot P2, BSM.

R factor

The R factor was calculated by doing the average of the three equations that fit better in the internal part of central Italy (chapter 2, Petroselli et al., 2021). The results are showed in table 5.1. Once the average was done, we created a raster map with the average value that was 3210.16 MJ*mm/ha/h/year (figure 5.2). As it possible to see from table 5.1, all three values are similar, the second and the third are almost identical. That is because the third equation, Ferreira and Panagopoulos equation (2014), is an adaptation of the one made by De Santos Loureiro and De Azevedo Coutinho (2001). Is interesting to note that the values are similar even if the first equation is completely different from the other two.

Table 5.1: the table shows the R factor values of the study area using the three equations chosen, and the average values of them. The unit of measurement is MJ*mm/ha/h/year.

Equation	Value
Yu and Rosewell (1996)	3432.75
De Santos Loureiro and De Azevedo Coutinho (2001)	3099.48
Ferreira and Panagopoulos (2014)	3098.25
Average	**3210.16**

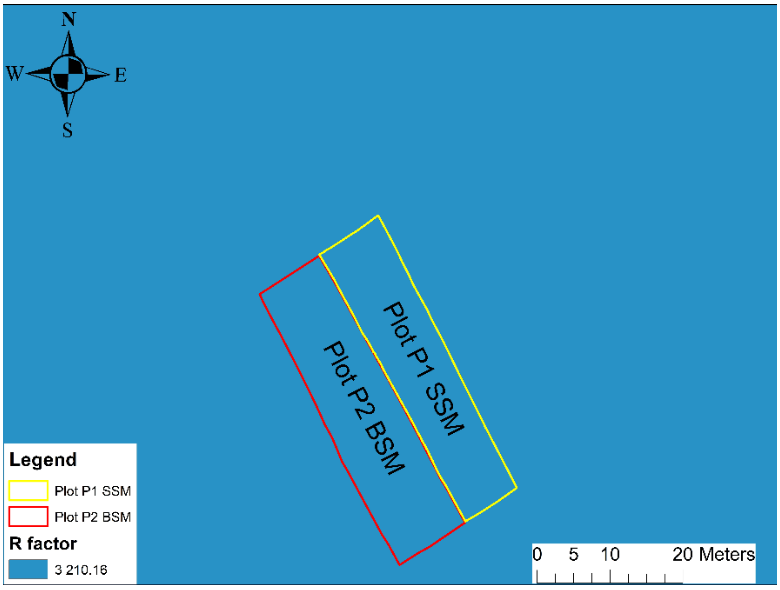

Figure 5.2: the figure shows the R factor map of the study area. The two polygons represent the two plots, in yellow plot P1, SSM in red Plot P2 BSM.

K factor

The K factor was created by using the software KUERY 1.5 (Borselli et al., 2012). Because our study area was very rocky, we had to put the percentage of rock fragments founded in the soil samples and then the percentage of sand and clay. The average of all the K factor was 0.0567 t*h/MJ/mm. As for the R factor map, we created a raster map with a single K factor value (figure 5.3).

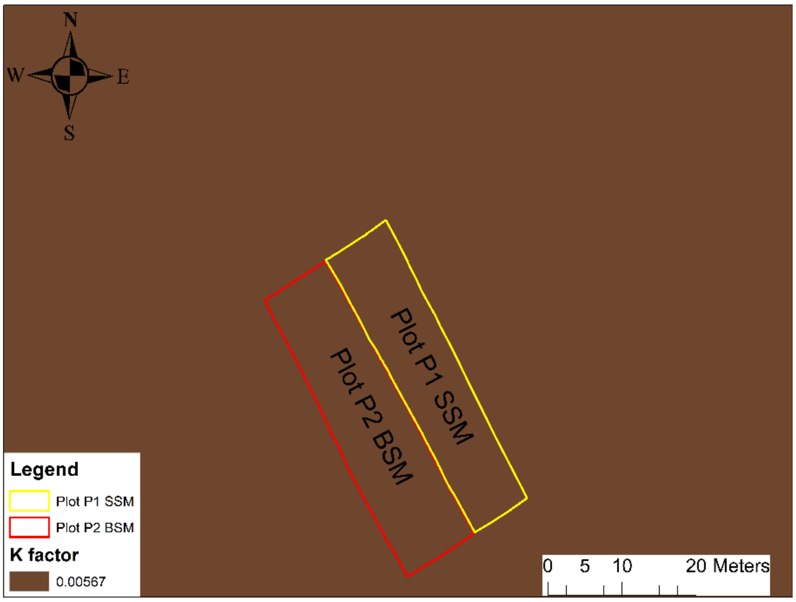

Figure 5.3: the figure shows the K factor map of the study area. The two polygons represent the two plots, in yellow plot P1, SSM in red Plot P2 BSM.

C factor

Regarding the C factor, differently from the other maps, we created two different maps. We first created a map containing the C factor values of the year before the logging was done (figure 5.4 A), and then a map containing the C factor value of the year after the logging was done (figure 5.4 B). As it possible to see in the figures, the colours vary from green to brown passing from low values to high values of the C factor. High values represent low NDVI values so low or no vegetation. It is clear seeing the maps, that the C factor of the study area changed a lot after the cut. The effect of the logging on the C factor and the NDVI is so strong that also other pixels outside the study area showed a decrease in the C factor. This is probably due to the dimension of the pixel, that is high for the type of the study that we did. Probably the C factor of our area could be less than what we had, but around the study area it could be greater than the result obtained.

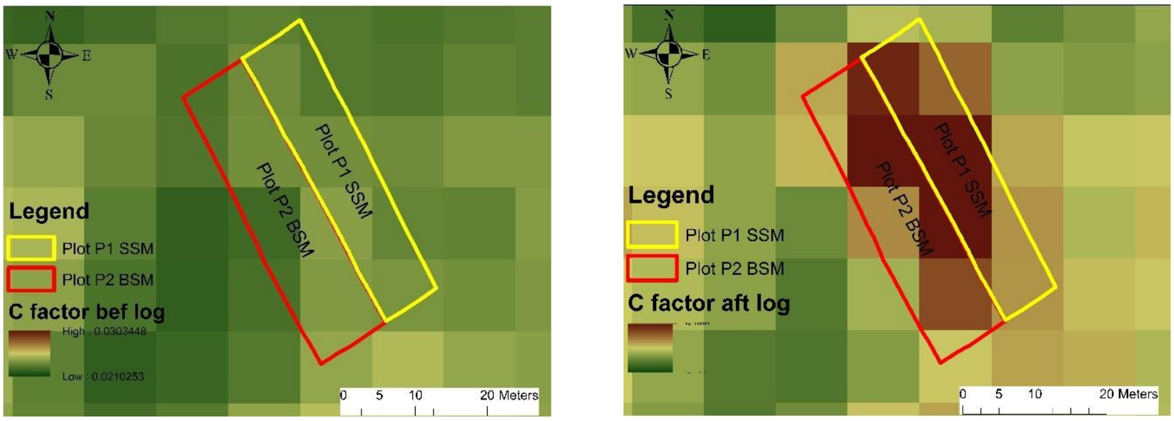

(A) (B)

Figure 5.4: This figure shows the c factor values of the study area before (A) and after (B) the logging.

RUSLE

Once all the maps were created, we multiplied the LS factor, R factor, K factor, once with the C factor map before the logging and then with the C factor map after the logging.

After that, using the polygon representing the two plots, we extracted a soil erosion map for each plot, before and after the cut and finally we calculate the mean soil erosion of them (figure 5.5 A and B). As it possible to see from the figures soil erosion increased after the logging and it was concentrated in the micro watershed where we had the higher LS factor values. The results showed an increase of soil erosion after the cut. Indeed, soil erosion in plot P1 passed from 1.84 t/ha/y to 2.24 t/ha/y, while in the plot P2 the soil erosion passed from 1.7 t/ha/y to 2.06 t/ha/y. In the plot P1 case we had a 21.74% increase of soil erosion, while in the plot P2 a 21.21% Increase. Because we saw that soil erosion had increased less in the Plot P2, the one logged using the Banded standard method, BSM, our proposed method, we calculated the percentage of decrease of soil erosion using the BSM method, compared with the Scattered Standard Method, SSM, the traditional method. We calculated an 8.21% decrease of soil erosion in plot P2 compared with the plot P1. Table 5.2 shows a resume of the results obtained.

Table 5.2: the table shows the RUSLE results for each plot both before and after the cut.

Soil erosion (t/ha/y)		
	Plot P1 SSM	**Plot P2 BSM**
Before logging	1.84	1.69612069
After logging	2.24	2.056034483
Difference	0.40	0.36
Soil erosion increasing (%)	21.74	21.21
Erosion degrease P2/P1 (%)	8.21%	

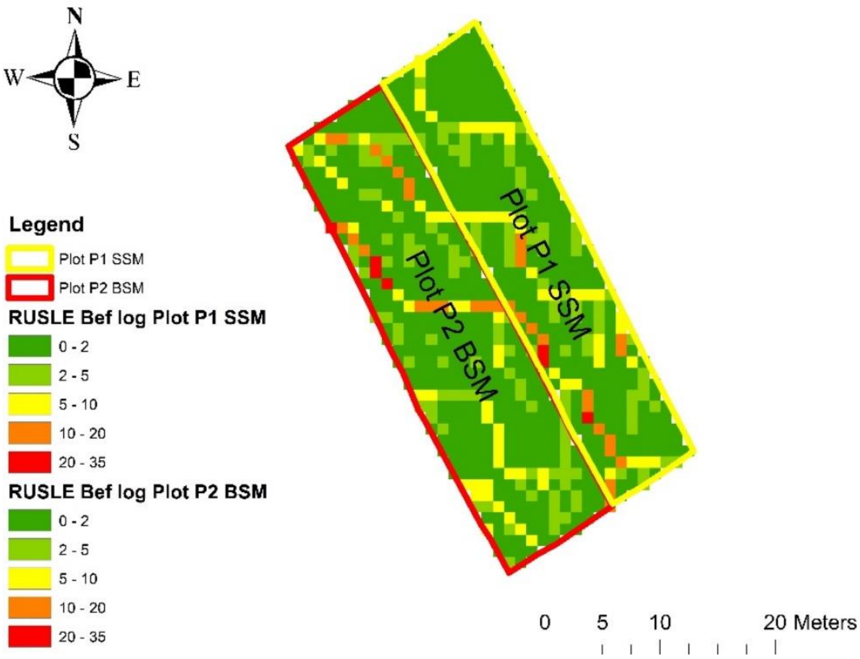

(A)

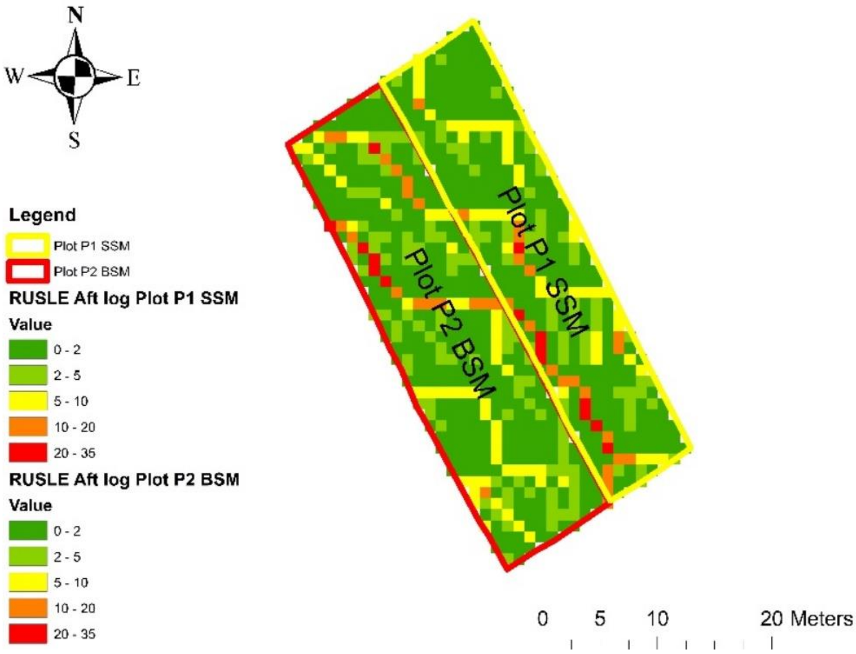

(B)

Figure 5.5: the figure shows the annual soil erosion before (A) and after (B) the cut, both in the two plots, plot P1 is represented by the yellow polygon, while P2 is represented by the red one.

Discussion and Conclusions

RUSLE is a good way to estimate the potential erosion of a place, its simple use overcomes the errors that the equation brings. The most important factor involved in the increase of soil erosion is the C factor, indeed, in our research we saw an increase of soil erosion passing from a situation of no log to the situation after the log, but the only map that change was the C factor map.

We noted an increase of soil erosion after the logging and also different erosion between the two plots. The Plot P2, the one where we used the BSM method, had less erosion than the plot P1. This result let us think that the banded standard arrangement, somehow modify the C factor decreasing it in comparison with the Scattered standard arrangement.

Comparing the results obtained with the results of our field experiment, we can see great differences between the real soil erosion after the logging and the potential soil erosion, the one made using the RUSLE. Infact, in the field experiment, we collected 0.224 t/ha/y in the plot P1, SSM, and 0.196 t/ha/y in the plot P2, BSM, while with the RUSLE model we obtained a potential soil erosion of 2.24 t/ha/y in plot P1 and 2.05 t/ha/y in plot P2. We also noted a difference in the percentage of decrease of soil erosion from the real experiment to the RUSLE model. In the real experiment the percentage of decrease from plot P2 to plot P1 was 14.32% while in the model was 8.21%. Actually, the percentage of decrease was even more, in this percentage we only counted the sediment and not the leaves collected, and the rock blocked by the standards and the bundle of twigs. The explanation of this difference is that the RUSLE consider only the canopy of the study area, but not the antierosive power of the sylvicultural model. The band of standards and the bundles of twigs posed on their top base, work as a real dam, and this effect is not contemplated in the RUSLE model. We can think that maybe it can be created a new factor, that can be called sylvicultural factor, that express the sylvicultural practice done with the aim of reducing soil erosion after the cut. This factor could work as the P factor.

Another interesting result is that the sediments collected by our soil erosion plots are less than the potential soil erosion before the logging. We think that it could be possible that the RUSLE model, even if is a good way to understand if there is erosion and where is located that erosion, is not well calibrated for steep forest. The USLE and the RUSLE were created for agricultural use and typically the agriculture is done in flat or not very steep lands. Agriculture in places with big slopes as our study area would be impossible, and there would be an incredible amount of erosion, mostly because of the agricultural practices. But a forest work differently from an agricultural field is not an artificial ecosystem, but an entire ecosystem working together. So naturally, a forest produces less erosion than an agricultural field. Unlucky the RUSLE model doesn't have a way to make a real distinction between the two ecosystem and is for that reason that we found great erosion in a place where we found less erosion even after the cut.

In any case the RUSLE model is useful to have a prediction of soil erosion, it can be a valid instrument in management, it can be used to understand the future prospective of a sylvicultural practice.

Finally, considering future studies, it could be good the implement of high detailed technologies as the use of drone technologies. Using a drone with multispectral camera, for example, it would be possible to create almost all the factor with the same size and the same position. Moreover, it would be possible to control the re-naturalization of the plots doing orthophotos regularly, something that is impossible to do using SENTINEL data because of the size of pixels ($100m^2$). This process, united with the collection on field of the soil erosion, could bring to a real validation of the RUSLE model and maybe a modification, implementing factors that consider the type of environment and if in forest the sylvicultural practice.

References

1. Almagro, A., Thomé, T. C., Colman, C. B., Pereira, R. B., Marcato Junior, J., Rodrigues, D. B. B., & Oliveira, P. T. S. (2019). Improving cover and management factor (C-factor) estimation using remote sensing approaches for tropical regions. *International Soil and Water Conservation Research*, *7*(4), 325–334. https://doi.org/10.1016/j.iswcr.2019.08.005
2. Borselli L, Torri D, Poesen J, Iaquinta P (2012). A robust algorithm for estimating soil erodibility in different climates. Catena 97:85-94. https://doi.org/10.1016/j.catena.2012.05.012
3. Collis, R. T. H. (1965). Lidar Observation of Cloud. Science, 149(3687), 978–981. https://doi.org/10.1126/science.149.3687.978
4. De Santos Loureiro, N., & De Azevedo Coutinho, M. (2001). A new procedure to estimate the RUSLE EI30 index, based on monthly rainfall data and applied to the Algarve region, Portugal. *Journal of Hydrology*, *250*(1), 12–18. https://doi.org/https://doi.org/10.1016/S0022-1694(01)00387-0
5. Durigon, V. L., Carvalho, D. F., Antunes, M. A. H., Oliveira, P. T. S., & Fernandes, M. M. (2014). NDVI time series for monitoring RUSLE cover management factor in a tropical watershed. *International Journal of Remote Sensing*, *35*(2), 441–453. https://doi.org/10.1080/01431161.2013.871081
6. Ferreira, V., & Panagopoulos, T. (2014). Seasonality of Soil Erosion Under Mediterranean Conditions at the Alqueva Dam Watershed. *Environmental Management*, *54*(1), 67–83. https://doi.org/10.1007/s00267-014-0281-3
7. Hrabalíková, M., & Janeček, M. (2017). Comparison of different approaches to ls factor calculations based on a measured soil loss under simulated rainfall. Soil and Water Research, 12(2), 69–77. https://doi.org/10.17221/222/2015-SWR
8. iPhone 14 pro, available on: https://www.apple.com/it/
9. Mikita, T., Krausková, D., Hrůza, P., Cibulka, M., & Patočka, Z. (2022). Forest Road Wearing Course Damage Assessment Possibilities with Different Types of Laser Scanning Methods including New iPhone LiDAR Scanning Apps. *Forests*, *13*(11). https://doi.org/10.3390/f13111763
10. Monsalve, A., Yager, E. M., & Tonina, D. (2023). Evaluating Apple iPhone LiDAR measurements of topography and roughness elements in coarse bedded streams. *Journal of Ecohydraulics*, 1–11. https://doi.org/10.1080/24705357.2023.2204087
11. Moore I.D., Burch G.J. (1986): Physical basis of the length-slope factor in the Universal Soil Loss Equation. Soil Science Society of America Journal, 50: 1294–1298.
12. Moore I.D., Wilson J.P. (1992): Length-slope factors for the Revised Universal Soil Loss Equation: Simplified method of estimation. Journal of Soil and Water Conservation, 47: 423–428.
13. NOOA: https://oceanservice.noaa.gov/facts/lidar.html
14. Petroselli, A., Apollonio, C., De Luca, D. L., Salvaneschi, P., Pecci, M., Marras, T., & Schirone, B. (2021). Comparative Evaluation of the Rainfall Erosivity in the Rieti Province, Central Italy, Using Empirical Formulas and a Stochastic Rainfall Generator. Hydrology, 8(4), 171. https://doi.org/10.3390/hydrology8040171
15. Pix4Dcatch, available on: https://www.pix4d.com/it/prodotto/pix4dcatch/
16. Pix4Dmatic, available on: https://www.pix4d.com/product/pix4dmatic-large-scale-photogrammetry-software/

17. Renard, K., Foster, G., Weesies, G., McCool, D. and Yoder, D. (1997) Predicting Soil Erosion by Water: A Guide to Conservation Planning with the Revised Universal Soil Loss Equation (RUSLE). US Department of Agriculture, Agriculture Handbook No.703USDA, USDA, Washington DC.
18. SENTINEL data available: https://browser.dataspace.copernicus.eu/
19. Tatsumi, S., Yamaguchi, K., & Furuya, N. (2023). ForestScanner: A mobile application for measuring and mapping trees with LiDAR-equipped iPhone and iPad. *Methods in Ecology and Evolution*, *14*(7), 1603–1609. https://doi.org/10.1111/2041-210X.13900
20. Schirone, B., Salvaneschi, P., Cianfaglione, K., Pecci, M., Andrisano, T., Vessella, F., & Petroselli, A. (2021). A proposal for modifying coppicing geometry in order to reduce soil erosion in the forest areas. *Notulae Botanicae Horti Agrobotanici Cluj-Napoca*, *49*(2), 1–17. https://doi.org/10.15835/nbha49212325
21. Van der Knijff JM, Jones RJ, Montanarella L (1999) Soil erosion risk assessment in Italy. European Soil Bureau, Joint Research Center of the European Commission. Scientific-Technical Reports, EUR 19044 EN, 34 pp.
22. Yu, B., & Rosewell, C. J. (1996). Technical notes: A robust estimator of the R-factor for the universal soil loss equation. *Transactions of the ASAE*, *39*(2), 559–561.
23. Wischmeier, W.H. and Smith, D.D. (1978) Predicting Rainfall Erosion Losses. A Guide to Conservation Planning. The USDA Agricultural Handbook No. 537, Maryland.

6. Conclusions

The forest environment, compared to the agricultural environment, is less studied concerning soil erosion and the risk of hydrogeological instability. Coppice stand arrangement is a form of forest management that has a greater impact on soil erosion and the increase of hydrological risk.

From our experiences, both theoretical and real, we can surmise that within coppice forests in sloping areas and where there is a real risk to human health, such as the presence of large rocky boulders, it might make sense to use our silvicultural model, the banded standards method. Our model was found to decrease post-cut erosion both theoretically and through field experiments. Our model was found to be effective in decreasing erosion, especially concerning large sediment, and in stopping the loss of leaves and consequently organic matter. This leads on the one hand to a decrease in the risk of disruption and consequently in the risk to human health, and on the other hand to an increase in fertility with respect to traditional coppice. These two phenomena are due to the action of the bands of standards and the bundle of twigs posed on them, which act as real barriers.

In addition to the positive effects related to erosion reduction resulting from logging, we believe that the Banded Standards Method can be an effective model to address certain issues related to forest regeneration after logging. Regarding seed regeneration, seeds that fall from trees, typically fewer in a coppice stand forest compared to a high stand forest, are easily washed away by runoff water. However, when obstacles like bands of standards and bundle of twigs are present, as in our case, seeds can be trapped, facilitating seed regeneration. Furthermore, the presence of these bands and bundles allows for blocking seeds of all sizes, without altering the biodiversity of the stand, as smaller and lighter seeds are more susceptible to being carried away by water.

The use of bands and bundle of twigs, by reducing erosion and promoting faster regeneration, may also limit the establishment of cosmopolitan herbaceous plants that negatively impact stand regeneration (both gamic and agamic).

Finally, by maintaining stand continuity in strips, the bands of standards can be considered true ecological corridors, benefiting both fauna and gene flow continuity.

Our soil erosion plot prototype, which we called N.E.T. (Natural Environment erosion Trap), proved to be effective in capturing sediment of all types. Since we were able to use it in a difficult context (coppice forest with an average slope of 48%), its use in any type of environment is conceivable. By adopting some modifications, it may also be able to obtain run-off, in addition to the data it is normally able to provide.

Concerning the USLE and RUSLE models, we realized that the choice of formulas forming the factors of the two equations is crucial for the calculation of total annual erosion. An incorrect choice of a formula can brings errors in the order of tens of t/ha/year, or more. An example would be the choice of formula to calculate the R-factor of the equations. The various existing formulas are very different from each other and are generally better in some places than others. This fact causes an enormous diversity of results. For this reason, in soil erosion studies, the most suitable formula should always be chosen for the location chosen for the investigation, perhaps using an average of several equations to obtain a more homogeneous result.

In our theoretical experiments, we observed greater soil erosion than in the field experiment. In our opinion, this could be caused by the very nature of the USLE and RUSLE models. Indeed, the two models were created in the agricultural field and later adopted for use within natural and forest environments. With the same slope and land cover, a natural and forest environment produces less erosion, because no tillage has been carried out within it, which is a source of erosion. For this reason, there could be a basis for creating an environmental factor that identifies the type of environment not only for land cover, i.e. the C-factor, to be implemented in the USLE equation and the RUSLE model. Furthermore, as part of the modelling of silvicultural projects, it would be useful to create an additional factor, a silvicultural factor, to represent the silvicultural operations carried out in favour of reducing soil erosion. This factor should identify the silvicultural practice chosen and give it a value based on its effect on reducing soil erosion. This factor should work somewhat like the P-factor works but related to silvicultural practices.

Clearly, these theses are merely deductions derived from a year of scientific experimentation in the field and from results obtained from models, but with clear limitations due to the difficulty of using detailed data. It would be desirable to continue the research in the Popoli study area, to monitor the evolution of soil erosion in the two plots over the years. Moreover, new plots should be created, so that the phenomena studied can be generalized.

As far as models are concerned, in order to optimize their use within small parcels such as ours, they should be created from ultra-detail data, e.g. using multispectral images obtained from drone flights, and not from low-detail data found online. The possibility of obtaining such high-detail models could allow a better comparison with real erosion obtained from soil erosion plots and minimize errors. This would give the possibility, if the data confirm the hypothesis, to seriously reason about the possible creation of new factors.

Acknowledgments

This PhD project was carried out thanks to the scientific collaboration and to the funds received from the Maiella National Park and the Department of Regional Affairs and Autonomies (DARA) – Presidency of the Council of Ministers. Their fund gave us the possibility to build the two erosion plots, as well as technical and technological products.

We would like also to thank the Raggruppamento Carabinieri Biodiversità di Pescara for their collaboration. Their workers carried out all the silvicultural operations and they help us building the two erosion plots.